CR-137616

DESIGN, FABRICATION, AND TESTING OF A CRYOGENIC THERMAL DIODE

INTERIM RESEARCH REPORT

GRUMMAN

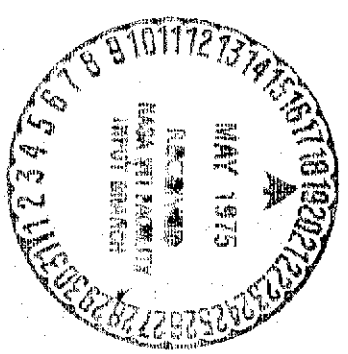

CR-137616

DESIGN, FABRICATION, AND TESTING OF A CRYOGENIC THERMAL DIODE

INTERIM RESEARCH REPORT

Prepared for
National Aeronautics and Space Administration
Ames Research Center
Moffett Field, California 94035

Under Contract NAS-2-7492

Prepared by
J. Quadrini
R. Kosson

Grumman Aerospace Corporation
Bethpage, New York 11714

December 1974

FOREWORD

The research described herein was conducted by the Heat Pipe Group, Thermodynamics Section of the Product Engineering Department of Grumman Aerospace Corporation. The authors wish to thank Dom Visceglie and Ed Leszak for development of special fabrication techniques and assistance during testing. The work was supported under Contract NAS 2-7492, "Design, Fabrication and Testing of a Cryogenic Thermal Diode." The Technical Monitor is Mr. Jac Kirkpatrick of the Systems Development Branch of the NASA Ames Research Center, located at Moffett Field, California.

CONTENTS

ILLUSTRATIONS

ILLUSTRATIONS (Cont)

TABLES

Section 1

SUMMARY

This interim research report reviews cryogenic heat pipe diode applications and describes a new heat pipe geometry. This new geometry employs excess liquid to block the vapor space of the evaporator and part of the transport section during reverse mode conditions. An orifice plate is positioned in the pipe at the blocking meniscus location, with the opening arranged to permit proper liquid distribution in both ground tests and zero "g" operation.

Experimental data are presented for a room temperature heat pipe modified to operate as a blocking orifice diode. The test results verify feasibility of the blocking orifice technique with the diode having a rapid shutoff characteristic.

The selection of a diode for fabrication and test was based mainly on a parametric investigation of the liquid trap and liquid blockage techniques. The blocking orifice form of liquid blockage was selected for the cryogenic diode based on its high throughput, small reservoir requirement, and small energy and time required for shutoff.

The design, fabrication and test of the blocking orifice engineering model is described. The cryogenic diode pipe was made of stainless steel having a .635 cm (.25 in.) outside diameter. The working fluid was methane and the capillary system was a spiral artery tunnel wick with an effective screen pore size of 38.1 microns (.0015 in.). Tests were conducted in both the forward and reverse mode. A throughput of 2794 watt-cm (1100 watt-in.) was achieved when level and 868 watt-cm (270 watt-in.) was achieved at 12.7 cm (5.0 in.) adverse tilt. Reverse-mode performance resulted in a rapid shutoff.

Section 2

INTRODUCTION

This interim research report covers work performed by Grumman Aerospace Corporation under Contract NAS 2-7492, "Design, Fabrication and Testing of a Cryogenic Thermal Diode." The report covers the period April 1973 through August 1974 and describes four major tasks:

I. Survey throughput requirements and shutoff characteristics of cryogenic diodes used for satellite and spaceborne equipment thermal control.

II. Analyze a variety of shutoff techniques for the requirements established in Task I.

III. Investigate a detailed design, selected in conjunction with ARC, with respect to throughput of the cryogenic diode and shutoff characteristics.

IV. Fabricate and test the cryogenic thermal diode.

In addition to the above tasks, a new geometry was developed for liquid blockage shutoff which would allow a marked increase in throughput over the ordinary liquid blockage technique. The geometry is based on the use of an orifice plate inserted in the vapor passage. Feasibility of this technique, considered as an additional task under this contract, was demonstrated in an existing room temperature heat pipe.

Task I resulted in the cataloging of throughput and boundary temperature requirements which would allow various shutoff techniques to be evaluated.

In Task II, primary consideration was given to determination of the shutoff technique which would result in the maximum throughput for the minimum reverse mode energy required during shutdown. Reliability, weight, complexity, and room temperature envelope pressure containment were all factors considered in the recommended design.

The selected diode design, employing liquid blockage with the blocking orifice, was fabricated and tested with methane as the working fluid. A throughput of 2794

watt-cm (1100 watt-in.) was achieved level and 868 watt-cm (270 watt-in.) at 12.7 cm (5.0 in.) adverse tilt. Shutoff of the heat pipe in the reverse mode was evident within 1 min., resulting in a sharp temperature gradient which is characteristic of conduction heat transfer in the blocked portion of the pipe.

Section 3

FORMULATION OF DESIGN REQUIREMENTS

This section of the report is concerned with the accumulation of thermal requirements for potential cryodiode applications and a review of that data to determine specific diode performance requirements. In most cases, throughput, forward mode, and reverse mode temperatures were obtained. The collected data consisted of current and future design specifications covering the intended applications (See Table 3-1).

This task has been divided into two categories:

- Potential applications including throughput and shutoff evaluations
- Selection of requirements for analysis and preliminary design.

Table 3-1 Potential Diode Applications

Intended Application	Length, cm			Load, w	Temperature, °K		Watt-cm
	L_{EV}	L_{TR}	L_{EFF}		T_{normal}	$T_{reverse}$	
• Detector Cooling							
– General: SWIR	5-15	213	305	20-30	100-200	–	6100-9150
LWIR	10-15	91	127	2 15 40	10 10-30 30-40	–	254 1905 5080
– Sensor W/PCM	15 15	45 45	68 68	5-10 50	150-160 100	300 300	340-680 3400
– Switching Radiators	8	10	38	10	90-100	–	380
• Detector Protection	15-30 8 8	60-30 28 91	76-61 38 127	35 6 10	100-110 200 100	268 250 150	2660-2135 228 1270
• Reverse Mode Operation for Cryogenic Tankage	20 64	51 91	137 127	10 5	200 90	– –	1370 635

3.1 POTENTIAL APPLICATIONS

Currently there is definite interest in the application of heat pipe thermal diodes to the cryogenic temperature range. As required, a phone and literature search was conducted to establish potential diode applications and determine associated diode specifications. From the results of this survey, the following areas were found to benefit:

- Detector cooling with a single or multiple radiator
- Detector protection
- Reduction of cryogen boiloff rates.

Diode specifications for each of the areas were catalogued and are listed in Table 3-1. Several observations regarding this information can be made:

- A wide variation in diode specifications prevail
- Reverse-mode hottest condenser temperature is estimated to be outside the cryogenic temperature range, i.e., $>170^{\circ}K$ ($>-154^{\circ}F$)
- No maximum acceptable limit of reverse-mode heat leakage was known.

Determining the hottest reverse-mode temperature for many of the intended applications required an educated guess. For the specific applications having immediate use this temperature is well defined. For future applications, involving primarily low earth orbits, little is known regarding this temperature. It will depend upon the satellite mission, orbital parameters, and time constants associated with the satellite/diode configuration and orientation of the radiator(s).

The maximum reverse-mode temperature is highly critical for liquid blocking diodes which require the working fluid to remain in the liquid state. It is less critical for diodes which shutoff by wick dry-out, though still important because of sensible heat storage. The high reverse-mode temperatures tend to be associated with low altitude orbits, which also have relatively short orbital periods, and the time required to reject the stored sensible heat can seriously reduce the available time for normal mode heat rejection. Obviously, the selection of the blocking technique is dependent upon this temperature and fluid properties, while the working fluid selection remains dependent upon fluid transport properties for the forward mode.

The amount of energy absorbed and transmitted by the diode in making the transition to the reverse-mode, and during the reverse-mode, is controlled by several factors:

- Amount of fluid inventory
- Mass of diode system
- Heat loads and temperatures imposed during transition.

These factors vary as a function of throughput, radiator thermophysical properties, and fluid properties, as well as with shutoff technique. While prediction of the exact amount of energy absorbed can be very complex, the magnitude should be minimized.

3.2 DESIGN GOALS

Because of the wide variation of diode specifications, the following groundrules regarding design requirements were formulated:

- In a system where the heat transfer distances are large, especially in an application where a radiator is employed, the watt-cm (watt-in.) capacity can be high even though the radiator heat rejection is small. The first diode applications, however, will probably be in the lower capacity range. Thus, design goal values chosen were 254-762 watt-cm (100 to 300 watt-in.), with a short evaporator and long condenser.
- The fastest possible transition to reverse-mode operation is necessary for minimum heat transfer during reversal. After transition, a reverse-mode heat leakage of less than parasitic heat inputs was taken as a design goal.
- Forward-mode operating temperature range of $100^{\circ}K$ ($280^{\circ}F$) to $160^{\circ}K$ ($-172^{\circ}F$).
- Thermal shutoff or reverse-mode temperature $30^{\circ}K$ ($54^{\circ}F$) to $50^{\circ}K$ ($90^{\circ}F$) above forward-mode temperatures. This is on the low side for the applications shown in Table 3-1, but is adequate for many initial applications.

From the above groundrules, a concept of the cryodiode design can be formulated, i.e., the type of shutoff techniques, throughput, working fluid, and the degree of room temperature pressure containment. Boundary conditions and geometry are then varied parametrically to obtain performance curves for each diode concept.

Section 4

REVIEW OF SHUTOFF TECHNIQUES

The shutoff techniques are considered for the case of a low-temperature sensor rejecting heat to space via a relatively large radiator. The evaporator is short and the condenser is long. Shutoff is desired when the radiator temperature rises due to incident solar flux, earth albedo, or earth emission.

A number of techniques for interfering with forward-mode heat pipe operation have been studied and reported in the literature (Reference 1). These techniques can be subdivided into two broad groups:

- Electromechanical
- Thermodynamic.

Although mechanical shutoff devices have been built, their designs are functionally centered around ancillary hardware and an external power source. For example, an electromechanical diode might employ a solenoid valve to disrupt normal heat pipe operation. Reverse-mode operation would be initiated by movement of a metal slug to block the vapor space. The motion commences when the coil is energized and remains energized for the entire reverse-mode time. Alternatively, a more complex latching solenoid valve can be used. In either case, shutoff is incomplete because of vapor forcing its way through the wick to bypass the valve.

Diode designs employing electromechanical devices have the following common disadvantages when compared to thermodynamic shutoff techniques:

- Inherently complex
- Requires external power source
- Inherently heavy
- High reverse-mode heat leakage
- Envelope compatibility problems
- Less reliable
- High cost.

Because of these factors, electromechanical devices were not considered part of this study effort.

Thermodynamic techniques for interfering with normal heat pipe operation have been subjected to some previous research and development. State-of-the-art, and optimal designs have been defined, fabricated and tested. Thermodynamic techniques employed for shutoff can be grouped as follows:

- Noncondensible gas blockage
- Freezing of the working fluid
- Liquid trap
- Liquid blockage.

4.1 NONCONDENSIBLE GAS BLOCKAGE

Functionally, shutoff is achieved by introducing a noncondensible gas into the single-component system. The gas tends to diffuse slowly throughout the system when the original source temperature drops below that of the original condenser. Once this occurs, a mixture of gas and vapor flows towards the original evaporator. The noncondensible gas accumulates at this end, and eventually completely blocks it.

The conditions for reservoir sizing are different than those for gas blockage variable conductance heat pipes (VCHPs). When the reservoir of a diode heats up during reversal, the gas partial pressure must equal the difference in vapor pressure between normal and reverse mode hot-end temperatures. This can be an order of magnitude larger than the gas pressure in the reservoir during normal-mode operation. The reservoir must therefore be relatively large compared with the liquid blockage technique.

4.2 FREEZING OF THE WORKING FLUID

This type of shutoff is applicable when the normal mode-evaporator becomes cold, and shutoff is desired. It is not applicable for cryogenic diodes, where shutoff is desired when the condenser end becomes hot.

4.3 LIQUID TRAP

Shutoff control depends upon the ability of liquid to accumulate within the inner wall and artery envelope and at the coldest portion of the pipe, except as displaced

by surface tension and gravity forces. Depleting the artery of normal fluid inventory causes a rapid reduction in throughput.

A reservoir is provided at the evaporator end to hold the fluid during and after reversal. For minimum heat transfer during shutdown, the reservoir must be sized to hold virtually all the liquid in the wick. Generally, because of the long condenser, the result will be a larger reservoir than that needed for liquid blockage.

4.4 LIQUID BLOCKAGE

This choice of shutoff control is dependent upon excess liquid shifting naturally from one end to the other as hot and cold ends are interchanged. Under reverse-mode operation, the excess liquid must have a volume sufficient to block the vapor space of the cold end and a large part of the transport section to minimize conduction heat transfer. A reservoir would be provided at the other end to contain excess liquid under normal-mode conditions. The reservoir size must be slightly larger than the absorber and transport section vapor space volumes, to allow for changes in liquid density with temperature.

This type of shutoff mechanism is most attractive for cryogenic applications where, under normal-mode operation, the evaporator is relatively short compared with the condenser and transport sections. This arrangement minimizes the excess liquid required for blockage. Since this technique was selected for detailed investigation, some additional discussion, particularly with respect to ground test requirements, is given in the following subsections.

4.4.1 Narrow Vapor Space

In a gravity environment, the vapor space in the blocked sections of the shutoff diode must be designed to insure that the capillary force, ΔP_{cap} will support the pressure head of the liquid slug. This is necessary if the vapor space is to self-fill with liquid, and remain filled in the reverse mode.

For use in the ATFE (Reference 2) this requirement resulted in extremely thin vapor spaces (see Figure 4-1), and consequently large vapor pressure drops during normal heat pipe operation. This limited the heat pipe capacity, restricting this type of diode to smaller heat transport applications, and use of working fluids such as ammonia, which combine good capillary rise characteristics with small vapor space requirements. The problem is particularly severe at cryogenic temperatures, where even the best fluid, methane, has a relatively poor capillary rise characteristic.

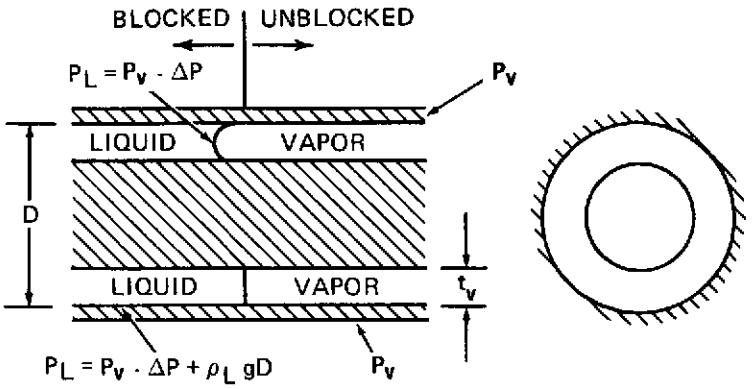

FOR BLOCKAGE IN LEVEL GROUND TESTING

$$\Delta P = \frac{\rho_L gD}{g_c} = \frac{2\sigma}{t_v}$$

Figure 4-1 Liquid Blockage of Vapor Space

4.4.2 Blocking Orifice

To get around the limitations on working fluid and capacity described in Subsection 4.4.1, a new geometry has been developed based on insertion of an orifice plate in the heat pipe at the blocking meniscus. The opening in the orifice plate is located at the bottom of the pipe, as shown in Figure 4-2. The orifice height may be greater or less than the annular vapor passage height, t_v. The use of large vapor passage areas more than compensates for the additional vapor pressure loss introduced by the orifice.

The blocking orifice geometry is particularly suited for thermal diode applications on space vehicles coupling moderately low temperatures detectors, i.e., 120°K to 150°K (-244°F to -190°F) to a radiator which periodically sees a slightly warmer environment. The evaporator would normally be relatively short compared with the overall length of the heat pipe. The available working fluids have relatively poor capillary rise characteristics, and the excess liquid reservoir can be coupled to the radiator to provide a rapid shutoff characteristic.

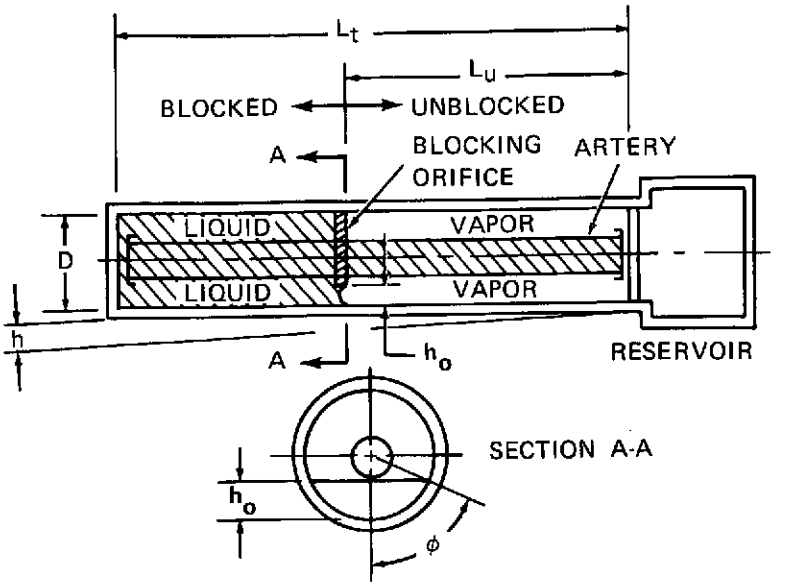

Figure 4-2 Blocking Orifice – Liquid Blockage

Having discussed the importance of the blocking orifice diode, a theory for heat pipe throughput, which takes account of the orifice plate follows.

The basic hydrodynamic equation for flow in the heat pipe is modified by addition of an orifice pressure loss, taken equal to the loss of the dynamic head of vapor flowing through the orifice:

$$\Delta P_o = \frac{\rho_{v,o} V_o^2}{2g_c} = \frac{Q^2}{2g_c (C_D A_o)^2 \rho_{v,o} \lambda^2} \tag{1}$$

Then the hydrodynamic equation can be written:

$$\Delta P_{LIQ} + \Delta P_{VAP} + \Delta P_o = \Delta P_{CAP} - \Delta P_{GRAV} \tag{2}$$

For laminar flow, the liquid and vapor viscous losses are proportional to flow rate and can be written (see Reference 2):

$$\Delta P_{LIQ} = C_L Q \tag{3}$$

$$\Delta P_{VAP} = C_v Q \tag{4}$$

where C_L and C_V are functions of fluid properties and pipe geometry.

In similar fashion we can define an orifice pressure loss coefficient:

$$\Delta P_o = C_o Q^2 \tag{5}$$

where $$C_o = \frac{1}{2g_c (C_D A_o)^2 \rho_{v,o}} \lambda^2 \tag{6}$$

Then the hydrodynamic equation can be written:

$$C_o Q^2 + (C_V + C_L) Q - (\Delta P_{CAP} - \Delta P_{GRAV}) = 0$$

with solution:

$$Q = \frac{(C_v + C_L)}{2 C_o} \left[\sqrt{1 + \frac{4 C_o (\Delta P_{CAP} - \Delta P_{GRAV})}{(C_V + C_L)^2}} - 1 \right] \tag{7}$$

For turbulent vapor flow:

$$\Delta P_V = C_{V,T} Q^2 \tag{8}$$

giving the hydrodynamic equation

$$(C_o + C_{V,T}) Q^2 + C_L Q - (\Delta P_{CAP} - \Delta P_{GRAV}) = 0 \tag{9}$$

with solution:

$$Q = \frac{C_L}{2 (C_o + C_{V,T})} \left[\sqrt{1 + \frac{4 (C_o + C_{V,T}) (\Delta P_{CAP} - \Delta P_{GRAV})}{C_L^2}} - 1 \right] \tag{10}$$

The maximum permissible orifice height, h_o, is computed for a two-dimensional meniscus of radius $h_o/2$ with surface tension at the temperature of the vapor space for the reverse mode condition. If the pipe is tilted with the blocked end high, the equation for hydrostatic equilibrium can be written:

$$\rho_L \frac{g}{g_c} \left(h_o + \frac{h L_u}{L_t} \right) = \frac{2\sigma}{h_o} \tag{11}$$

from which:

$$h_o = \tfrac{1}{2} \left\{ \left[\left(\frac{hL_u}{L_t} \right)^2 + \left(\frac{8\sigma}{\rho_L g/g_c} \right) \right]^{\frac{1}{2}} - \frac{hL_u}{L_t} \right\} \tag{12}$$

The lengths L_u, L_t and tilt h are indicated in Figure 4-2.

The orifice opening is assumed to be a circular segment at the bottom of the pipe (Figure 4-2), with height h_o, and half angle ϕ given by:

$$\phi = \cos^{-1} \left[1 - \frac{2\,h_o}{D} \right] \tag{13}$$

Orifice area is then:

$$A_o = \left(\frac{D}{2} \right)^2 \left[\frac{\pi \phi}{180} - \sin \phi \cos \phi \right] \tag{14}$$

Section 5

FEASIBILITY OF BLOCKING ORIFICE TECHNIQUE

This section describes the fabrication and reverse mode testing for demonstrating the feasibility of the blocking orifice concept based on the principles of Section 4. To expedite this task, an existing aluminum ammonia heat pipe was used.

5.1 DESIGN MODIFICATIONS

The aluminum heat pipe used to demonstrate feasibility had a stainless steel flexible spiral/tunnel wick with .152 cm (.060 in.) diameter tunnel. The artery outer diameter was .795 cm (.313 in.), whereas the pipe inner diameter throughout was 1.257 cm (.495 in.). The pipe shell was a 66 cm (26 in.) piece of internally threaded tube having approximately 31 grooves/cm (80 grooves/in.) with a full 180° 4.76 cm (1.875 in.) radius "U" bend.

Since ammonia was the previous working fluid, an orifice opening of .146 cm (.0575 in.) was selected which would provide blockage up to a temperature of 372°K (210°F). Beyond this temperature, the orifice opening is too large to sustain liquid for a level pipe in a 1-g force field.

5.2 FABRICATION

To accommodate both an orifice plate and reservoir for excess liquid, the pipe was sectioned in two areas: at the entrance of the transport region and at the end of the condenser portion of the pipe. An aluminum orifice plate was secured to the artery without removal of the artery from the envelope. "Swagelok" fittings were used to provide a leak tight closure between evaporator and transport sections.

A liquid reservoir was added to the condenser end of the pipe to trap excess fluid added to the normal charge inventory in order to obtain liquid blockage in the evaporator and 5.08 cm (2 in.) of the transport sections during the shutoff mode operation. The reservoir was made from the same pipe diameter tubing with "Swagelok" fittings providing the enclosure. The reservoir wick consisted of rolled up stainless steel screen and was non-communicating with the main wick system.

After bakeout, the pipe was charged with 35.0 grams of processed ultra high purity ammonia. Both evaporator and reservoir sections were then equipped with heaters and cooling systems in order that both modes of operation could be tested. Figure 5-1 shows a sketch of the pipe and thermocouple locations.

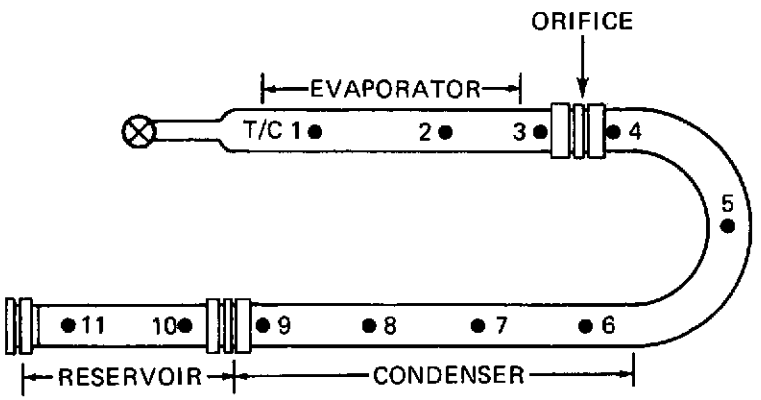

Figure 5-1 Feasibility Model

5.3 TEST RESULTS

The rework of the pipe caused some damage to the evaporator web-to-wall contact, resulting in an erratic evaporator wall temperature profile, and making determination of burnout very difficult. Maximum throughput obtained in the normal mode of operation at 2.54 cm (1 in.) adverse tilt with and without the orifice plate installed was approximately 185 and 275 watts, respectively. Results are too crude to compare directly with theory, but the orifice pressure drop at 185 watts should be about one-quarter to one-third of the total.

For transition testing, the pipe was initially at a cold isothermal condition, 284°K, (52°F) established by applying a cold spray bath to the reservoir and condenser. The evaporator and transport sections were insulated, with no power applied to the pipe. The water valve was then switched to hot and time $\theta = 0$ was taken corresponding to the first rise noted in condenser or reservoir outer wall temperature. The resulting transient response of representative thermocouples is shown in Figure 5-2. Thermocouple 2 shows an initial rise indicative of normal heat pipe action, quickly followed

by a drop indicative of shutoff. Shutoff for thermocouple 2 seems to occur in about 30 sec. From the shapes of the curves, shutoff seems to occur sooner for thermocouple 1 and later for thermocouple 3. The temperature drop following shutoff is simply due to the heat capacity of the wall. A significant temperature differential can be noted across the orifice (thermocouples 3 and 4) starting with the first data printouts.

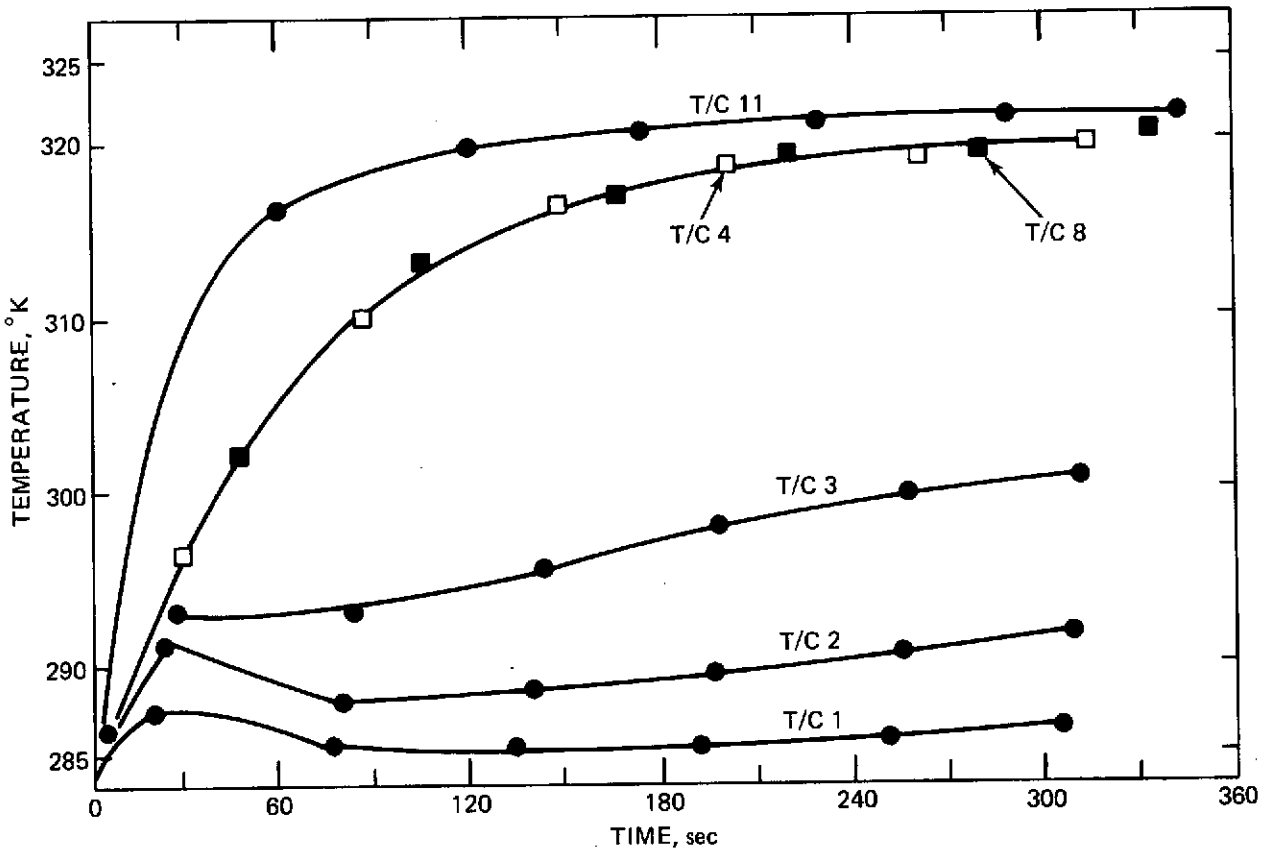

Figure 5-2 Diode Pipe Transition from Forward to Reverse Mode

The resulting steady-state reverse-mode temperature profile is shown in Figure 5-3 with the condenser and reservoir heated to a temperature well above evaporator temperature. As shown, a relatively steep temperature gradient exists on the evaporator side of the orifice plate, indicating proper liquid blockage. An even steeper gradient would be anticipated if the pipe envelope were made of stainless steel rather than aluminum.

From these tests, the concept of using a thin orifice plate for liquid blockage as a means of heat pipe shutoff was considered demonstrated.

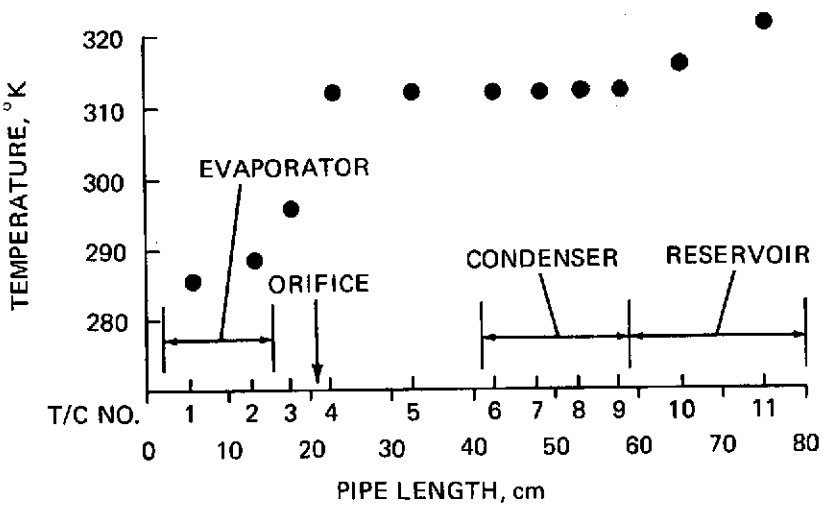

Figure 5-3 Reverse-Mode Performance of Diode Pipe with Ammonia

Section 6

CRYOGENIC DIODE ANALYSIS AND DESIGN

This section contains a brief discussion of the principal factors which are involved in the design of cryogenic heat pipes, and in particular, cryogenic thermal diodes. Consideration of these factors leads to an analysis survey and determination of a diode system design consistent with the study objectives. Finally, a description of the selected diode system fabrication steps are given.

6.1 DIODE DESIGN FACTORS

The intention of this section is to examine cryogenic diode design factors while deleting a discussion on common heat pipe design considerations such as heat pipe materials compatibility, economics and reliability. The principal factors discussed include:

- Fluid selection
- Pressure containment
- Blockage technique.

6.1.1 Heat Pipe Fluid

The maximum permissible temperature range over which any heat pipe operates in the forward mode is bounded by the working fluid thermodynamic triple point and critical temperature. For most cryogens this range is small when compared to room temperature and liquid metal candidate fluids: e.g., 19.1°K (34.4°F) and 102.4°K (184.3°F) for the cryogens hydrogen and methane, respectively; 210.3°K (378.5°F) and 374.1°K (673.4°F) for ammonia and water, respectively; and 6266°K (11279°F) for silver.

The heat pipe vapor pressure within the operating temperature range should be from approximately 1.4×10^4 to 69×10^4 Nm^{-2} (2 to 100 psia). Figure 6-1 presents the vapor pressure of candidate cryogens. At low vapor pressures, the vapor velocity is high and the vapor pressure drop becomes the dominant viscous loss, limiting pipe throughput. More important for many applications, however, is the drop in saturation

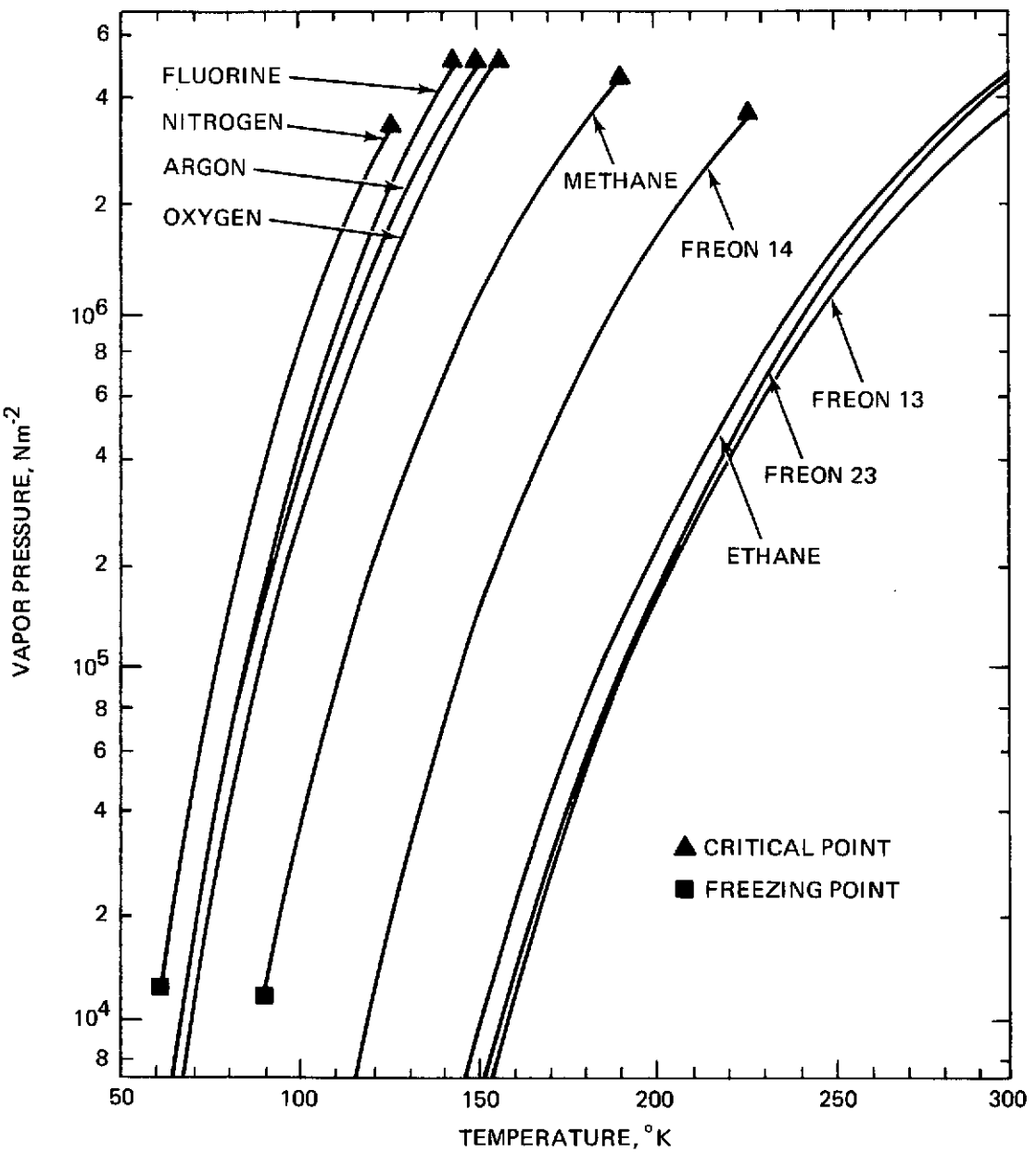

Figure 6-1 Vapor Pressure of Cryogens

temperature associated with this vapor pressure drop. The vapor entering the condenser will be superheated at condenser vapor pressure, and this superheat represents a temperature drop which is in addition to the usual evaporator and condenser temperature drops.

Assuming the vapor pressure drop is nearly equal to the capillary pressure drop, the saturation temperature drop is obtained from the Clausius-Clapeyron relation. Presented in Figure 6-2 are the corresponding saturation temperature drops for candidate cryogens for an effective pore size of 38.1 microns (.0015 in.). At higher vapor pressures, liquid pressure drop becomes the dominant concern, and throughput for forward mode operation is dependent on the liquid transport factor, $\sigma \rho_\ell \lambda g_c/\mu_\ell$, shown in Figure 6-3. It should be noted that this relationship of fluid thermodynamics and transport properties is a relative measure of the heat pipe's throughput.

For heat pipe diodes, another consideration is the fluid phase change thermal capacity ($\lambda \rho_\ell$). Liquid trap diodes and some liquid blockage diodes require liquid reservoirs which have no liquid flow path connection with the heat pipe wick. Such reservoirs fill by condensation and empty by evaporation. The heat transfer required to fill or empty the reservoir is proportional to the phase change fluid capacity. The amount of energy required to effect reversal should be minimal. In Figure 6-4, the thermal capacity of candidate cryogens are shown. It may be noted that low values of ($\lambda \rho_\ell$) imply low values of liquid transport factor.

Figure 6-5 presents the nucleation tolerance factor for the cryogens. This factor is an indication of the cryogens capacity for radial heat transfer up to the limit when boiling is initiated within the fluid. As shown in Figure 6-5, this factor is a decreasing function of temperature.

The hydrostatic liquid pressure head of the heat pipe operating in a 1-g field may have a pronounced influence upon its characteristics. Figure 6-6 presents the ratio of surface tension to body forces ($\sigma g_c/\rho_\ell g$) for the cryogens and shows this ratio to be a decreasing function of temperature. The lower the ratio, the more sensitive the heat pipe performance becomes to gravity effects, and the more care is required in laboratory tests to assure that results will be applicable to zero-g conditions.

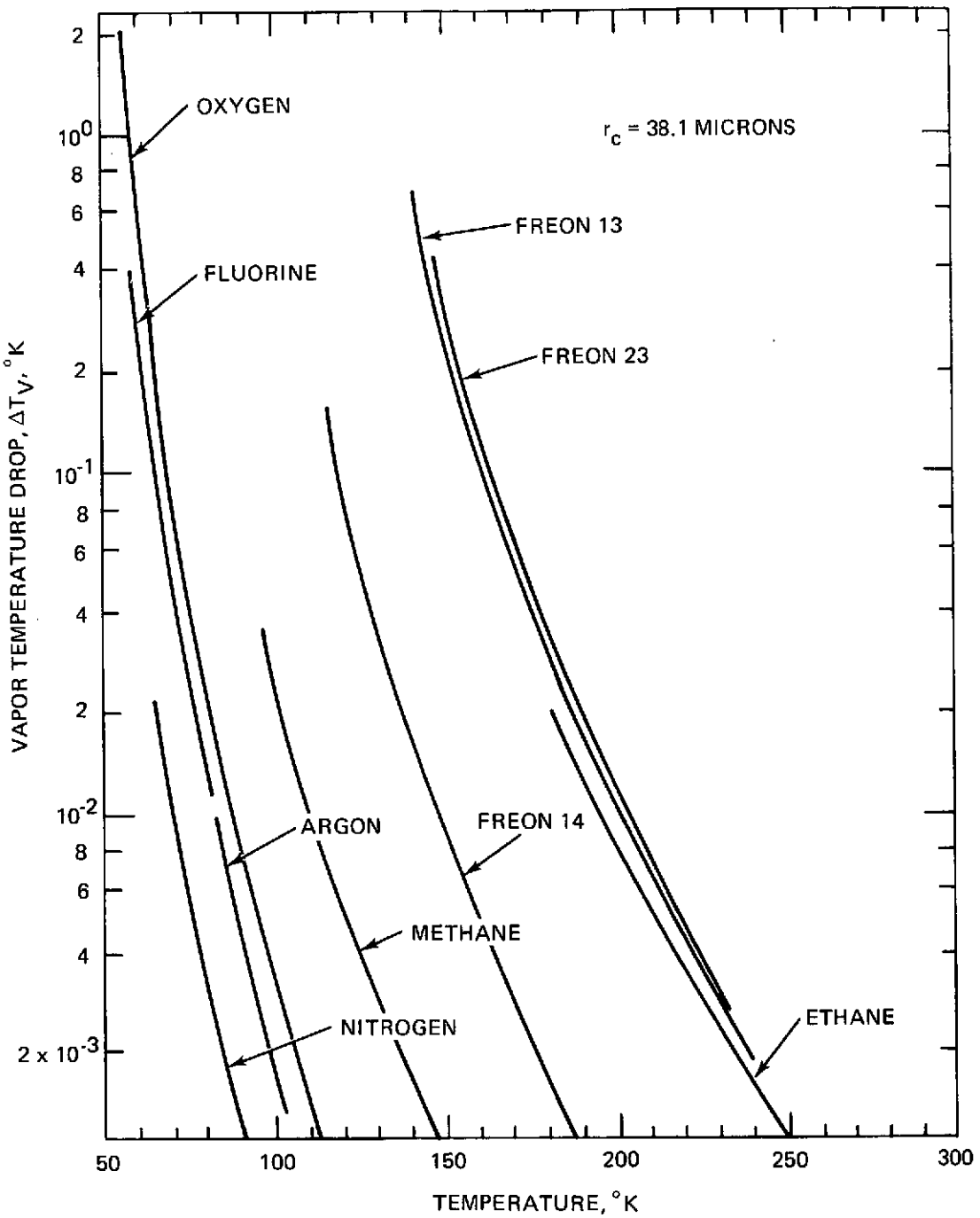

Figure 6-2 Clausius-Clapeyon Temperature Difference for Cryogens

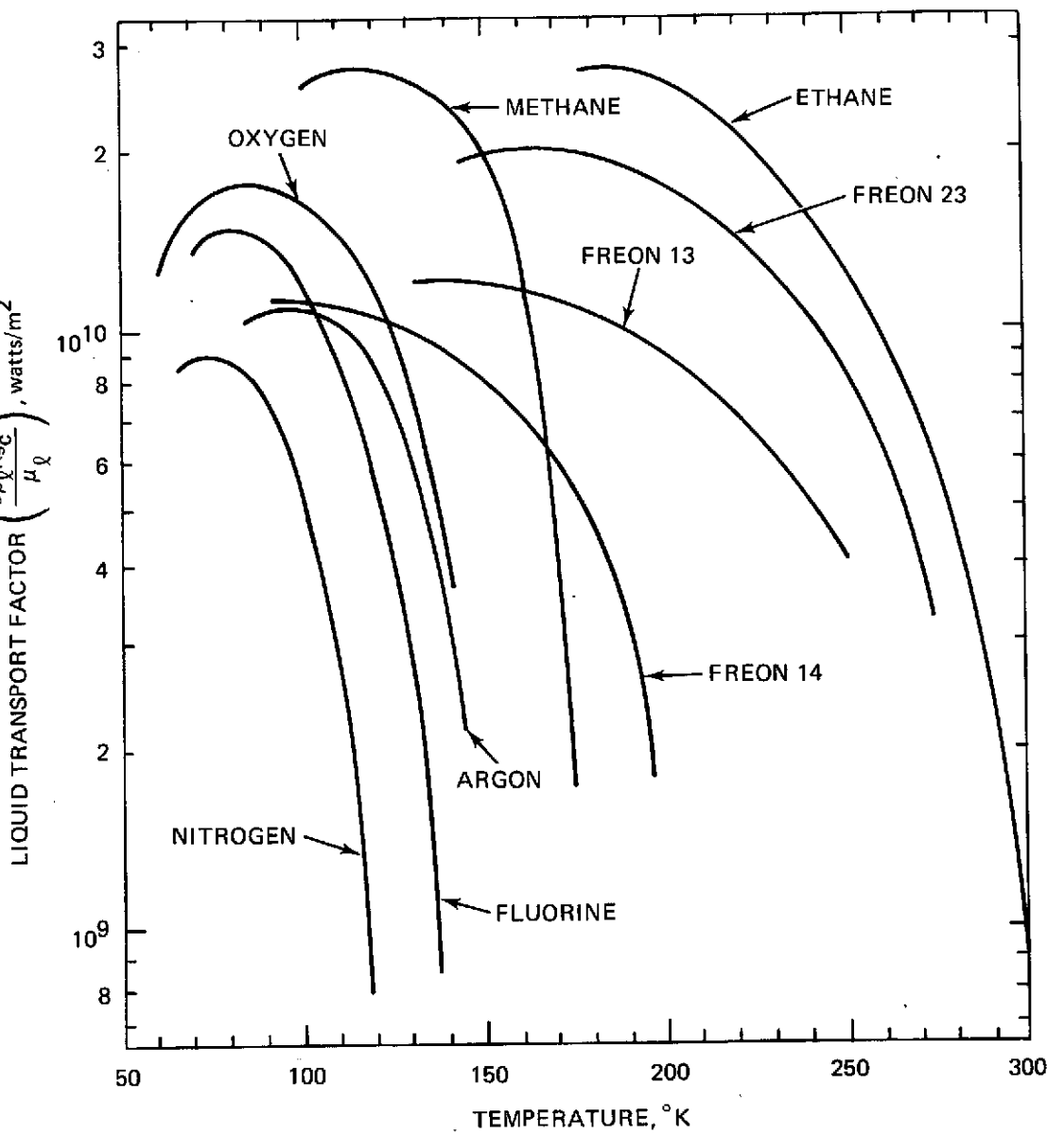

Figure 6-3 Liquid Transport Factor for Cryogens

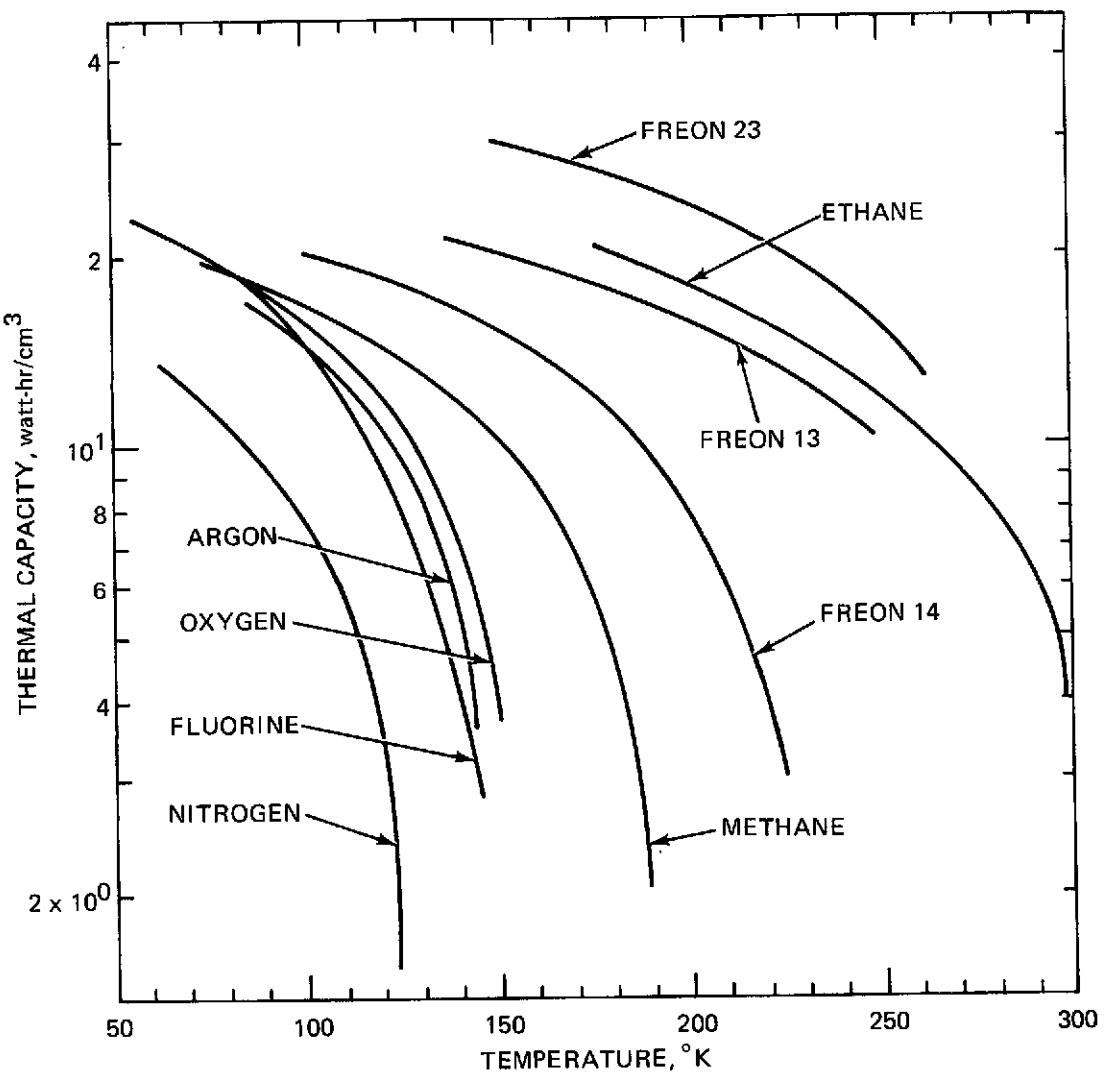

Figure 6-4 Cryogen Thermal Capacity

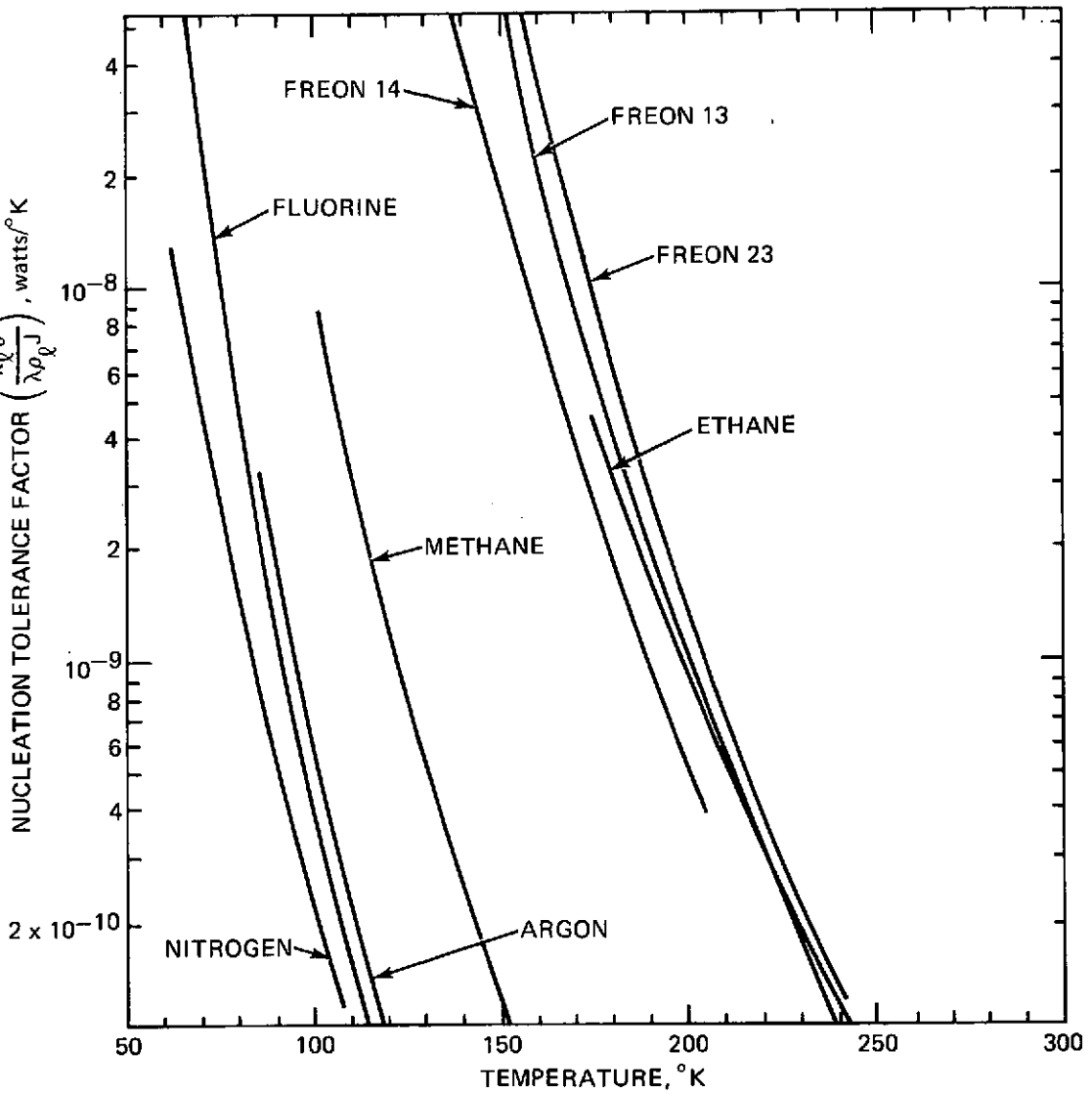

Figure 6-5 Nucleation Tolerance Factor for Cryogens

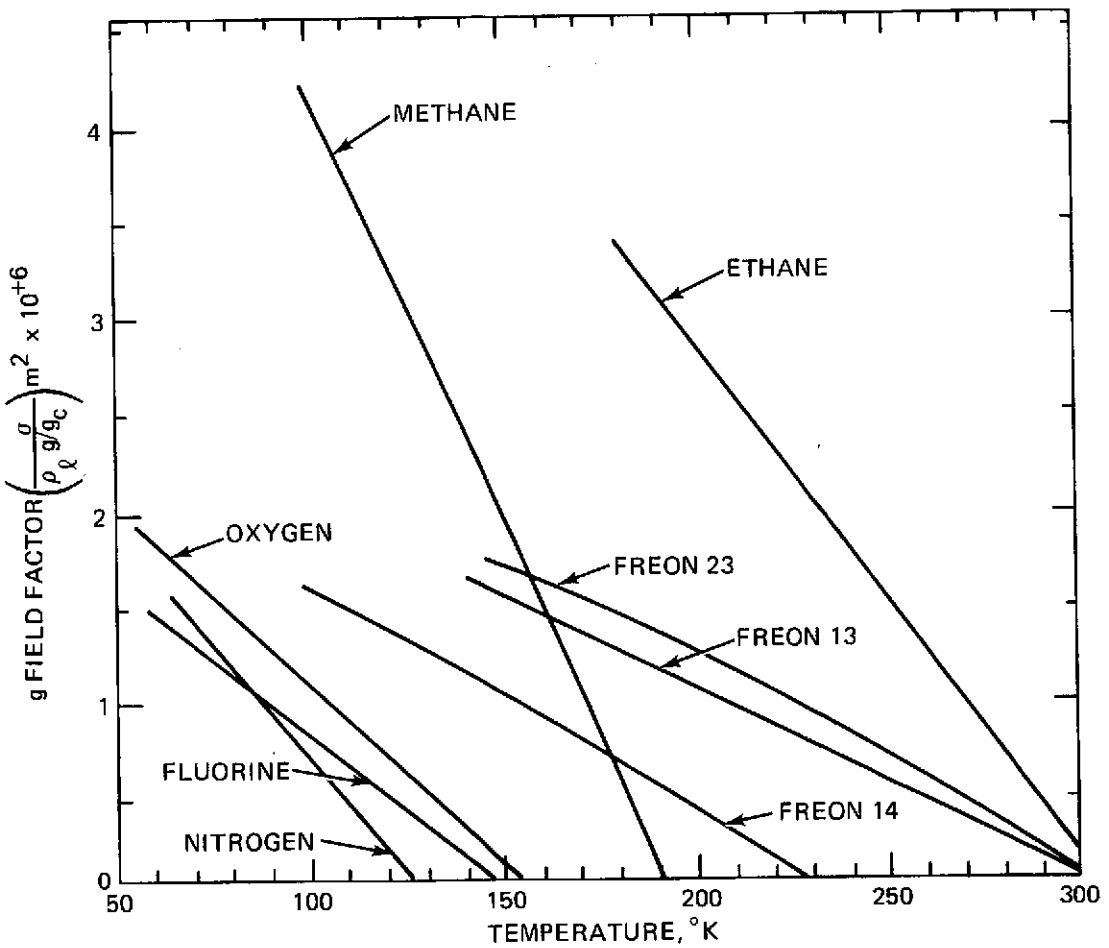

Figure 6-6 "g" Field Factor for Cryogens

When a heat pipe experiences an acceleration or deceleration, additional body forces act on the liquid and consequently alter the liquid flow characteristics. In the case of rotation, the maximum hydrostatic pressure difference becomes

$$\Delta P_{ROT} = \rho_\ell \frac{\Omega^2}{2g_c} (r_o^2 - r_i^2) = \rho_\ell \frac{\Omega^2 \bar{r} (\Delta r)}{g_c}$$

where the mean radius $\bar{r} = \frac{r_o + r_i}{2}$

and Ω = angular velocity. The effect of rotation on heat pipe performance is similar to that of gravity, with mean centripetal acceleration, $\Omega^2 \bar{r}$, analogous to gravity, and differences in end-to-end radii from the spin axis (Δr), analogous to pipe tilt. The ratio of surface tension to rotational forces would thus be indicated by the "g" field factor, $\sigma g_c / \rho_\ell g$, shown in Figure 6-6. Low values of $\sigma g_c / \rho_\ell g$ indicate high sensitivity to rotational forces.

The g-field factor ($\sigma g_c/\rho_\ell\ g$) is significant in blocking orifice designs because it controls the maximum permissible blocking orifice height (h_o). For zero pipe tilt,

$$h_o = \sqrt{\frac{2\sigma}{\rho_\ell (g/g_c)}}$$

Values for candidate pipe fluids are shown in Figure 6-7. As stated previously, the appropriate temperature to be used in evaluating h_o is the temperature of the unblocked vapor space for the reverse-mode condition.

For blocking orifice diodes, combining equations (5) and (6) from Subsection 4.4.2,

$$\Delta P_o = \frac{Q^2}{2g_c (C_D A_o)^2 \rho_{v,o} \lambda^2}$$

from which it can be seen that pressure drop depends on the ($2g_c \rho_{v,o} \lambda^2$) product as well as h_o (which controls A_o). Values for orifice pressure loss factor, $1/(2g_c \rho_{v,o} \lambda^2)$ are shown in Figure 6-8 for candidate fluids. Low values indicate low pressure drop. It may be noted that methane and ethane are particularly attractive for blocking orifice diodes, combining relatively low values of blocking loss factor and high values of orifice height.

6.1.2 Pressure Containment

The structural design approach for cryogenic heat pipes subject to internal pressures two to three times a cryogens critical pressure follows the practice of thin-walled cylinders:

$$P = \frac{2St_w}{D}$$

The determination of tube wall thickness is predicated on the maximum storage temperature and cryogen specific volume. When supercritical data is unavailable for the pressures an appropriate equation of state such as the reduced Benedict-Webb-Ruben equation can be applied for hydrocarbons and non-hydrocarbons (see Reference 3).

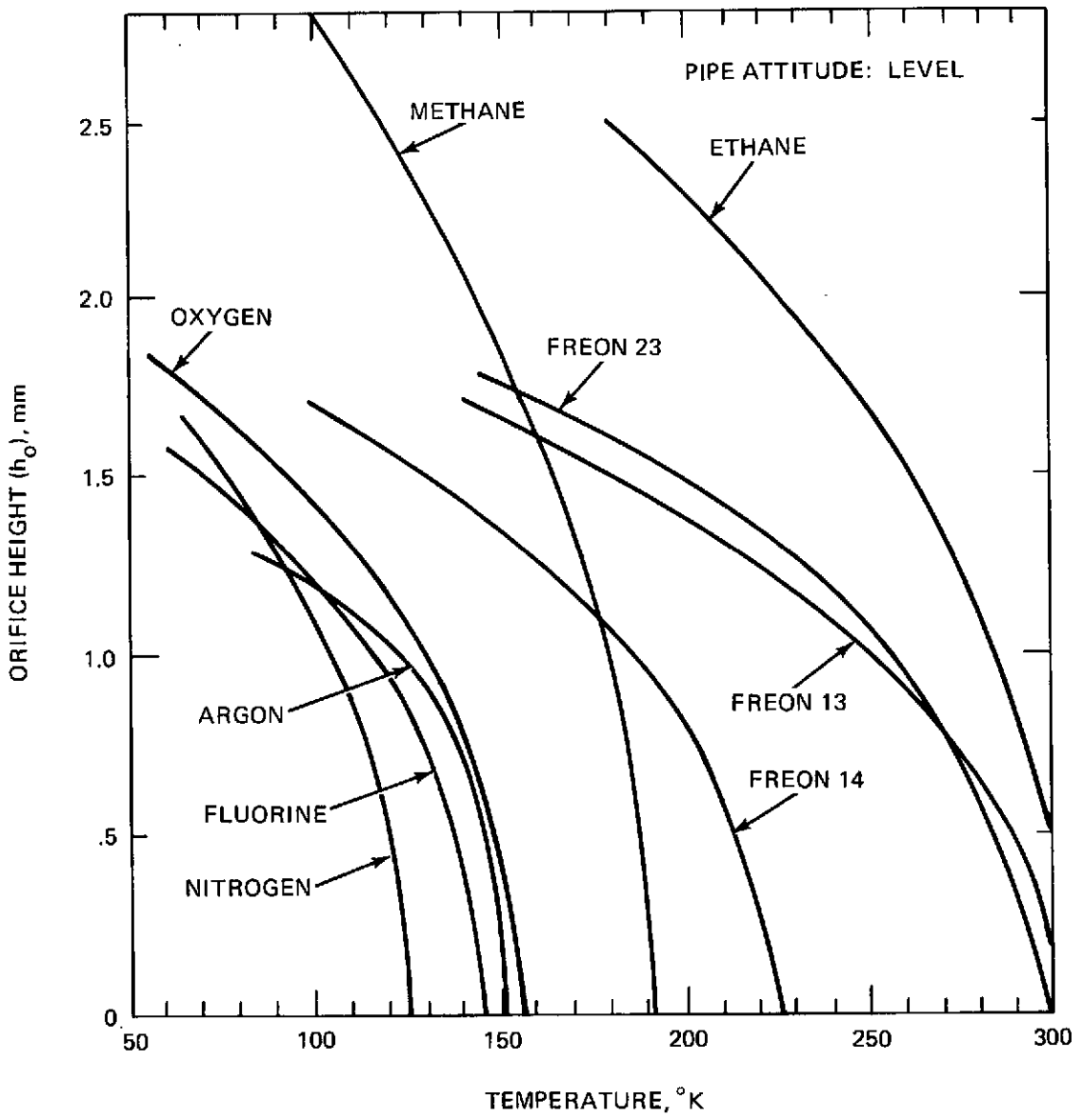

Figure 6-7 Orifice Height for Cryogens

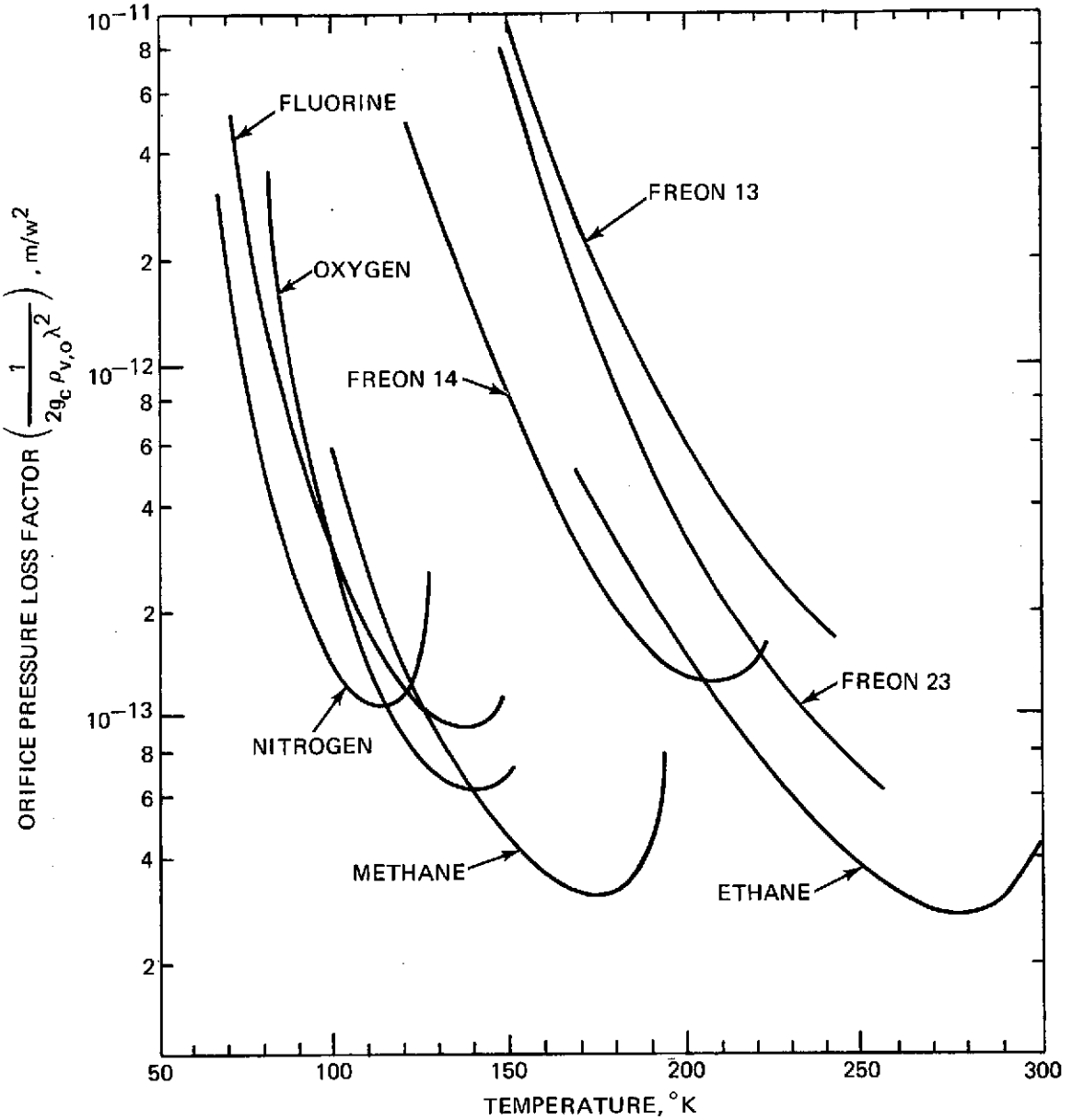

Figure 6-8 Orifice Pressure Loss Factor for Cryogens

In general, the equation predicts pressures that are within .5% of the true values for densities up to 1.8 times the critical density. The equation of state in dimensionless reduced form becomes:

$$P_r = T_r/\tau + (B_o' T_r - A_o' - C_o'/T^3)/\tau^2 + (b' T_r - a')/\tau^3 + a'\alpha'/\tau^6 + \left[c'(1 + \gamma'/\tau^2)\, e^{-\gamma'/\tau^2} \right] /\tau^3 T_r^2$$

where the terms T_r, P_r, and τ are reduced temperature, T/T_c, reduced pressure, P/P_c, and the modified reduced volume, respectively. The modified reduced volume takes the form:

$$\tau = \frac{P_c}{RT_c \rho}$$

The pressure ratios (P/P_c) of the candidate cryogens based on this equation of state for a storage temperature of ambient and 344°K (160° F) are shown in Figures 6-9 and 6-10.

6.1.3 Blocking Technique

From our review of cryogenic diode applications, the most common type of application involves heat rejection to a radiator during normal mode operation, with shutoff when the radiator is exposed to a hot environment. The conventional liquid blockage or the liquid blockage technique using an orifice to interrupt normal mode operation is attractive in this case for several reasons:

- The liquid reservoir can be easily heated by the hot environment to prevent liquid retention in the shutoff mode
- Generally, the evaporator is short compared with the condenser and total pipe length, minimizing blocking fluid requirements
- No liquid reservoir is required if the blocked length liquid requirement is less than the normal mode fluid inventory
- Liquid reservoir volumes are less sensitive to reservoir temperature when compared to the noncondensible gas blockage technique

- Small reservoir volumes when compared to the noncondensible gas reservoir volumes (ranging from 10.1 to 38.6 times the vapor space volume).

The liquid trap concept for blockage in this case is less attractive because of packaging considerations. For reverse-mode operation, the reservoir to collect the normal inventory of working fluid must become an integral part of the source package. Thus, not only must there be a thermal interface between the heat pipe evaporator and source but between source and heat pipe reservoir. This arrangement complicates the source package assembly.

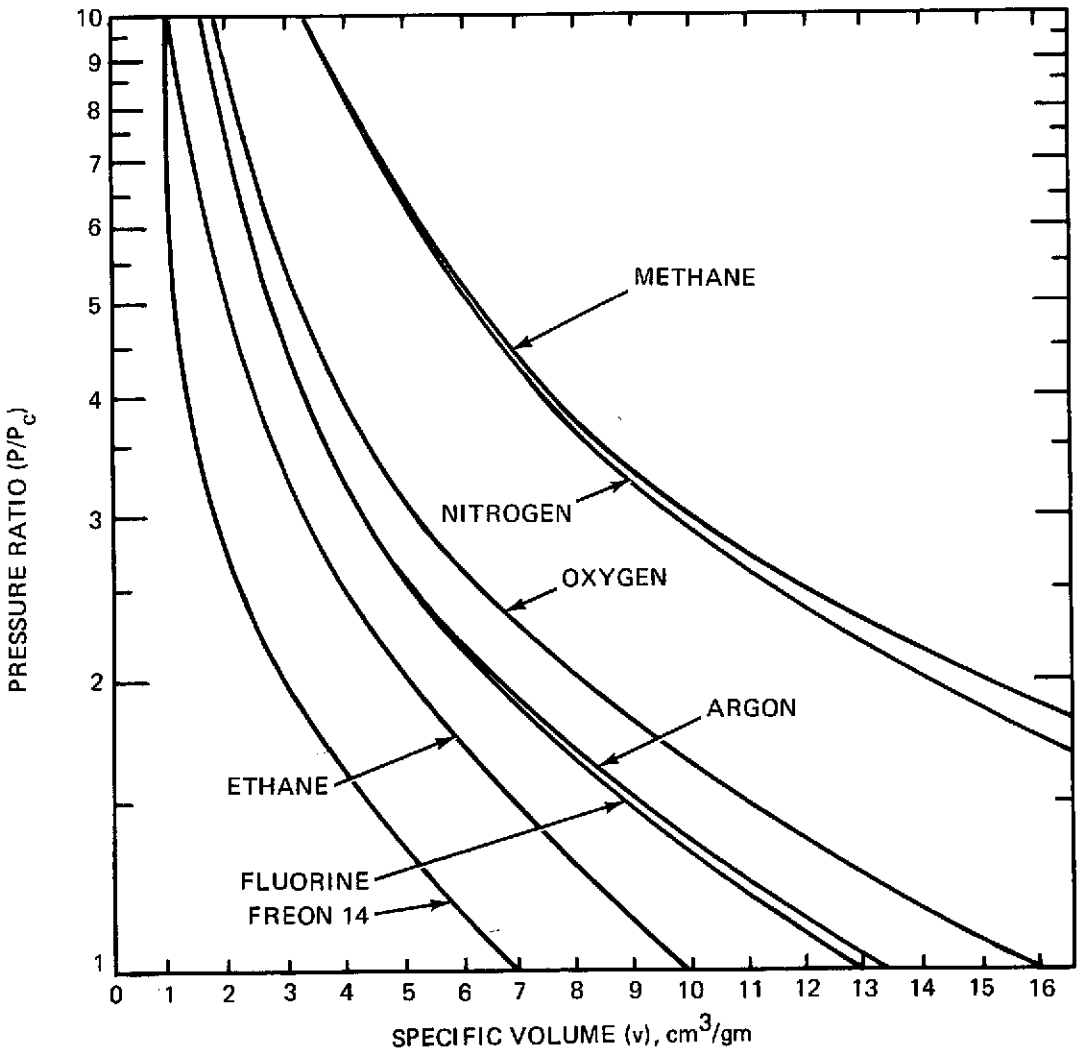

Figure 6-9 Pressure Ratio for 300° K (80° F)

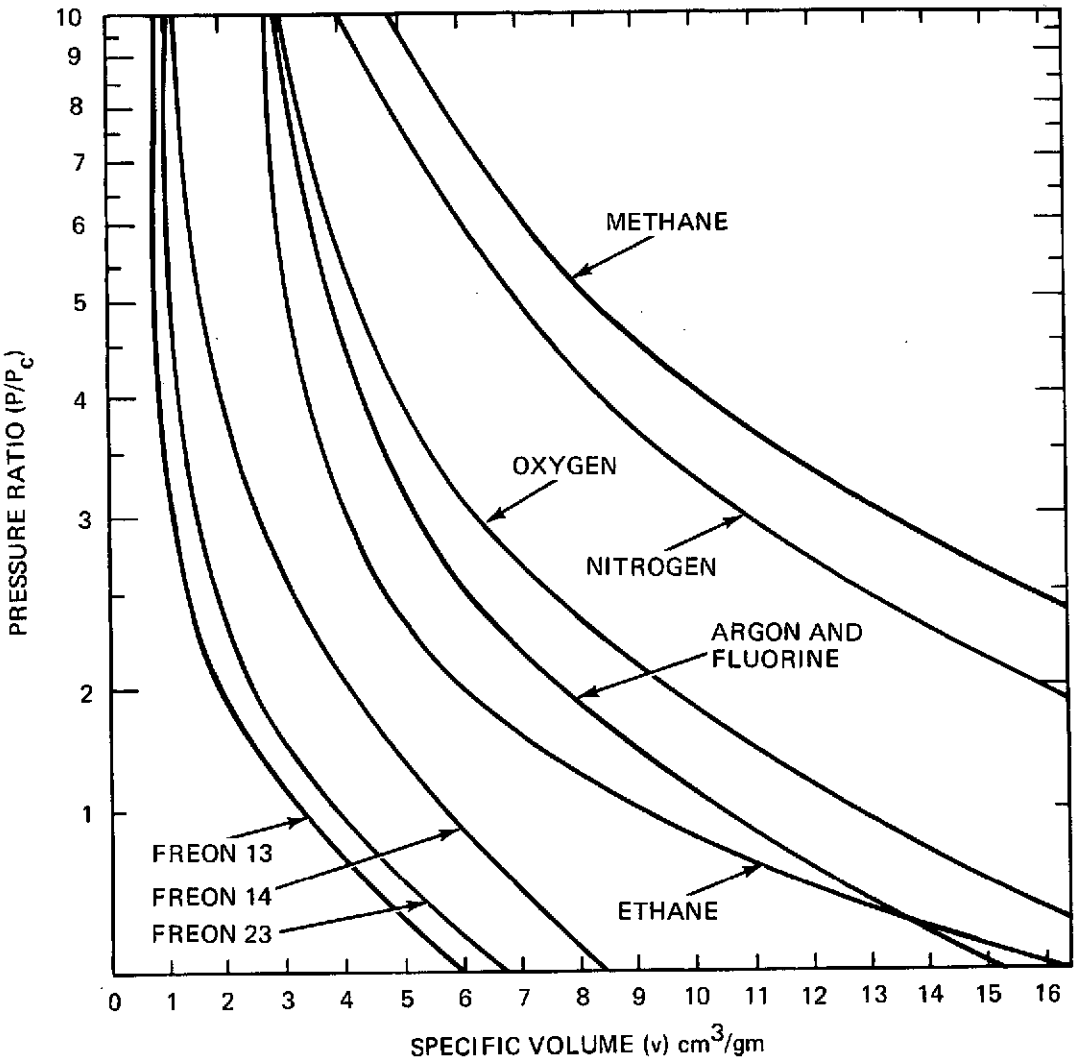

Figure 6-10 Pressure Ratio for 344°K (160°F)

6.2 SELECTION OF DIODE BLOCKAGE

Prior to the selection of diode shutoff technique, an evaluation illustrating the effect of pipe diameter and fluids for the liquid trap, blocking orifice, and concentric artery liquid blockage techniques was performed. The pipe geometry and pertinent information are listed in Table 6-1.

The evaluations were performed for 1-g performance with the pipe in a level attitude for both forward- and reverse-mode operation. Artery outside diameter is .163 cm (.064 in.) greater than tunnel diameter for all cases.

Table 6-1 Pipe Geometry for Parametrics

Pipe Parameter	Dimension
Evaporator Length	10.16 cm (4.0 in.)
Transport Length	50.8 cm (20.0 in.)
Condenser Length	30.48 cm (12.0 in.)
Effective Length	71.12 cm (28.0 in.)
Web Thickness	.083 cm (.0328 in.)
Web Number	6.0 (evaporator and condenser only)
Pipe Outside Diameter	.635, .953, 1.27 cm (.25, .375, .50 in.)
Pipe Wall Thickness	.071 cm (.028 in.)
Wick Pore Size	38.1 microns (.0015 in.)
Fluids	Methane, Freon 14, Ethane
Pipe and Wick Material	Type 304 Stainless Steel, 1/8 Hard

The parametric results for the various blocking techniques are shown in Figures 6-11 through 6-27. Each figure presents the variation of maximum heat throughput, reservoir volume, and shutdown energy plotted against artery tunnel diameter for several pipe outside diameters. The solid lines, except where noted on these figures, represent liquid trap blockage and the dashed lines portray the blocking orifice technique. For the concentric artery blockage, the above parameters are plotted against pipe outside diameter. In addition, two other parameters are considered: vapor space annular thickness required for blockage and total liquid blocked length. All figures indicate fluid, pipe attitudes, and forward- and reverse-mode temperatures.

The cases for methane (Figures 6-11 through 6-14) illustrate that for increasing pipe outside diameters, maximum throughput increases, then decreases with increasing artery tunnel diameter. For a given pipe outside diameter, small tunnel diameters result in high artery liquid flow pressure losses, thus reducing the maximum throughput. The vapor pressure loss becomes the dominant term for large tunnel diameters, again reducing the maximum throughput.

For equal artery and pipe diameters, higher throughput is obtained with liquid trap compared with blocking orifice with the difference representing the blocking orifice pressure loss. The blocking orifice height is largely independent of pipe

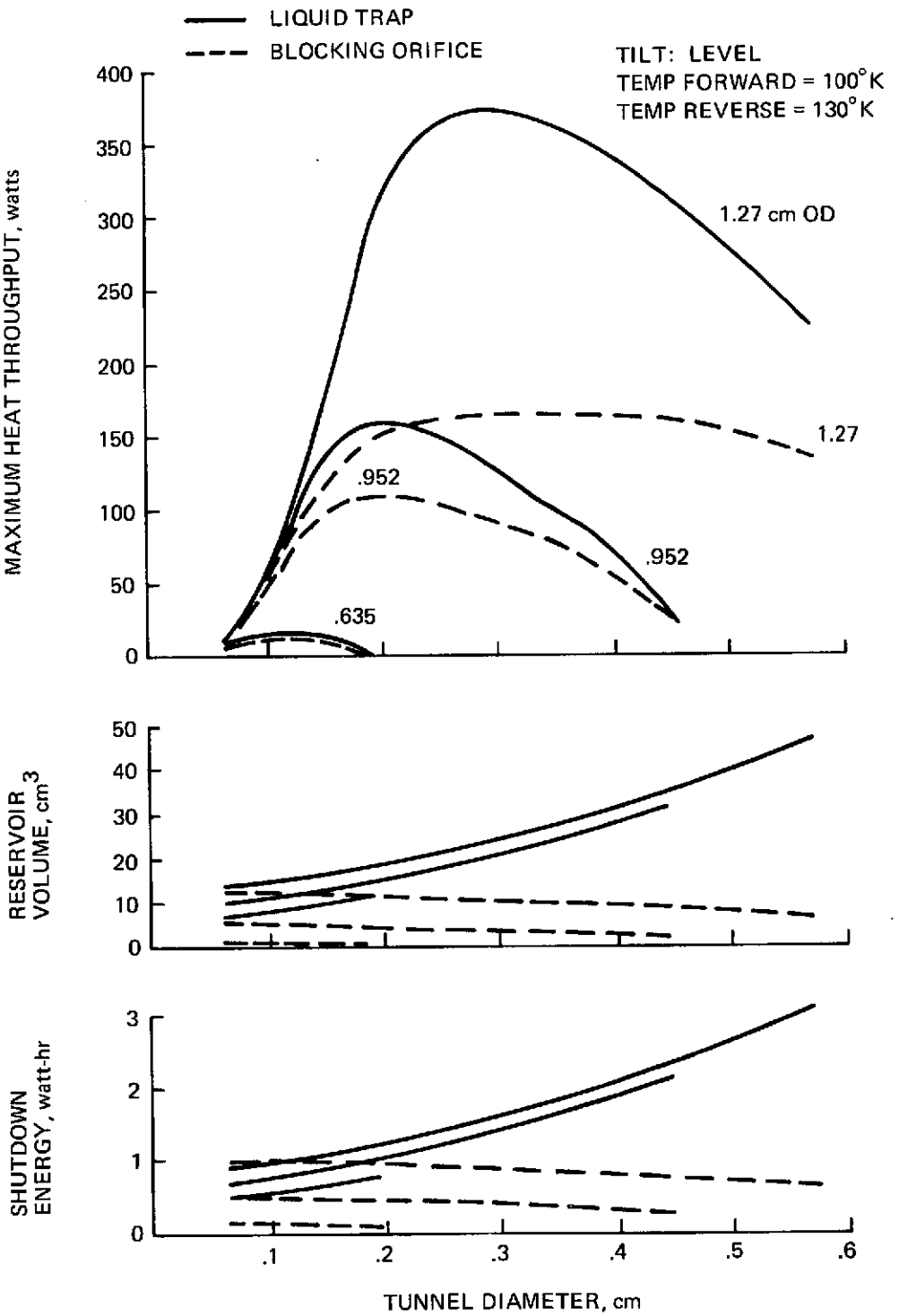

Figure 6-11 Diode Performance, Methane

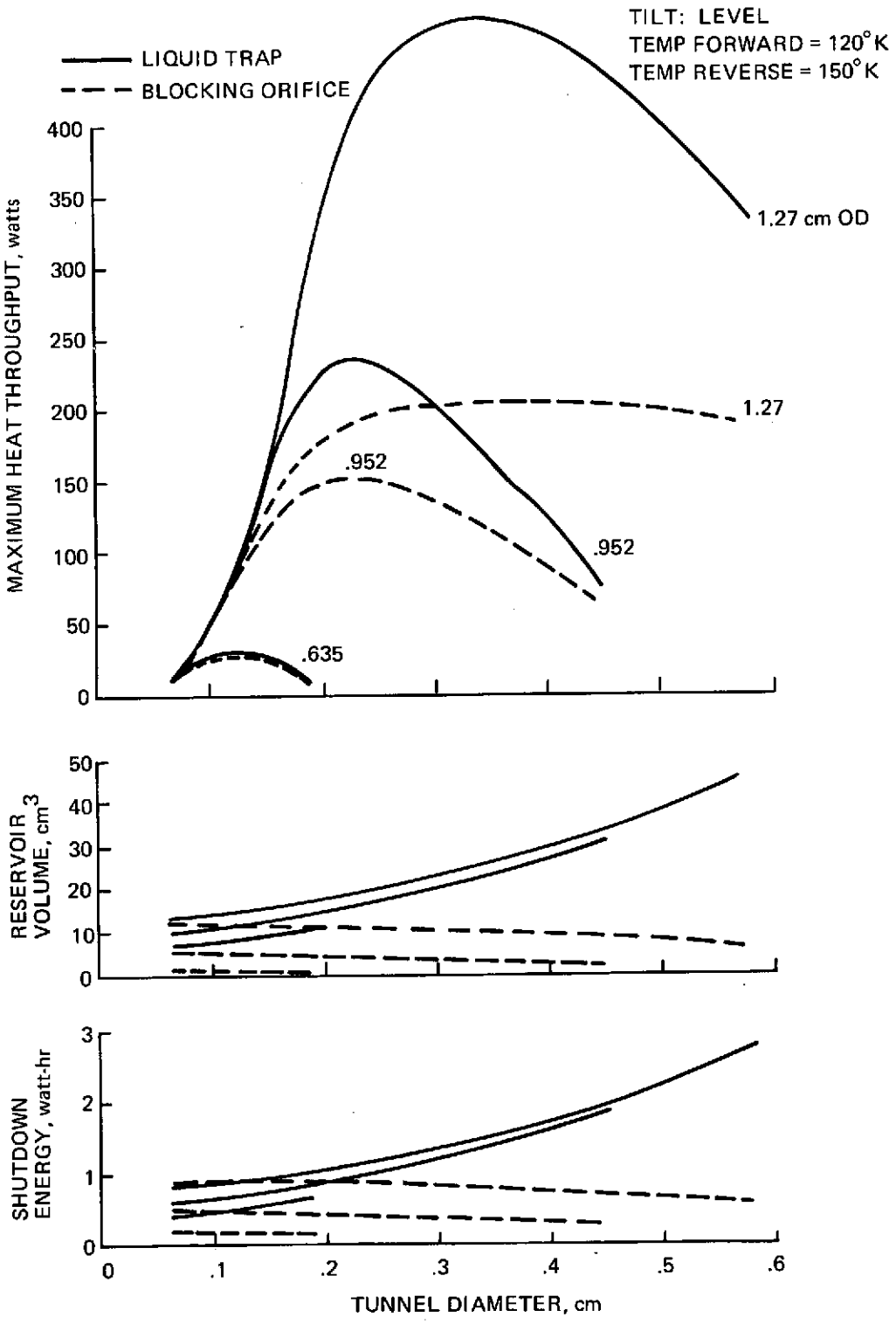

Figure 6-12 Diode Performance, Methane

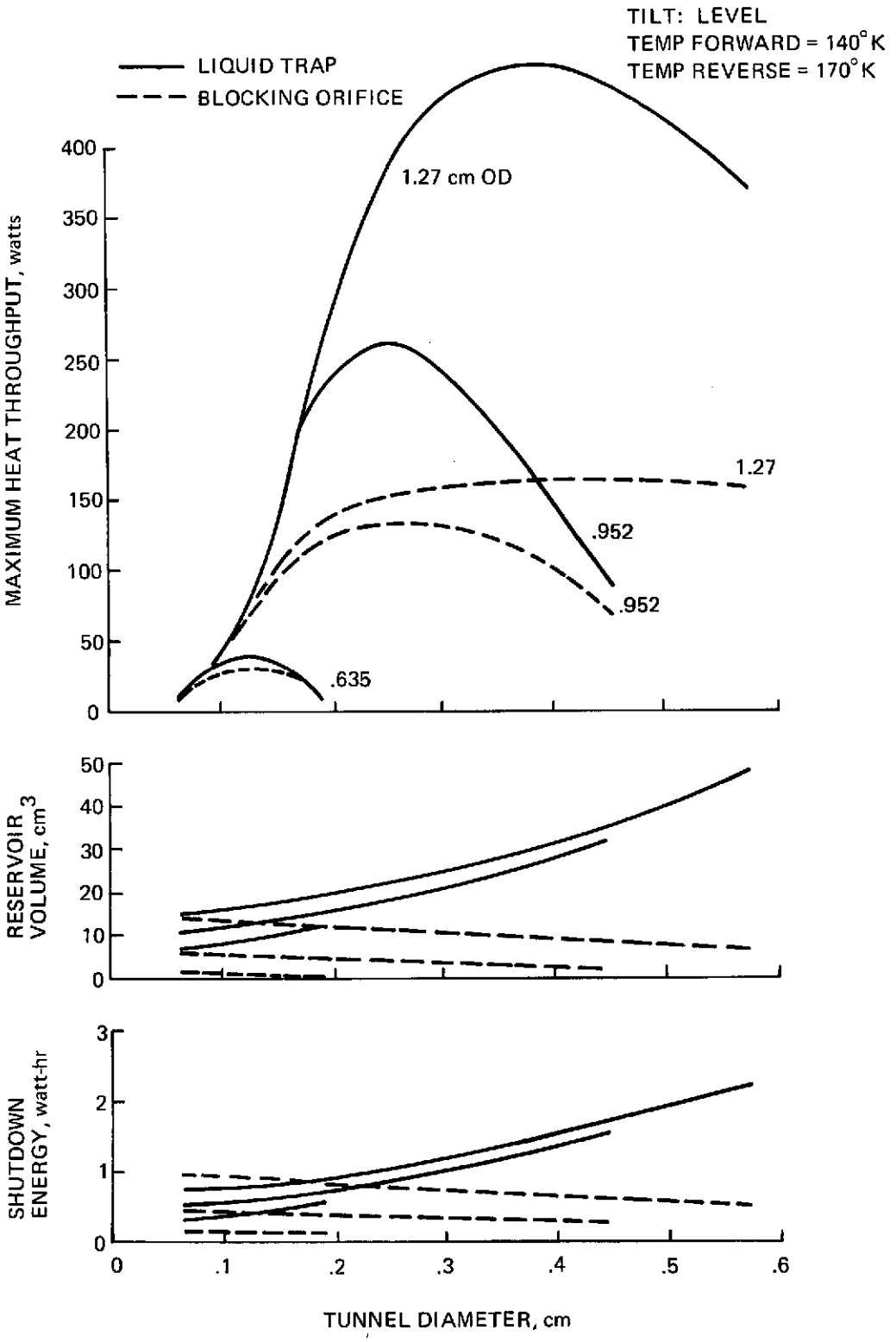

Figure 6-13 Diode Performance, Methane

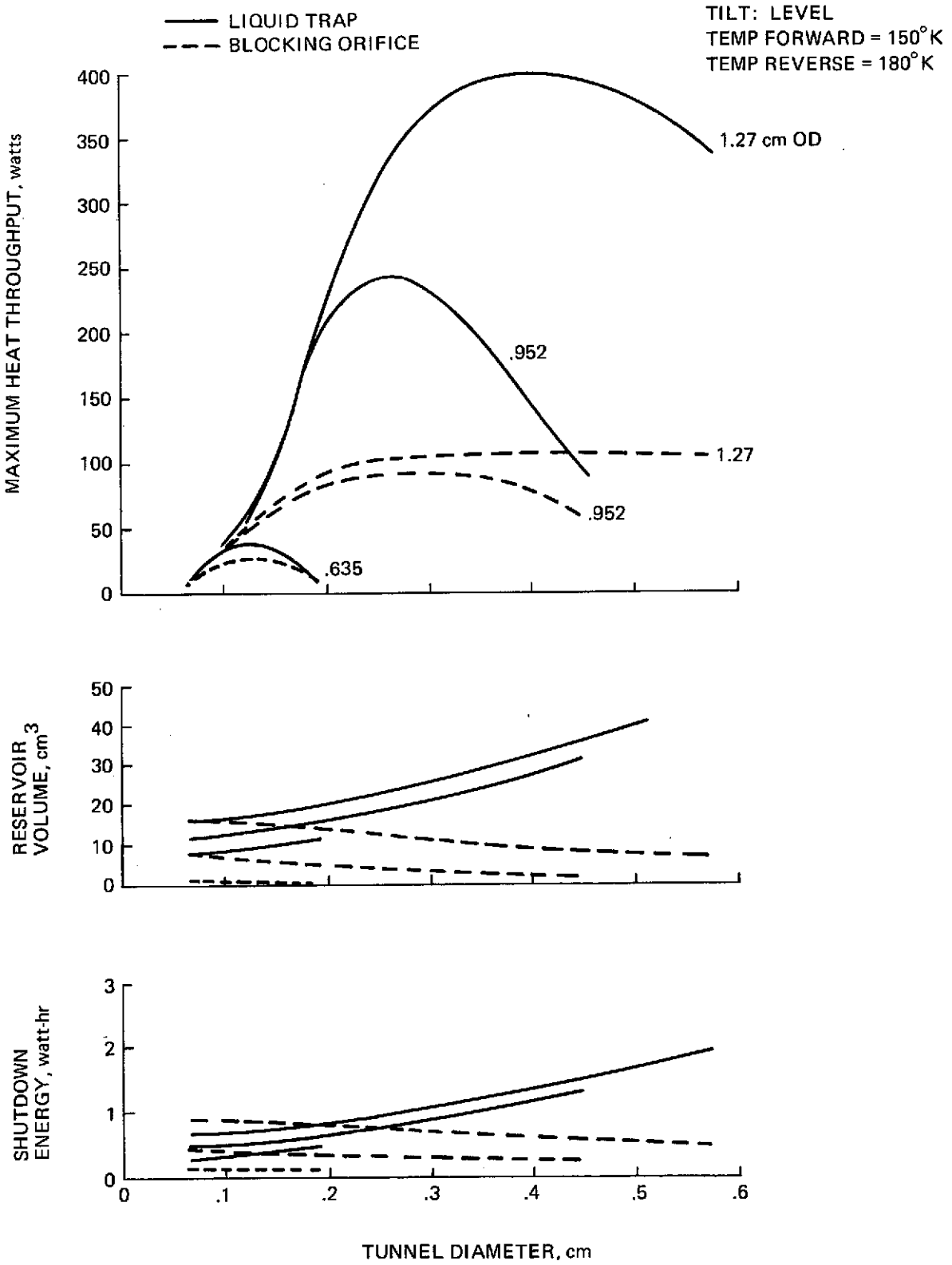

Figure 6-14 Diode Performance, Methane

diameter. As pipe diameter increases, the vapor passage and artery flow resistance tends to decrease much faster then the orifice flow resistance. Hence, the orifice loss becomes relatively more significant at large diameters. This can be seen by comparing maximum throughput for different ODs. The difference in maximum throughput for blocking orifice and liquid trap is negligible at .635 cm (.25 in.) OD and quite substantial at 1.27 cm (.50 in.) OD.

From the plots of reservoir volume and shutdown energy, the blocking orifice requires considerably less reservoir volume and shutdown energy. Shutdown energy is defined here as the energy required for transition from the forward-mode to the reverse-mode plus the reverse-mode heat leakage for 1 hr. Shutdown energy does not account for the transmittal of energy due to partial heat pipe operation during this transition period.

As shown in Figures 6-11 through 6-14, maximum throughput increases as forward mode temperature increases, then decreases. This behavior is attributed partly to the fluid's liquid transport factor and partly to the increasing vapor pressure. The percentage decrease for the blocking orifice technique is seen to be greater with increasing forward-mode temperature since the orifice height or vapor passage opening is decreasing, resulting in the orifice pressure drop becoming the dominant loss term (despite the increase in vapor pressure). Increasing the pipe outside diameter from .952 to 1.27 cm (.375 to .500 in.) only produces a slight increase in blocking orifice throughput whereas the liquid trap increase is considerable (see Figure 6-14).

In addition to the parameters plotted in Figures 6-11 through 6-14, another important parameter of interest is the pipe pressure under ambient conditions. For a constant outside diameter envelope and given artery geometry, the highest specific volume is obtained with the liquid trap technique, resulting in lower pipe pressures. Also, because of lower pressures, the pipe wall thickness can be reduced with a corresponding reduction in shutdown energy. Although the amount of reverse-mode heat leakage under steady state conditions is small for liquid trap blockage, the reduction in the shutdown energy, plotted in Figures 6-11 through 6-14, will not approach the magnitudes plotted for the blocking orifice technique. The liquid trap amount is primarily due to the energy required to evaporate all of the normal working fluid, hence as tunnel diameter increases, shutdown energy increases accordingly, as shown.

Single outside diameter concentric artery blockage results are plotted in Figure 6-15 for methane. Maximum throughput is reduced from the previous two techniques due to narrow vapor space requirements necessary to retain liquid for proper reverse-mode blockage in ground testing. For the outside diameters studied, the vapor space pressure drop is the dominant loss term. The maximum permissible annular height of the vapor space decreases with increasing pipe diameter and increasing reverse-mode temperature, as shown. For an annulus without webs, vapor pressure loss is inverse with the cube of vapor annulus height, and throughput would decrease with increasing diameter and temperature. The presence of the webs reduces this effect, and can cause a reversal as shown in Figure 6-15A. The .635 cm (.25 in.) outside diameter case shows low Q_{max} values at 100°K (-280°F) primarily because the calculations were done with six relatively thick webs, i.e., .083 cm (.033 in.) for all cases, reducing the vapor passage area severely. The use of a larger outside diameter in the unblocked region to open up the vapor space is discussed on page 6-40.

Reservoir volumes and shutdown energy, because of the narrow vapor space, are somewhat less than for the blocking orifice technique. Both parameters increase with pipe outside diameter and decrease with an increase in reverse-mode temperature. Figure 6-15B shows reservoir volume increasing to a maximum then decreasing with an increase in pipe outside diameter. This small reservoir volume at .635 cm (.25 in.) is due to the relatively large web liquid volume which is less important at larger diameters.

Liquid blocked length, as shown, increases with pipe outside diameter and increasing reverse-mode temperature. This length is inverse with the vapor space areas in the unblocked portions of the pipe. For all the cases studied, the minimum blocked length is specified as the evaporator length plus 5.08 cm (2.0 in.) of the transport section. The amount of excess liquid required for shutoff is compared to the steady state reverse-mode requirements. If this excess produces a blocked length greater than initially specified, the blocked length is adjusted accordingly up to a maximum equal to the total pipe length. A blocked length greater than pipe length results in a system whereby the liquid is in a compressed state in the reversal mode. This is shown in Figure 6-15B and C when the blocked length remains constant [maximum of 91.4 cm (36.0 in.)] for an increase in pipe outside diameter.

The specific volumes associated with single outside diameter concentric artery blockage are the lowest of the techniques studied. Consequently, the pipe pressure under ambient conditions is the highest. Based on the pressures obtained and taking

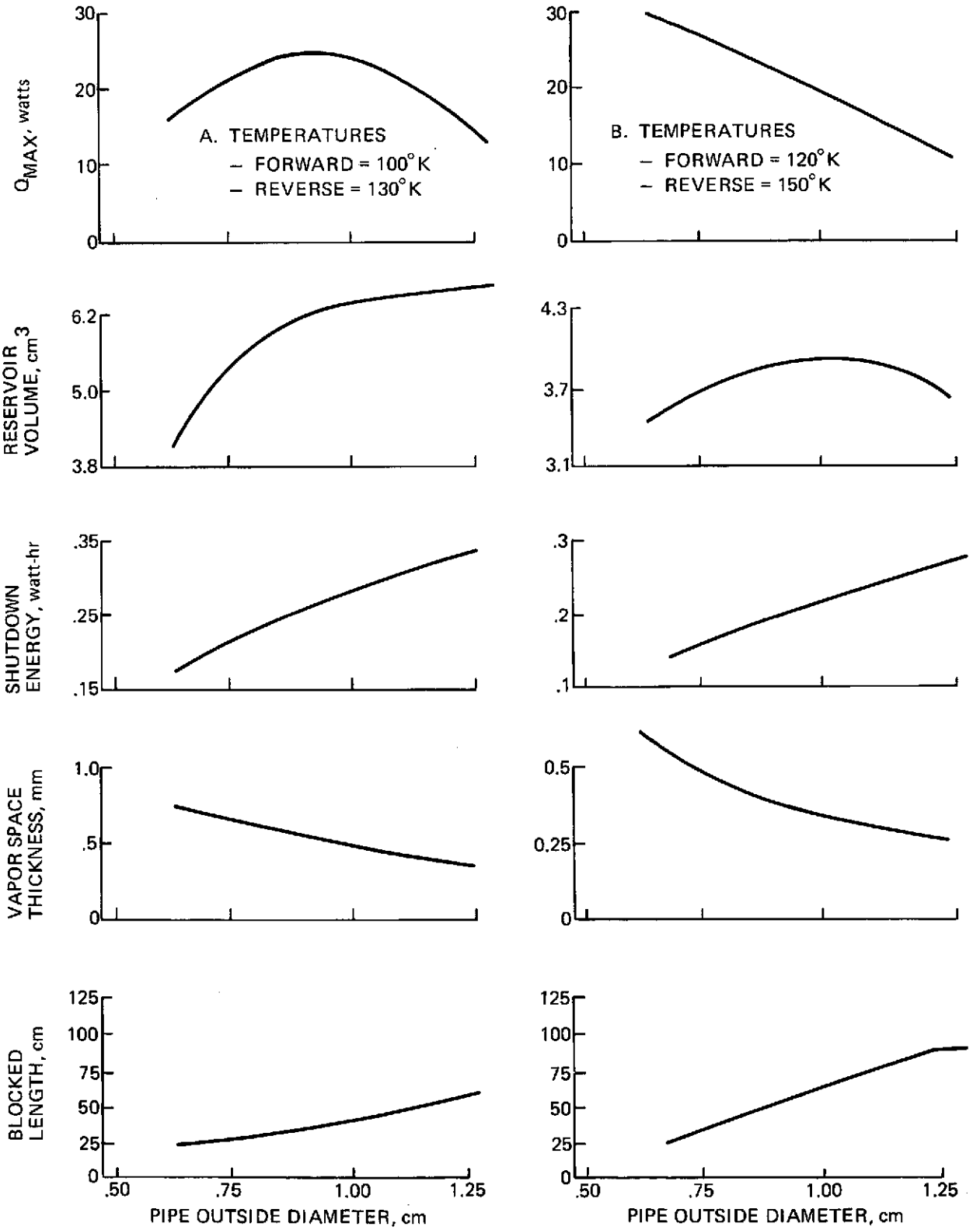

Figure 6-15 Concentric Artery Blockage Performance of Methane in a Level Heat Pipe (Sheet 1 of 2)

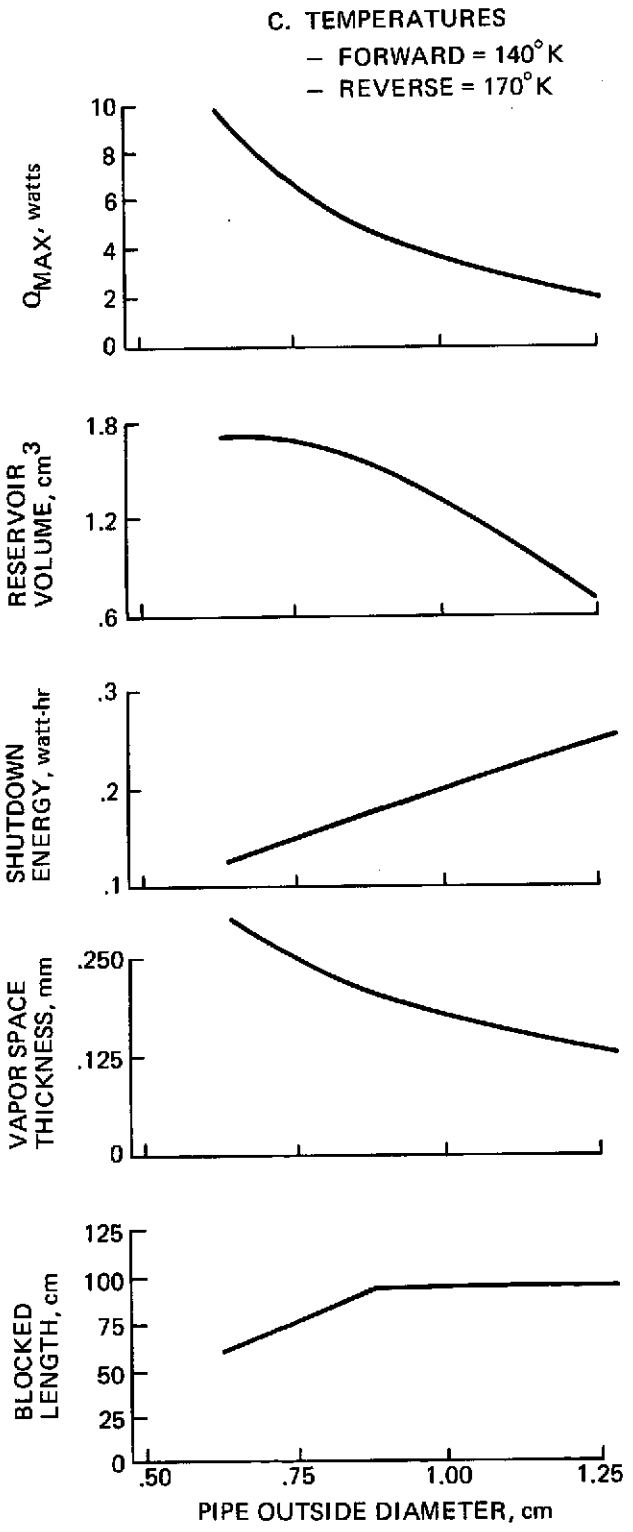

Figure 6-15 Concentric Artery Blockage Performance of Methane in a Level Heat Pipe (Sheet 2 of 2)

an allowable stress of 1.38×10^8 Nm^{-2} (20,000 psi), the wall thickness requirements for the .635 cm (.25 in.) outside diameter pipes are satisfactory but must be increased to over .381 cm (.150 in.) for an outside diameter of 1.27 cm (.500 in.). Obviously, going to a design whereby a stepped outside diameter is employed, as in the ATFE diode, retaining the smaller diameter associated with the blocked portions of the pipe will increase the pipe's specific volume, consequently reducing the pipe pressure under ambient conditions.

Performance characteristics with Freon-14 for the blocking techniques studied are shown in Figures 6-16 through 6-20. These evaluations were performed with the identical pipe geometries previously used with methane.

The comparison of the .635 cm (.25 in.) OD case at 110°K (-262°F) is not plotted in Figure 6-16 because of the relatively high pressure drop associated with the vapor passages, thus reducing the maximum throughput. Maximum throughput in general, as expected, is lower than that obtained with methane as the working fluid. Reservoir volumes are slightly lower with Freon-14 for equal maximum throughputs and temperature compared with methane, but shutdown energy is higher since Freon-14 has a higher liquid density-latent heat product than methane.

Single-diameter concentric artery results, as shown for the 110°K (-262°F) case were terminated with the .953 cm (.375 in.) OD due to high vapor loss coefficients. This coefficient is inverse to the product of vapor density and vapor space thickness cubed resulting in a high vapor pressure drop. For warmer forward-mode temperatures, the increase in vapor density more than offsets the decrease in vapor space thickness to produce higher values of throughput. Regardless of the pipe OD, the maximum throughputs obtained are very small when compared either to methane concentric artery results or to Freon-14 results for blocking orifice and liquid trap.

The results for blockage comparisons with ethane as the working fluid are presented in Figures 6-21 through 6-27. The curves show trends similar to those for the other fluids. Comparison with Freon-14 at a forward-mode temperature of 150°K (-190°F) and equal maximum throughput shows reservoir volumes and shutdown energies to be similar. Compared to Freon-14, ethane pressures under ambient conditions will be lower.

In terms of fluid comparisons for the single-diameter concentric artery cases at 150°K (-190°F) and 170°K (-154°F), ethane is a far superior fluid than Freon-14

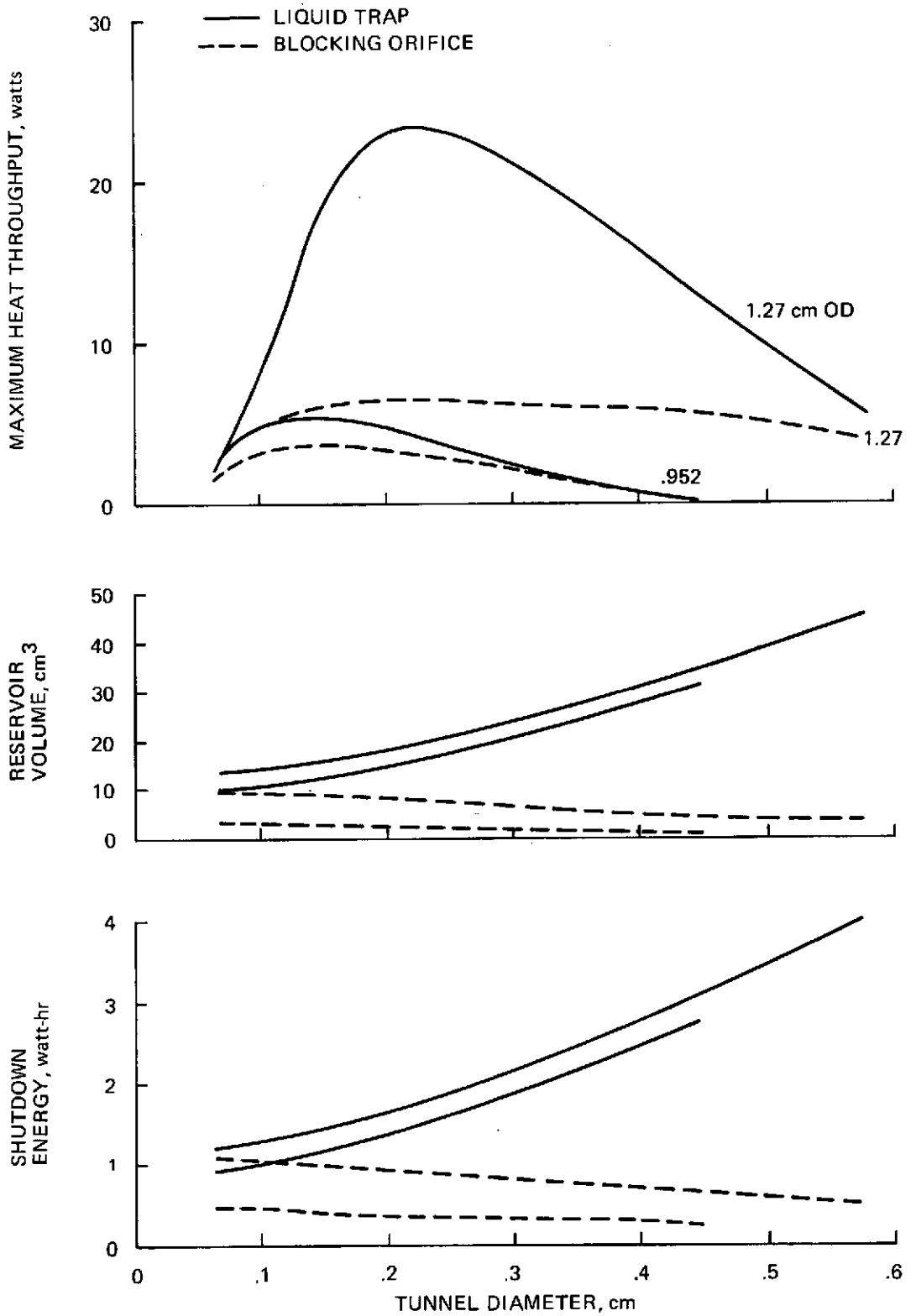

Figure 6-16 Level Diode Performance with Freon-14 (Temperatures: 110°K Forward; 140°K Reverse)

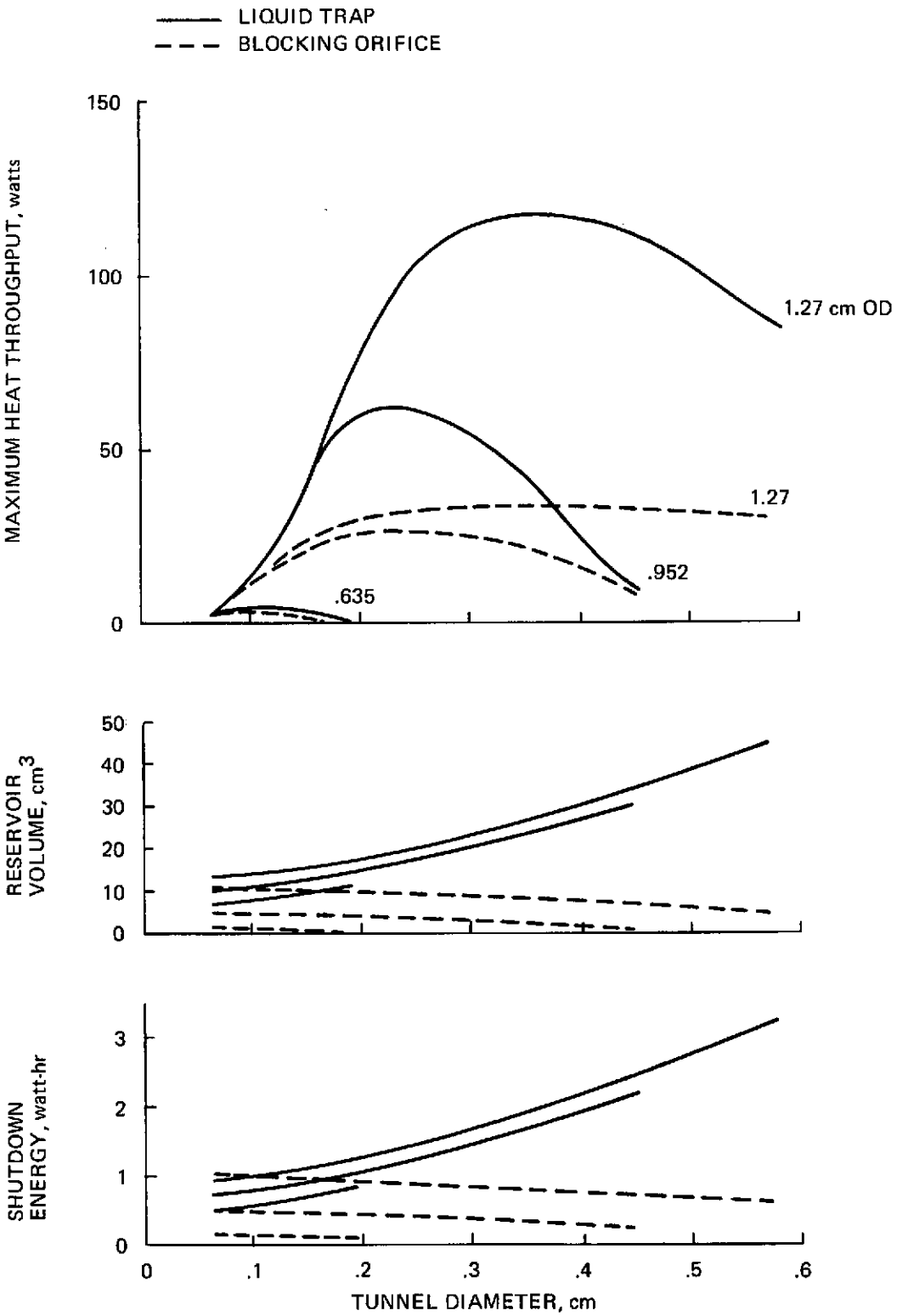

Figure 6-17 Level Diode Performance with Freon-14 (Temperatures: 130° K Forward; 160° K Reverse)

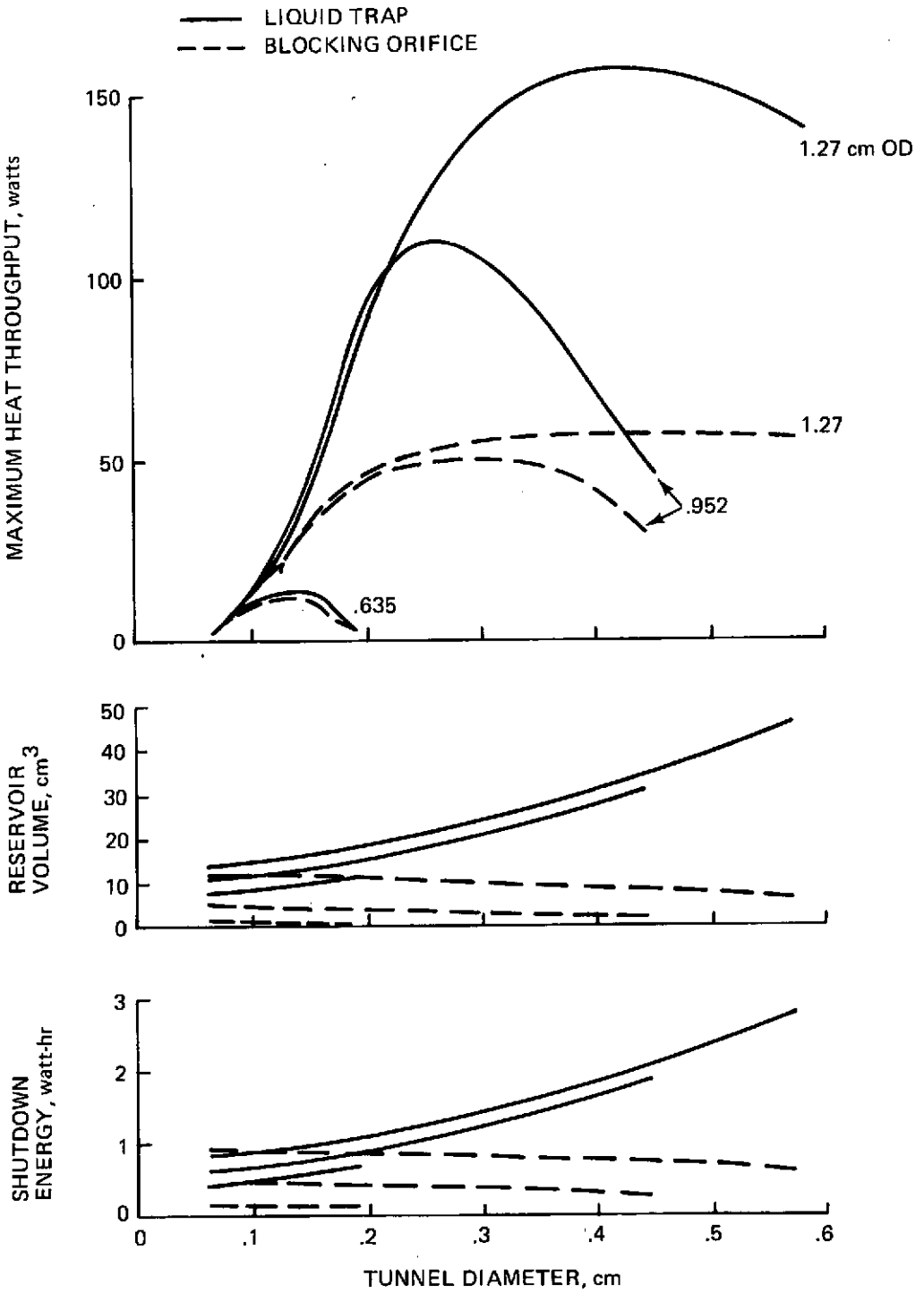

Figure 6-18 Level Diode Performance with Freon-14 (Temperatures: 150° K) Forward; 180° K Reverse)

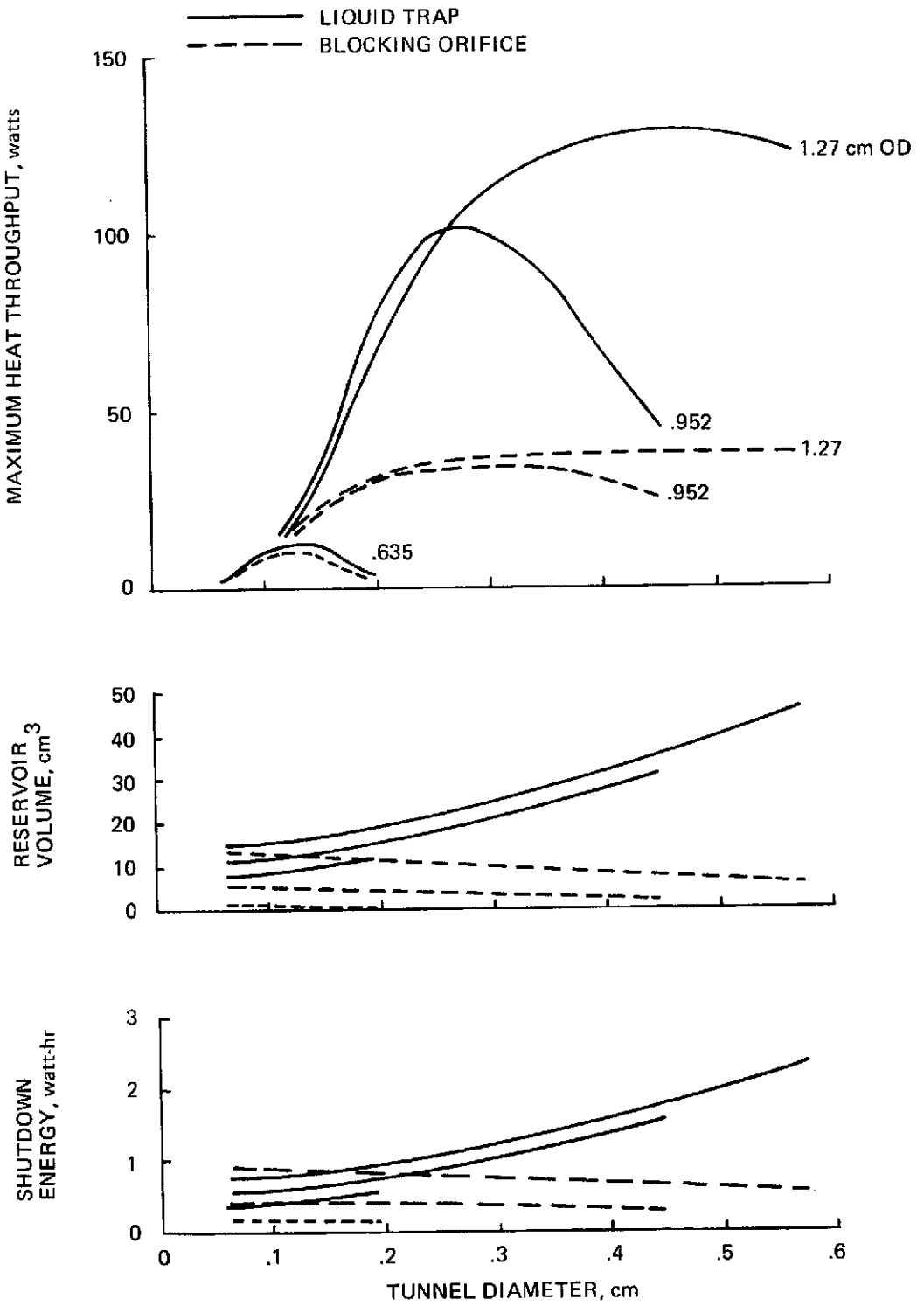

Figure 6-19 Level Diode Performance with Freon-14 (Temperatures: 170° K Forward; 200° K Reverse)

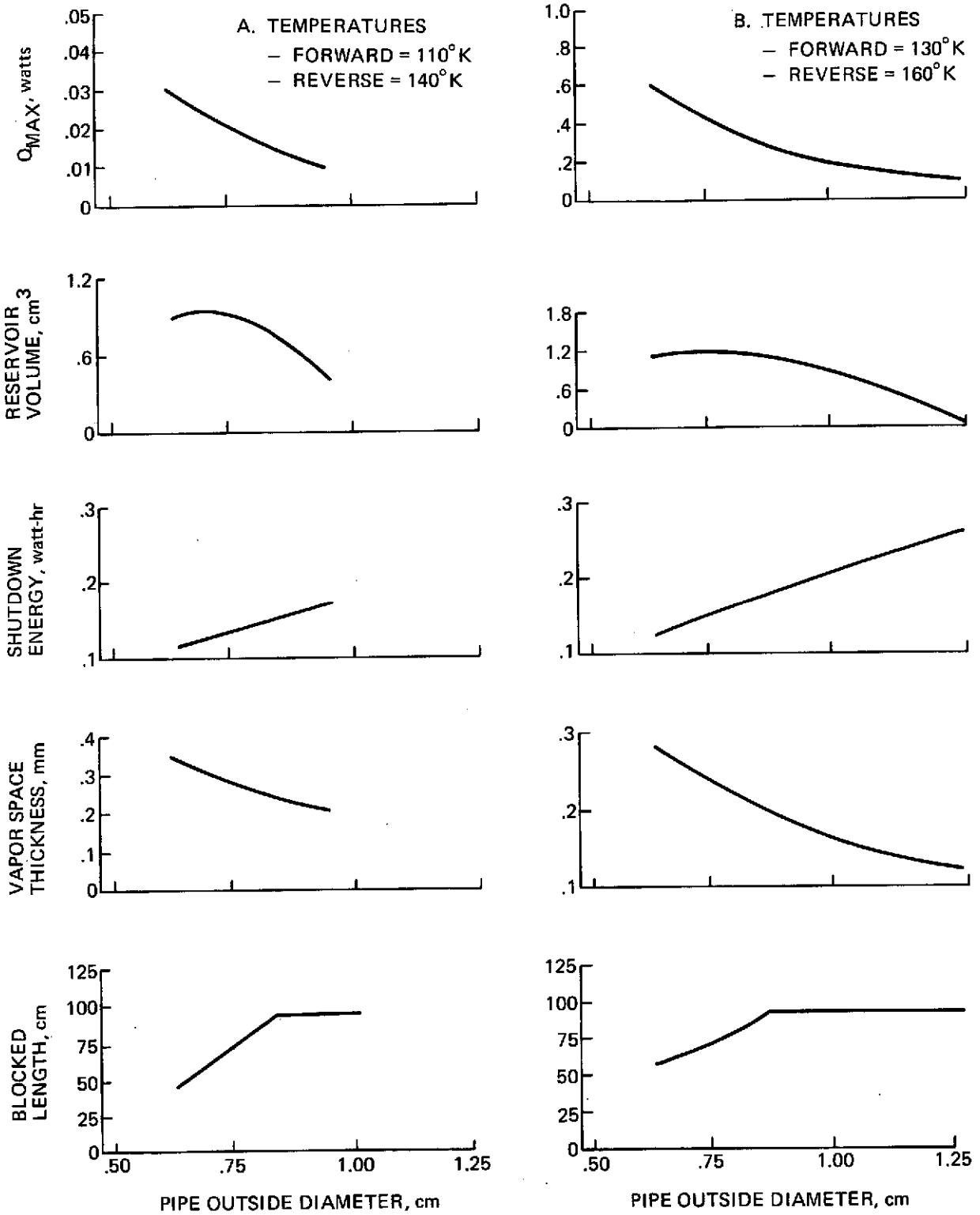

Figure 6-20 Concentric Artery Blockage Performance of Freon-14 in a Level Heat Pipe (Sheet 1 of 2)

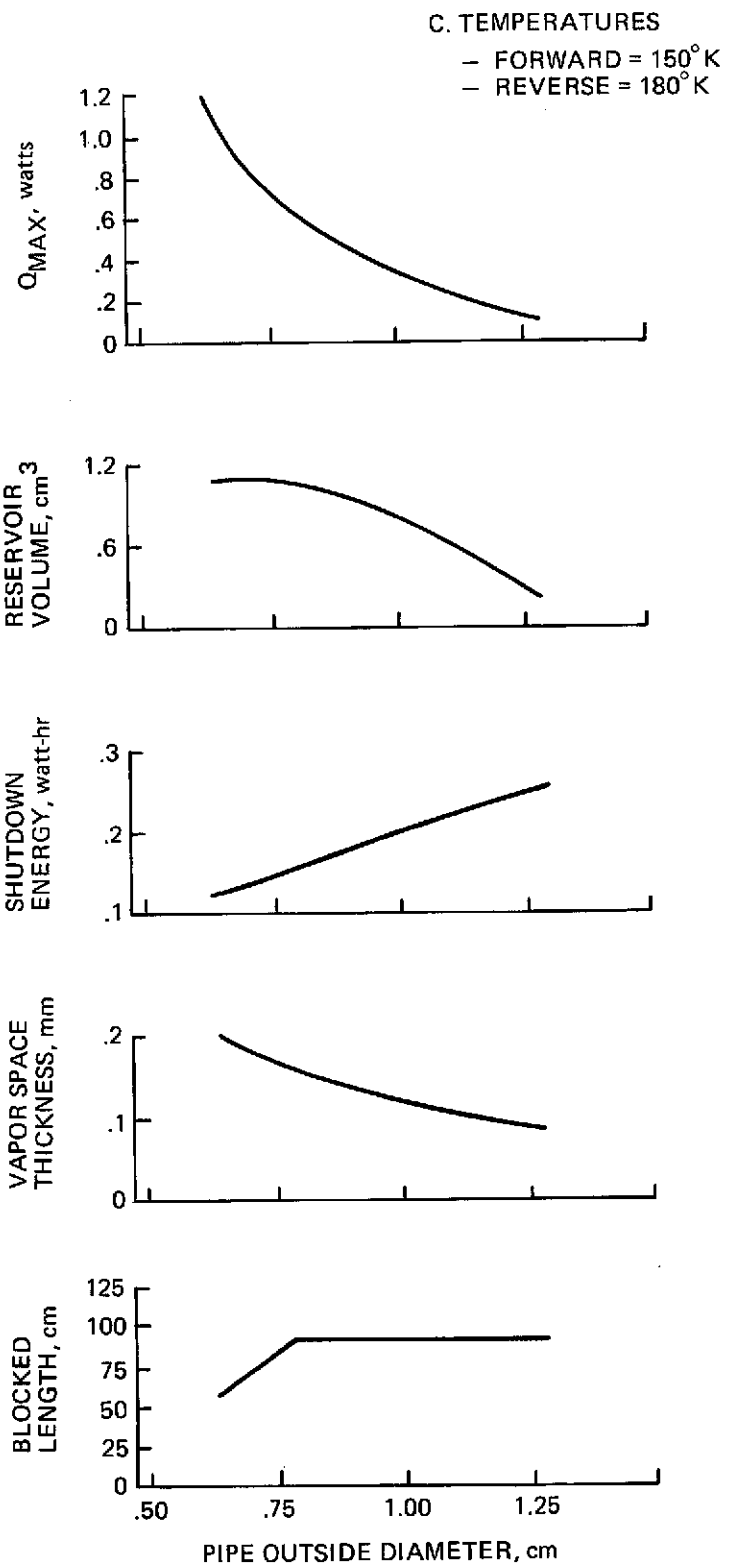

Figure 6-20 Concentric Artery Blockage Performance of Freon-14 in a Level Heat Pipe (Sheet 2 of 2)

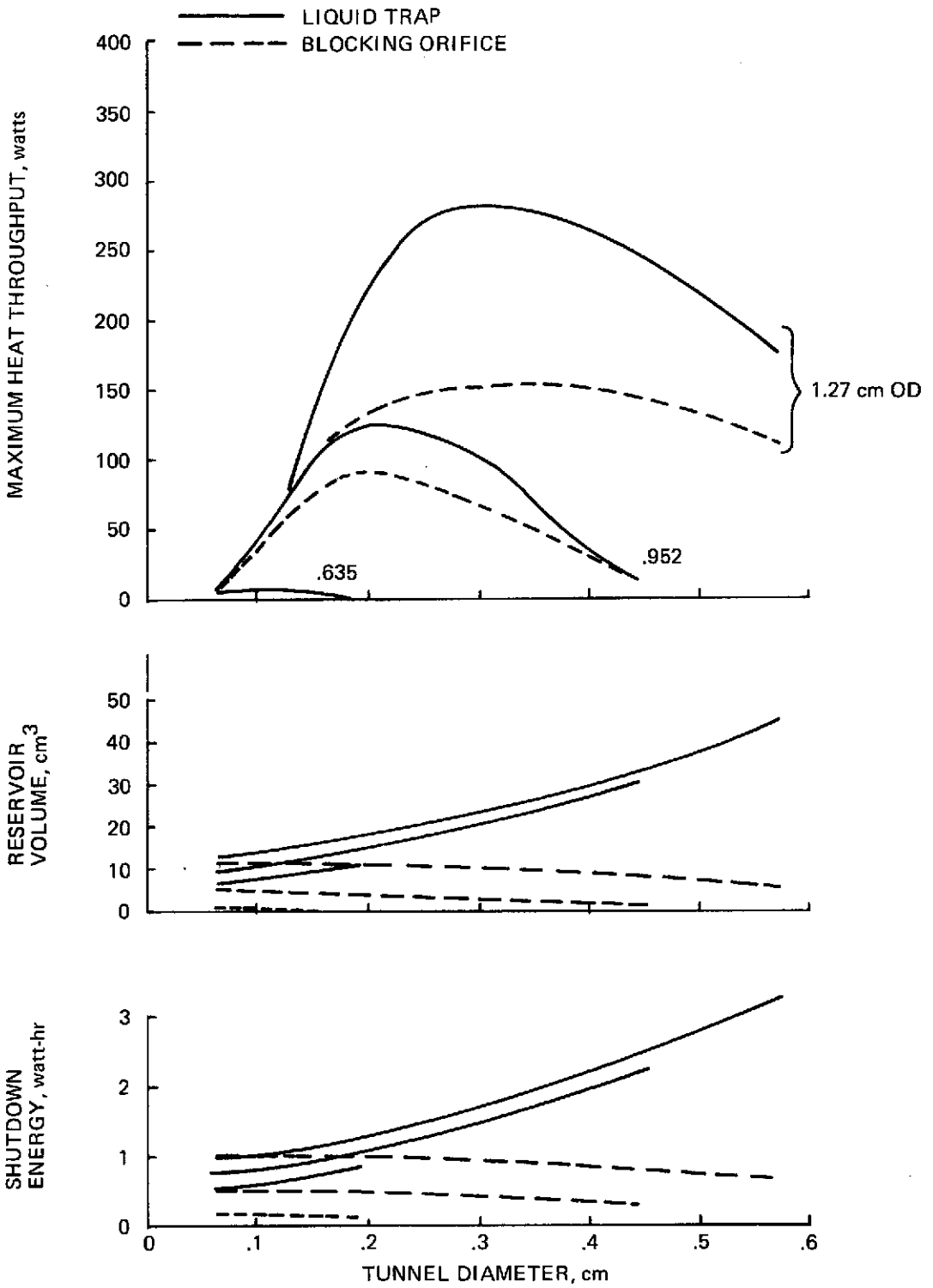

Figure 6-21 Level Diode Performance with Ethane (Temperatures: 150°K Forward; 180°K Reverse)

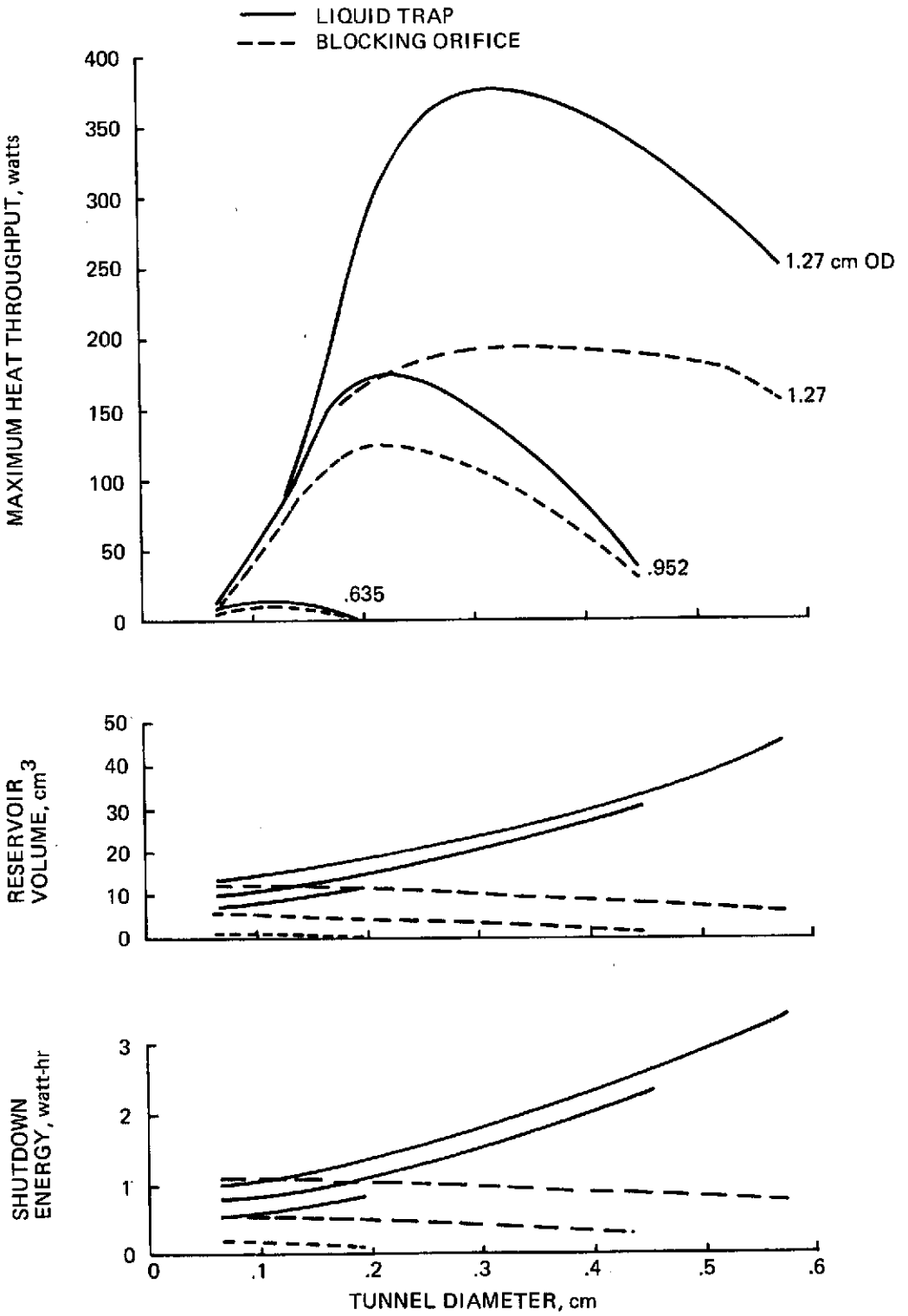

Figure 6-22 Level Diode Performance with Ethane (Temperatures: 170°K Forward; 200°K Reverse)

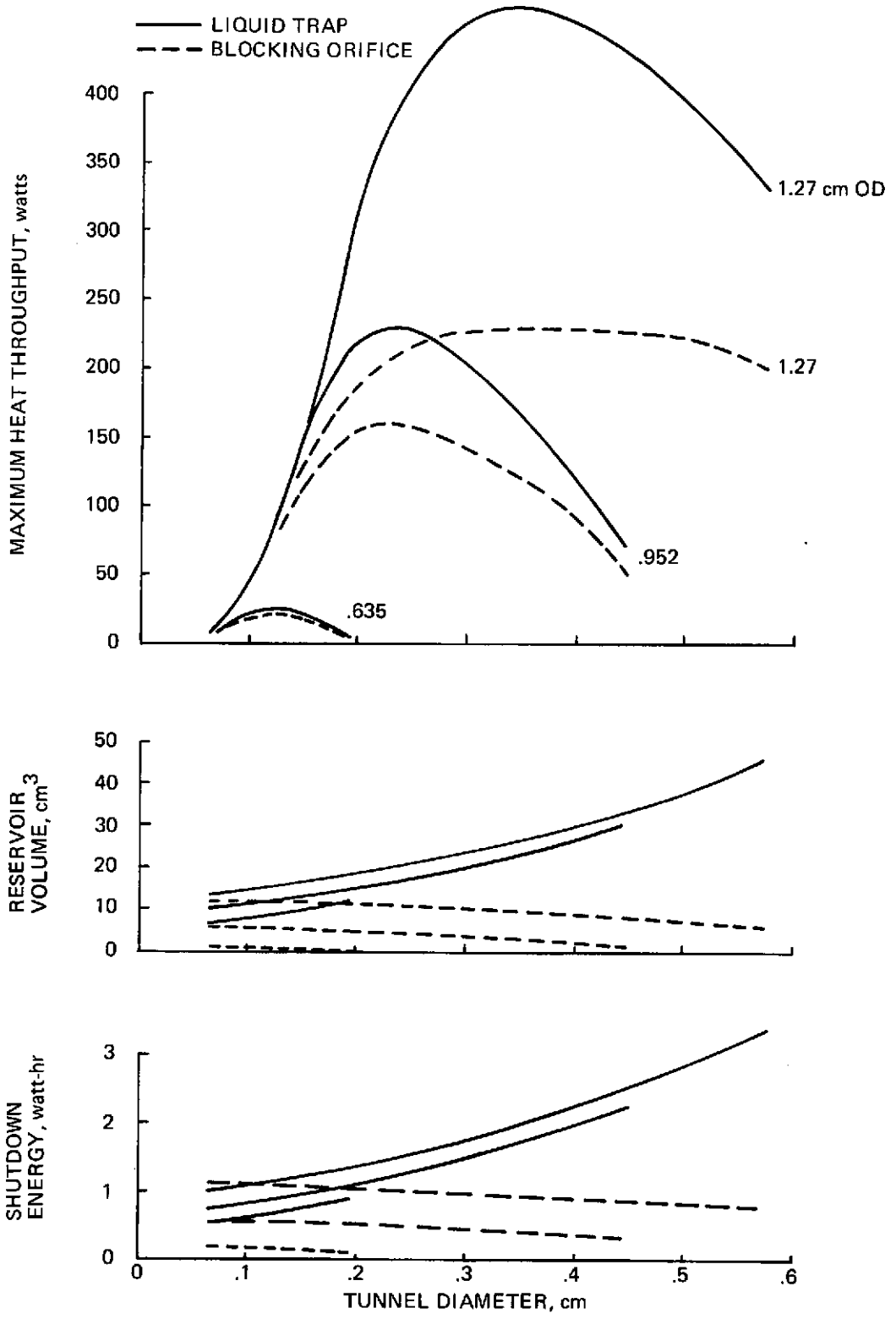

Figure 6-23 Level Diode Performance with Ethane (Temperatures: 190°K Forward; 220°K Reverse)

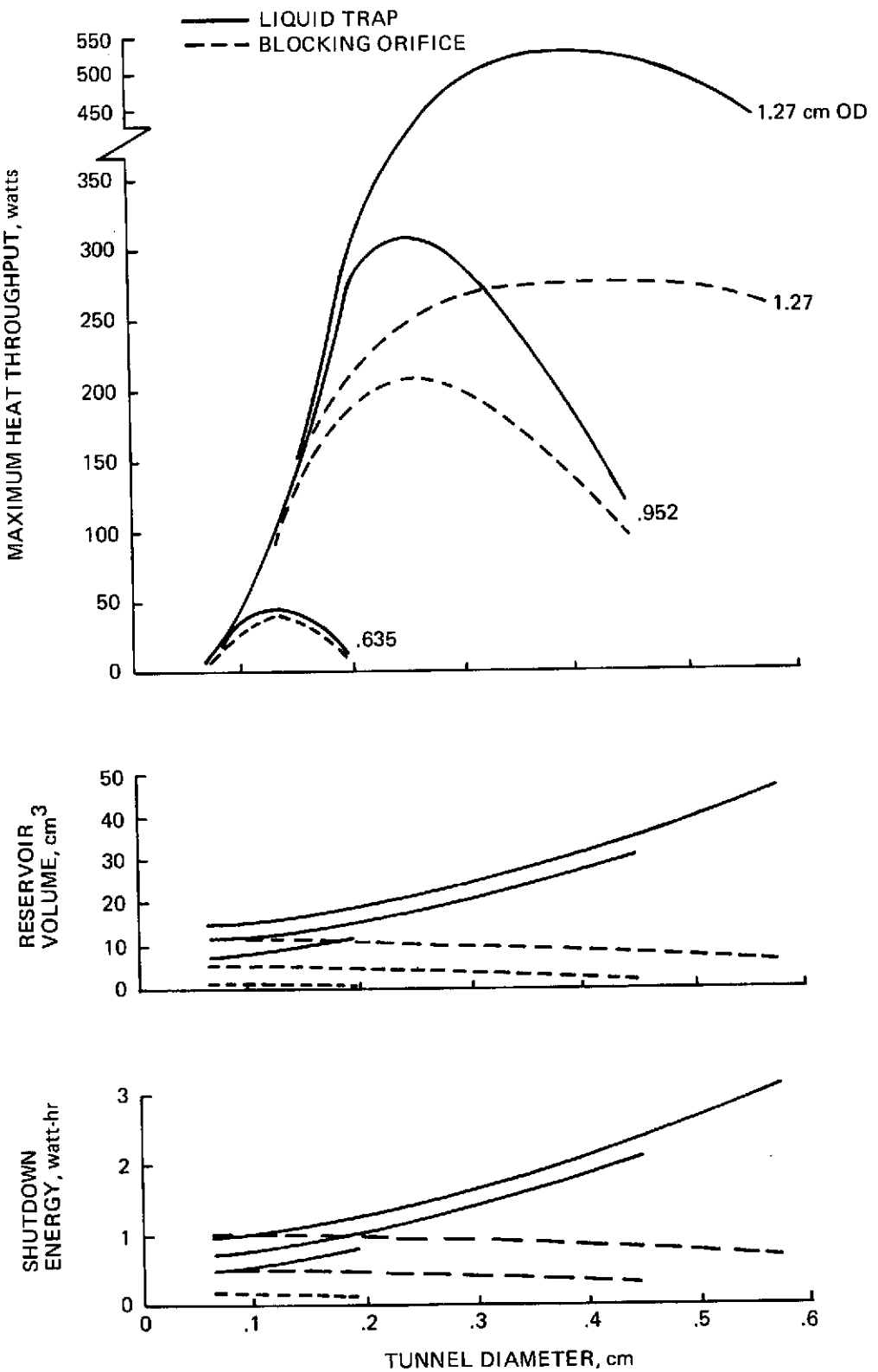

Figure 6-24 Level Diode Performance with Ethane (Temperatures: 210° K Forward; 240° K Reverse)

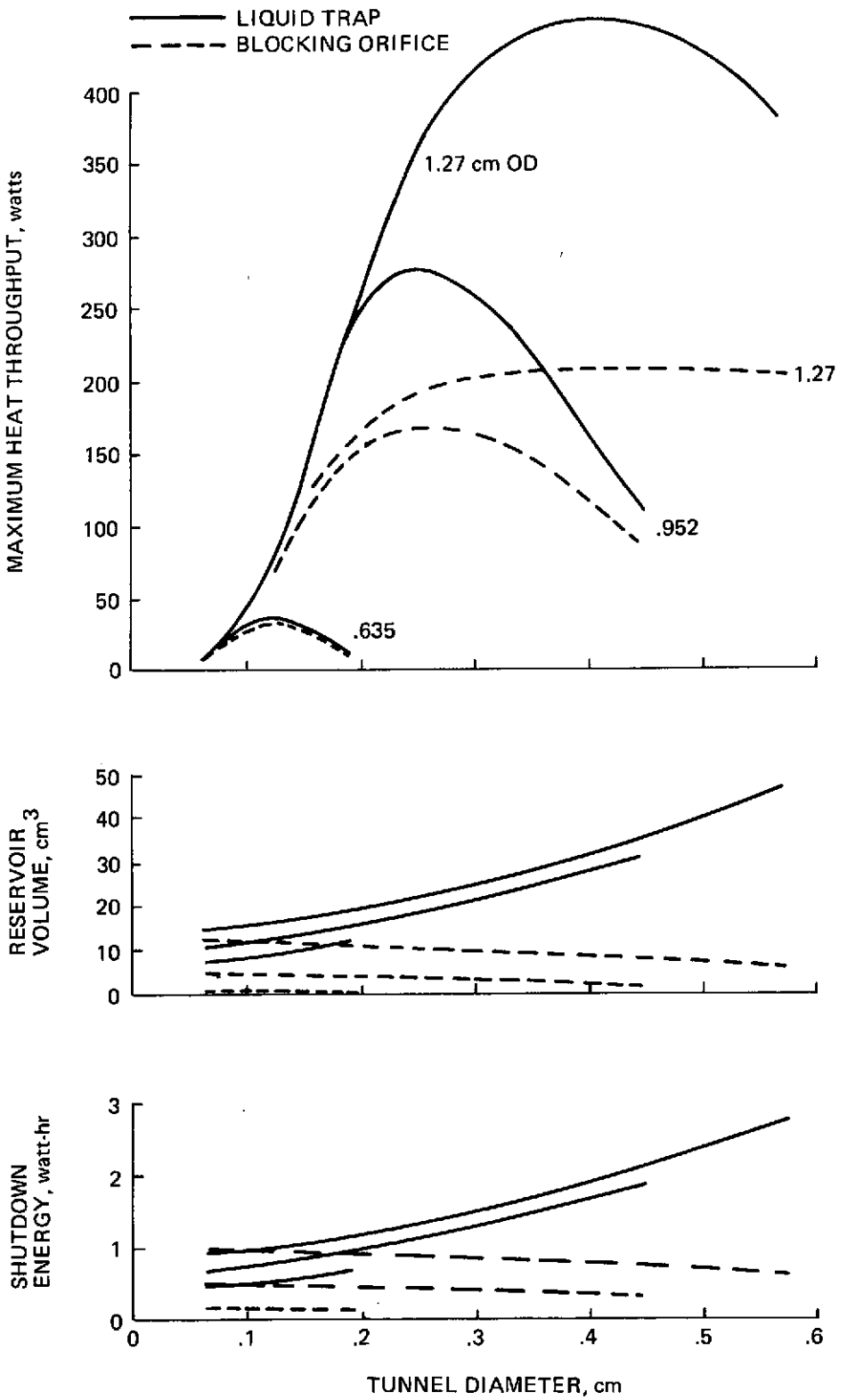

Figure 6-25 Level Diode Performance with Ethane (Temperatures: 230°K Forward; 260°K Reverse)

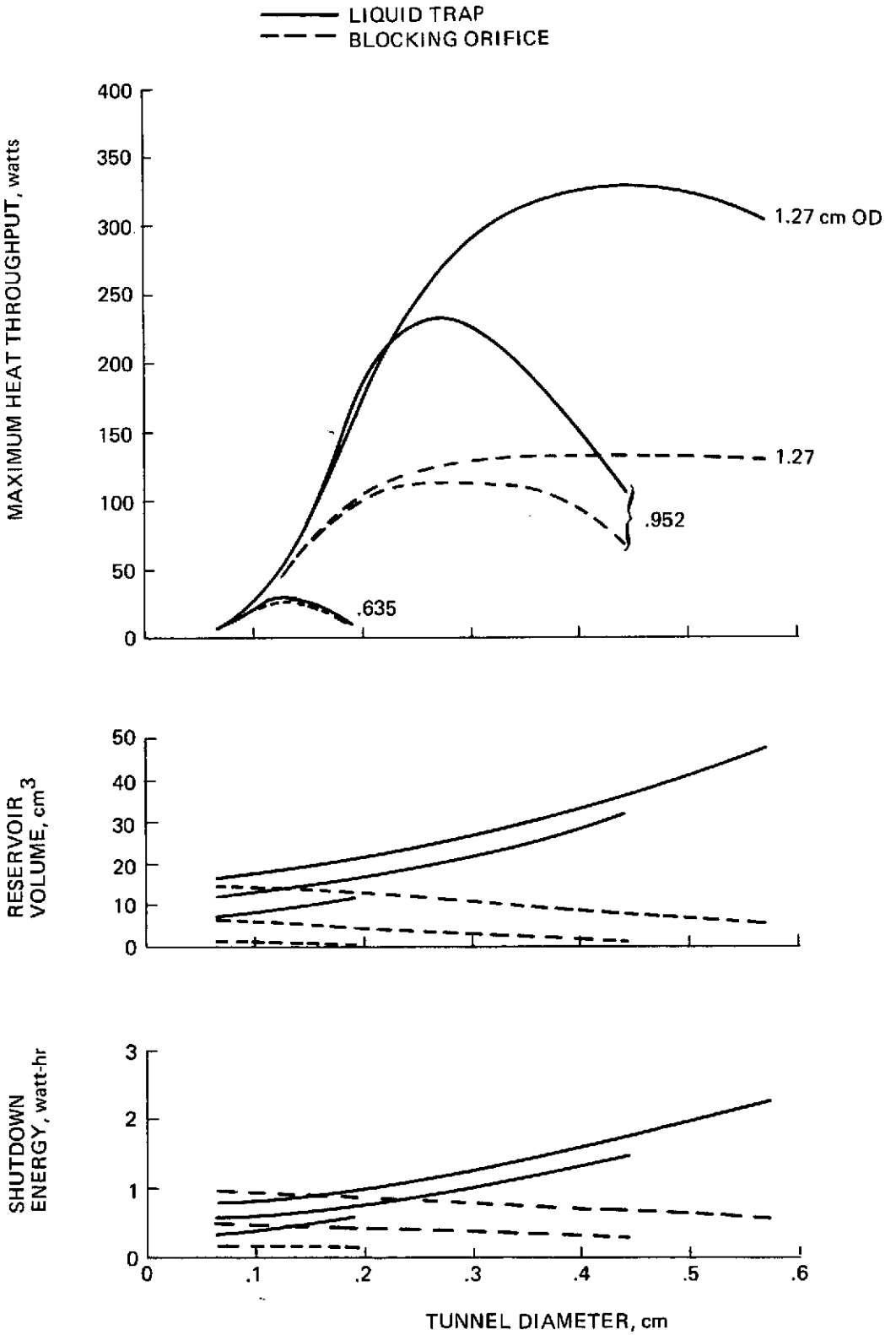

Figure 6-26 Level Diode Performance with Ethane (Temperatures: 250°K Forward; 280°K Reverse)

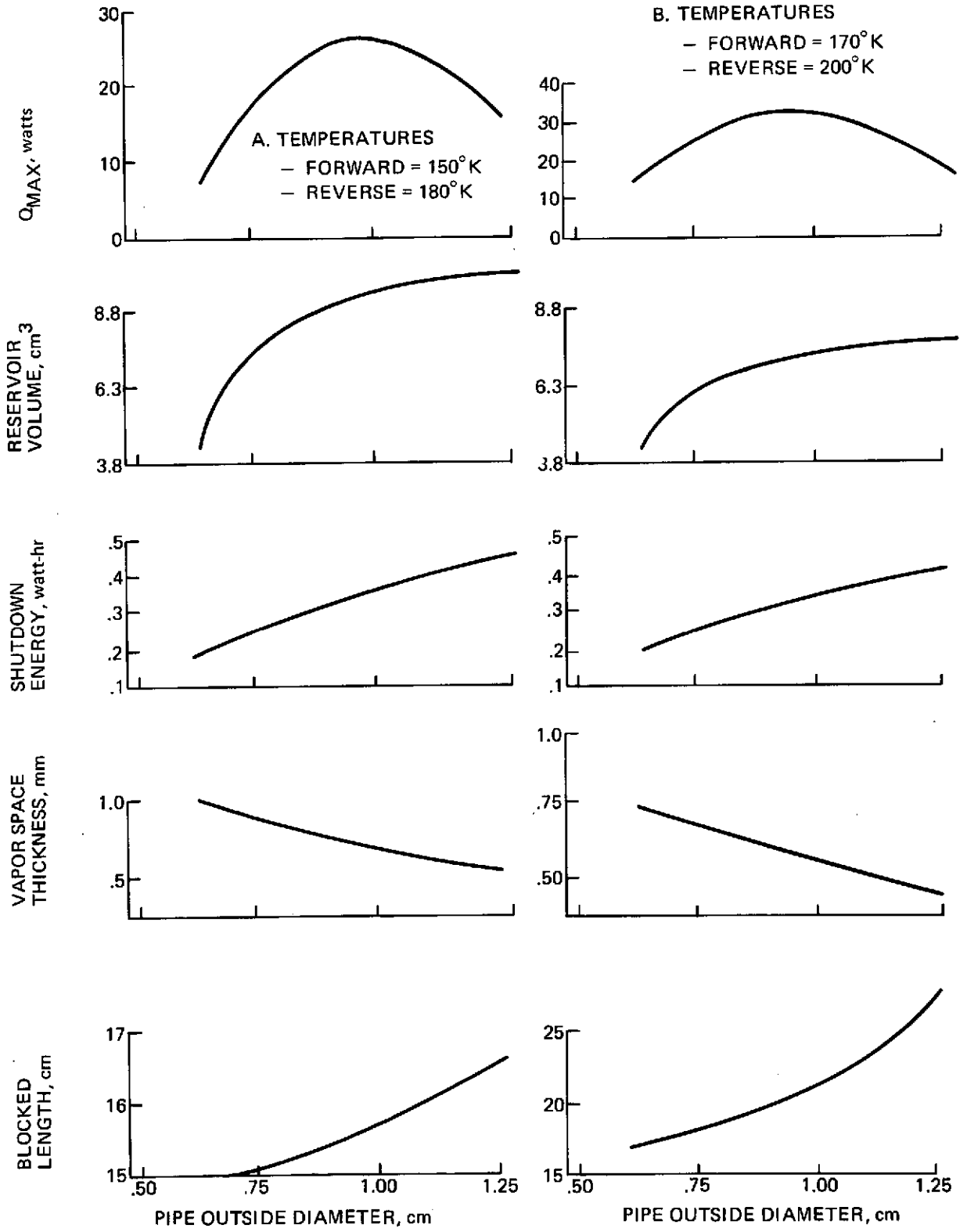

Figure 6-27 Concentric Artery Blockage Performance of Ethane in a Level Heat Pipe (Sheet 1 of 3)

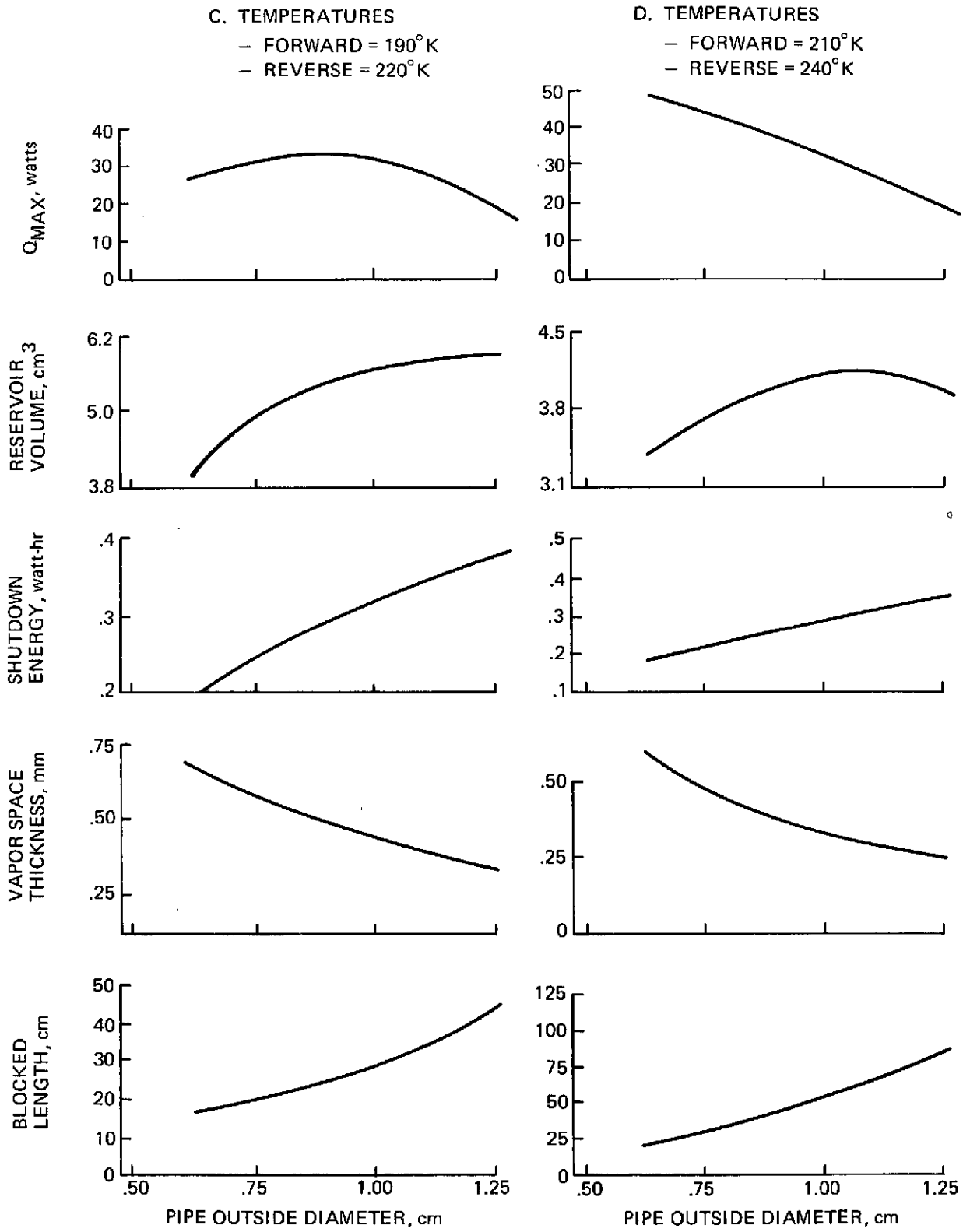

Figure 6-27 Concentric Artery Blockage Performance of Ethane in a Level Heat Pipe (Sheet 2 of 3)

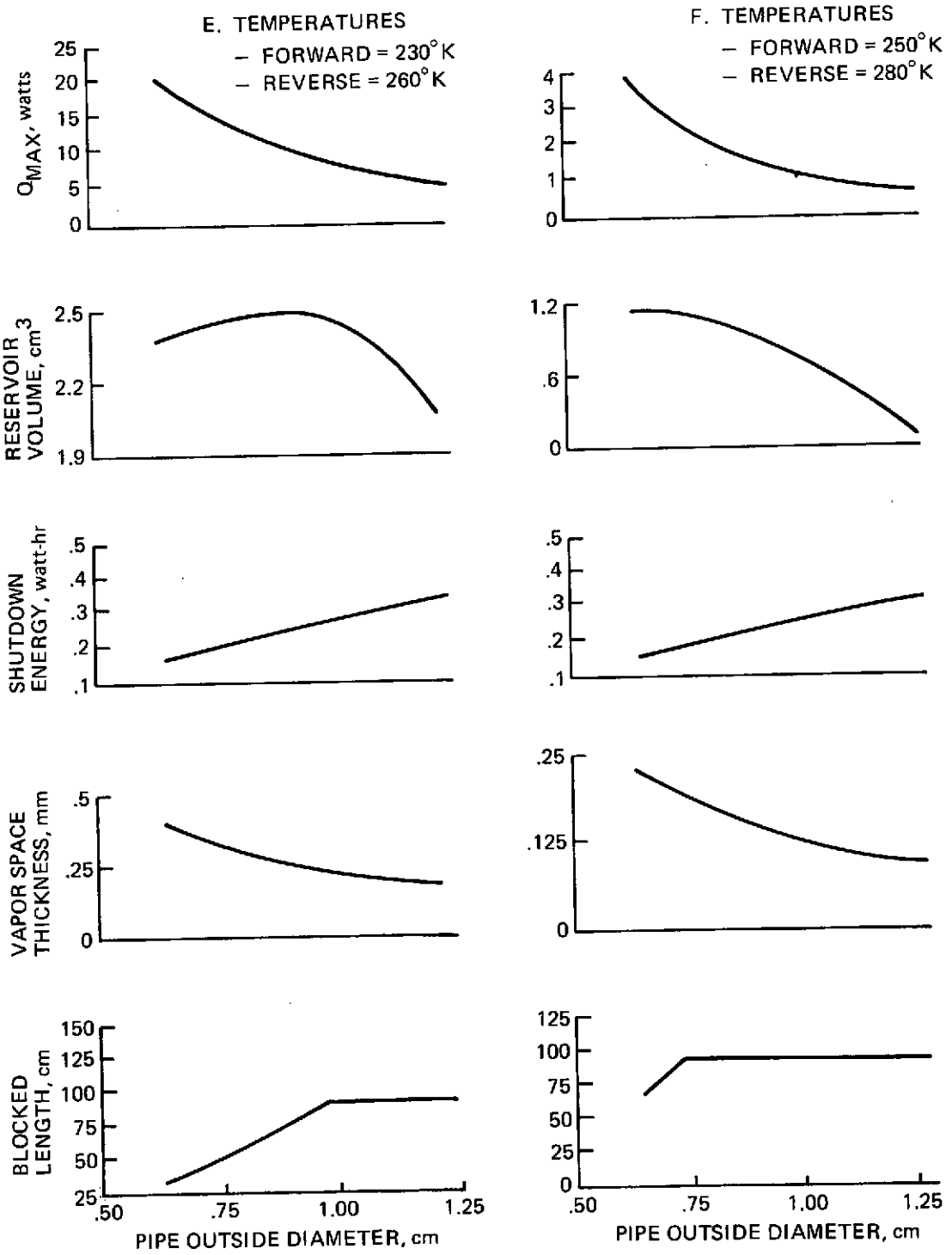

Figure 6-27 Concentric Artery Blockage Performance of Ethane in a Level Heat Pipe (Sheet 3 of 3)

for maximum throughput. This is primarily due to the vapor space opening which is approximately five times that of Freon-14, thus reducing the vapor pressure drop considerably. Shutdown energy is higher for ethane because of the large amounts of excess fluid required to fill up the larger vapor annulus for reversal. This is also evident in total blocked length comparisons. Freon-14, for instance, has its liquid in a compressed state at steady state reversal conditions whereas only a relatively short blocked distance beyond the specified blocked length results with ethane.

Analytical results with ethane illustrating the variation of maximum throughput with orifice discharge coefficient (C_d) for a fixed geometry are shown in Figure 6-28. The geometry used is similar to the previous analytical cases except where noted. The plot shows a 20% change in maximum throughput for a 33% change in discharge coefficient. For these cases, the orifice loss coefficient term dominated. A change of C_d from .9 to .5 produced a change in orifice pressure drop from 38% to 61% of the total drop. If the artery or vapor pressure drops become the controlling factor in the pipe hydrodynamics, the variation of maximum throughput with orifice loss coefficient would be negligible.

Previous discussions on concentric artery blockage dealt with a constant diameter envelope. Compared with liquid trap or blocking orifice blockage, the resulting concentric artery throughputs were small because of the narrow vapor space. For the constant diameter envelope, this vapor space extends the entire length of the pipe. Restricting the narrow vapor space to the evaporator and blocked portion of the transport section only, and with a larger vapor annulus beyond the blocked portion, greater throughput values result. In addition, the increase in vapor space volume for the same total fluid inventory (normal plus excess for blocking) results in larger pipe specific volumes, or lower pipe pressures under ambient conditions.

This design concept is illustrated in Figure 6-29 for ethane and the geometry of Table 6-1, except where noted. Plotted on the ordinate is the multiplier associated with the .635 cm (.25 in.) diameter case. As shown, maximum heat throughput increases over the single diameter case. Inspection of the results for the .952 and 1.27 cm (.375 and .500 in.) constant diameter cases shows the two diameter .635/.952 cm (.25/.375 in.) design throughput to be greater except when the artery liquid pressure loss is the dominant term.

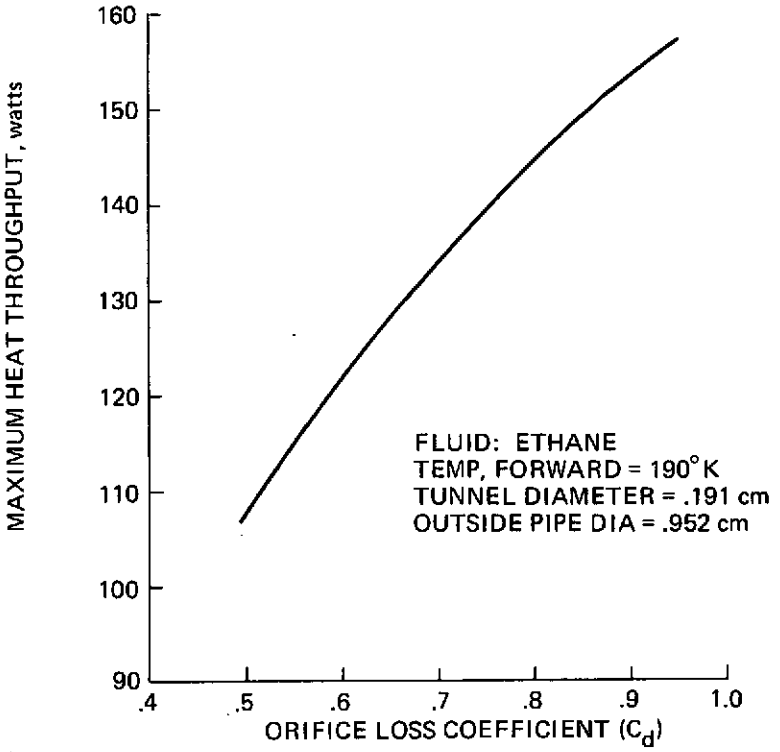

Figure 6-28 Effect of Orifice Loss Coefficient on Throughput

Energy for transition is somewhat less for the two-diameter design because excess liquid for blockage is reduced. Excess mass requirements up to 170°K (-154°F) are based on blockage at transition temperature, while above 170°K (-154°F), steady state requirements prevail because of the high vapor density under reverse mode conditions.

Another feature of the two diameter design is the lower pipe pressures under ambient conditions, as shown in Figure 6-29. Reductions of 50% to 75% are obtained due to a decrease in liquid requirements and increase in pipe total volume.

Comparison of the liquid blockage shutoff technique to the liquid trap technique for methane, Freon-14, and ethane are shown in Figures 6-30 through 6-32. For maximum diode effect, the shut-down energy curve must remain below the curve for maximum heat throughput. As indicated in the figures, the blocking orifice is better than liquid trap with methane as the working fluid up to 144°K (-200°F); Freon-14 up to 160°K (-170°F); and ethane up to 250°K (-10°F). In making these comparisons, note again that the shut-down energy curve is based on a one-hour reverse-mode heat leakage. The single-diameter concentric artery is worse than liquid trap for all

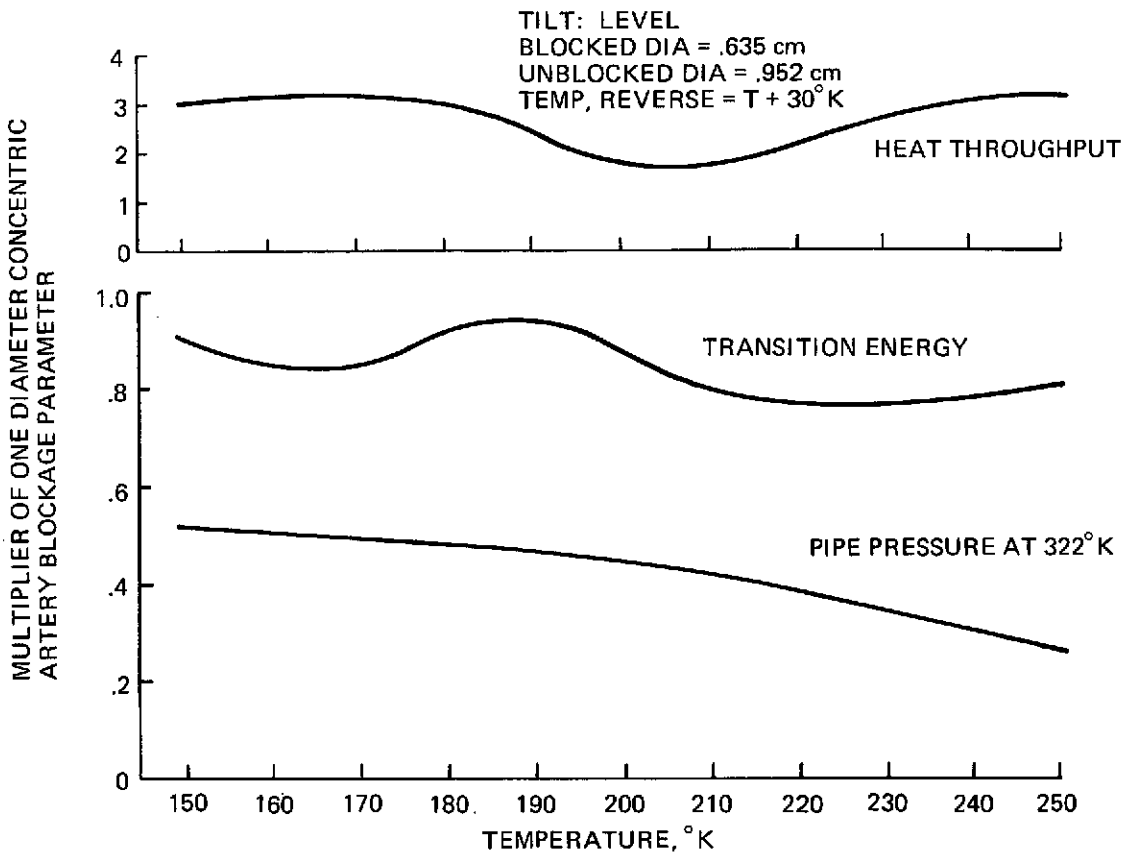

Figure 6-29 Two- and One-Diameter Concentric Artery Comparison, Ethane

temperatures and fluids considered. A closer examination of blocking technique formulations shows liquid trap to be attractive in terms of maximum diode effect for applications involving long evaporators and short condensers.

Based on this maximum diode effect evaluation and the design goals previously mentioned in Subsection 3.2, the blocking orifice design was selected as the most suitable type for fabrication and test.

6.3 DESIGN ANALYSIS

The design of the blocking orifice heat pipe had to accommodate additional considerations including those mentioned in Subsection 3.2. First, hardware fabricated would be tested with several working fluids. Second, overall length of pipe including charging stem and valve had to remain within a prescribed length, since the system would be tested with a radiator in a thermal vacuum chamber at NASA/ARC.

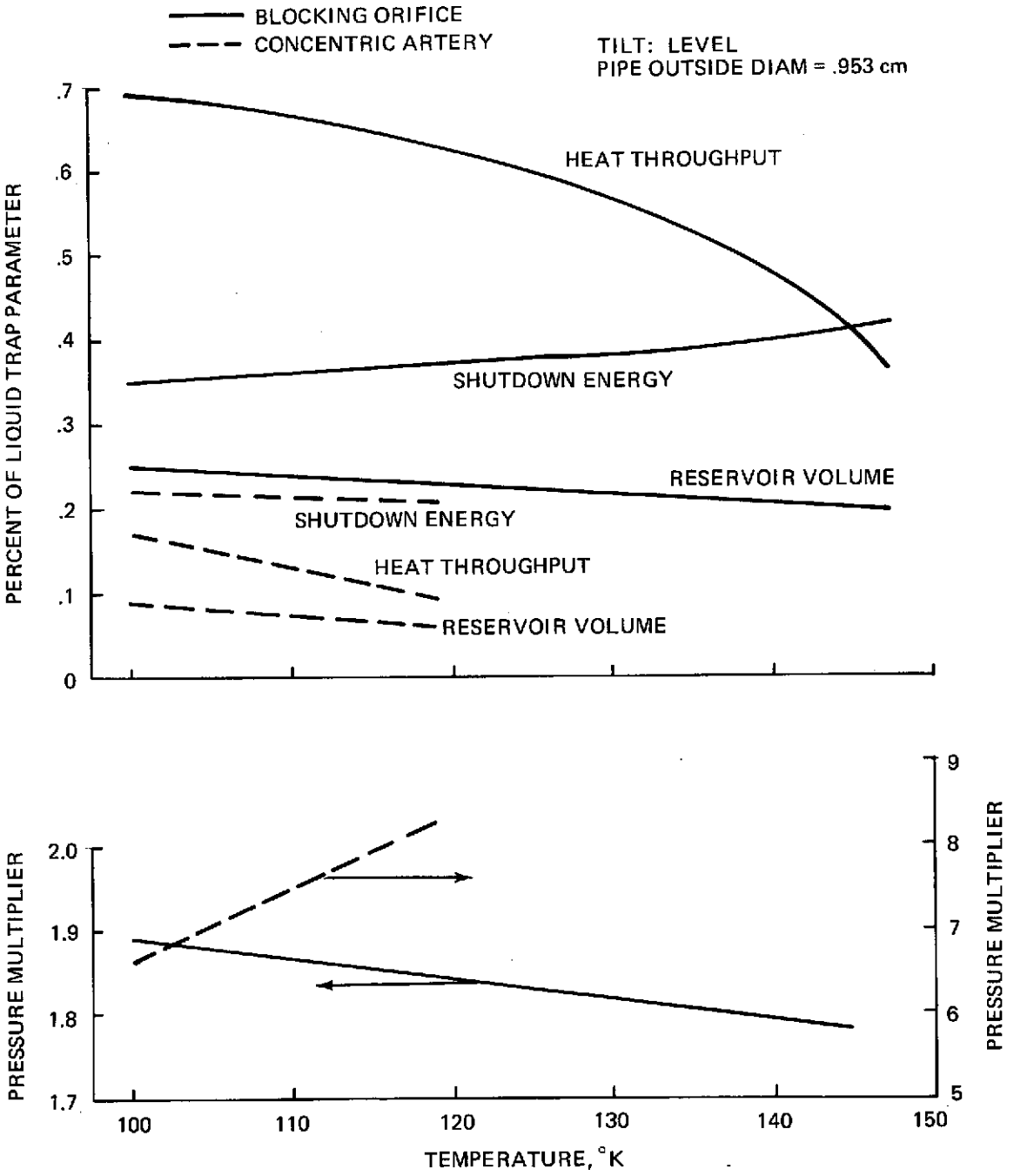

Figure 6-30 Comparison of Blocking Techniques Using Methane

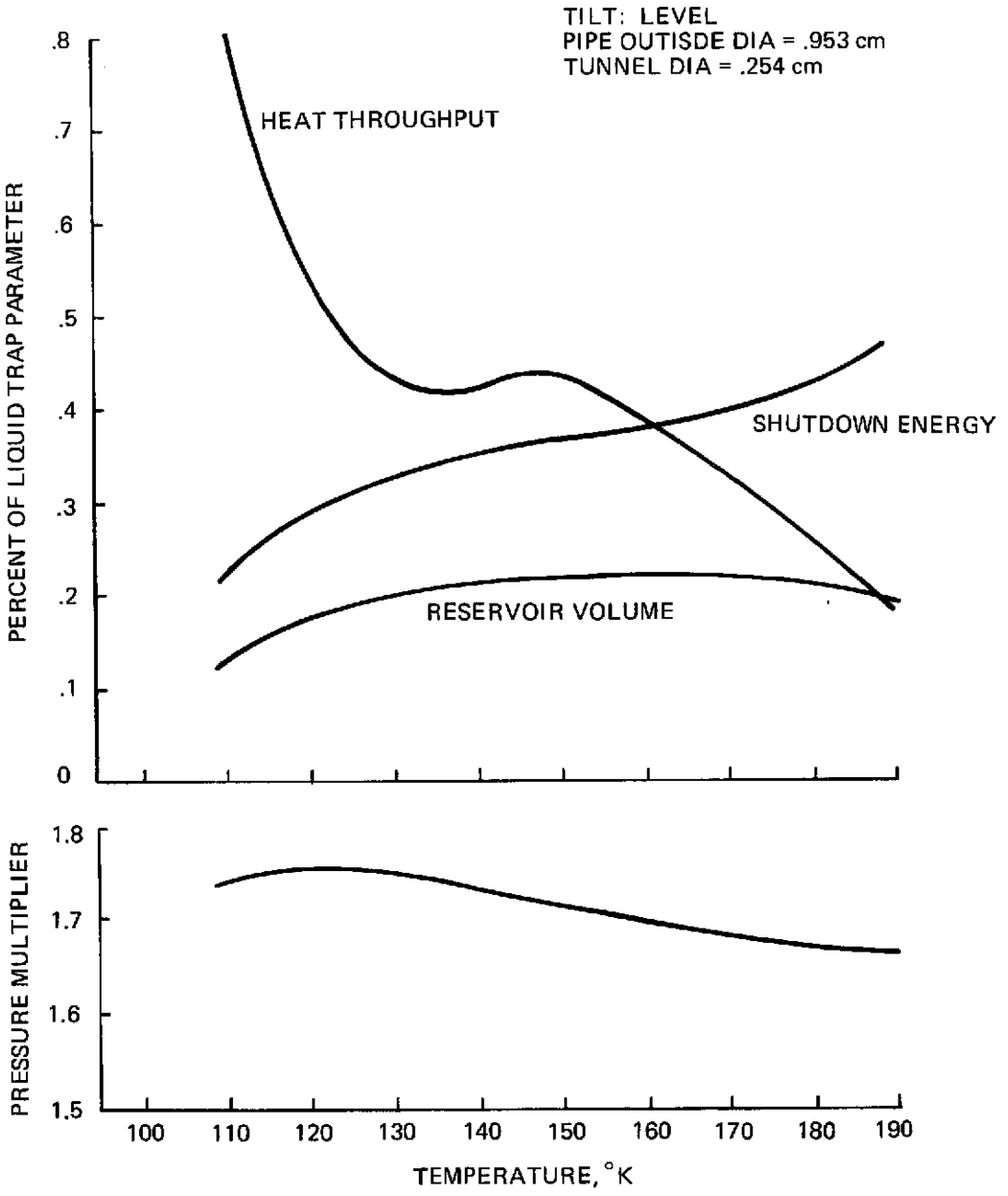

Figure 6-31 Comparison of Blocking Orifice Technique Using Freon-14

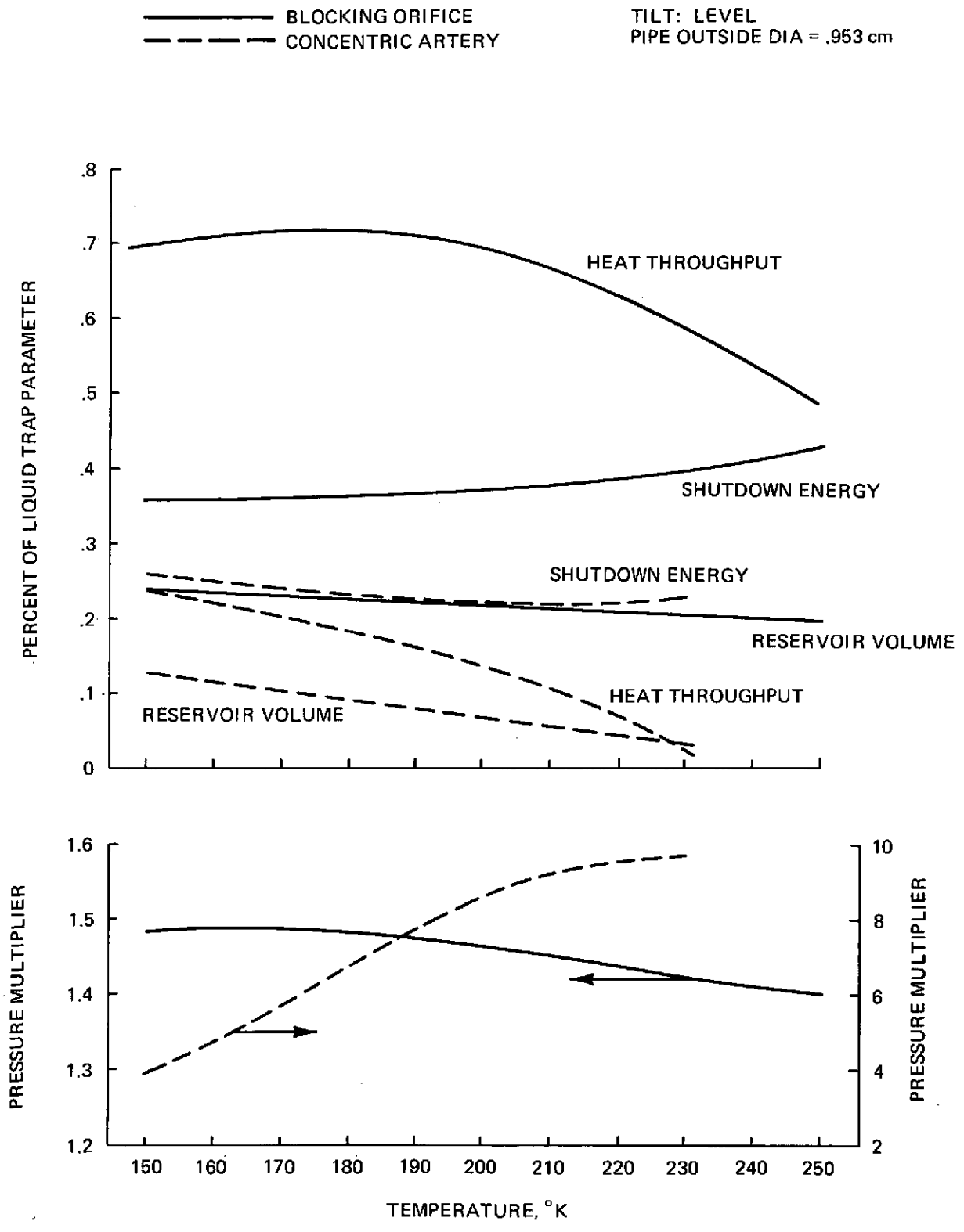

Figure 6-32 Comparison of Blocking Techniques Using Ethane

As previously noted, the blocking orifice concept seems particularly suited to coupling a moderately low temperature, i.e. 120°K to 150°K (-244°F to -190°F), detector on a space vehicle to a radiator which is periodically exposed to a slightly warmer environment. Normal-mode maximum load would be limited by the radiator heat rejection capability; hence, pipe transport capacity in the range of 760 watt-cm (300 watt-in.) was considered representative. Earlier parametric studies indicated this could be met with a pipe outside diameter of .635 cm (.250 in.). Even smaller pipes might have sufficient capacity, but would present fabrication problems.

The geometry selected is shown in Table 6-2. These values are the same as Table 6-1, except for the reduced transport section length and use of three webs instead of six. The wick is a spiral artery tunnel wick, formed of 250-mesh stainless steel screening (Reference 4). Parametric results for this geometry, shown in Figure 6-33 indicate this design would be suitable, with appropriate choice of working fluid, for a wide range of temperatures. Theoretical capacity exceeds 760 watt-cm (300 watt-in.) with Freon-14, and 2032 watt-cm (800 watt-in.) for methane and ethane. The .089 cm (.035 in.) blocking orifice height permits reverse-mode blockage in ground tests at temperatures up to 181°K (-135°F) for methane, 192°K (-114°F) for Freon -14 and 288°K (59°F) for ethane. The curves in Figure 6-33 are shown solid for temperatures 30°K (54°F) or more below these values, and dashed at higher temperatures.

Table 6-2 Low Temperature Diode Geometry

Length	Dimension, cm (in.)	
Evaporator	10.16	(4.0)
Transport Section	28.58	(11.25)
Condenser	30.48	(12.0)
Blocked Transport Section	10.16	(4.0)
Diameter		
Pipe OD	.635	(.250)
Pipe ID	.493	(.194)
Artery OD	.274	(.108)
Tunnel	.114	(.045)
Orifice Height	.089	(.035)
Screening 250-Mesh Stainless Steel		
Wall Grooves	63/cm	(160/in.)
Reservoir Volume	1.966 cc	(.12 cu in.)

It may be noted from Figure 6-33 that methane and ethane provide much higher transport capacity than does Freon-14. There may, however, be applications with reverse-mode hot-end temperature above the methane range, and normal-mode temperatures below the ethane range. For these, Freon-14 may be considered.

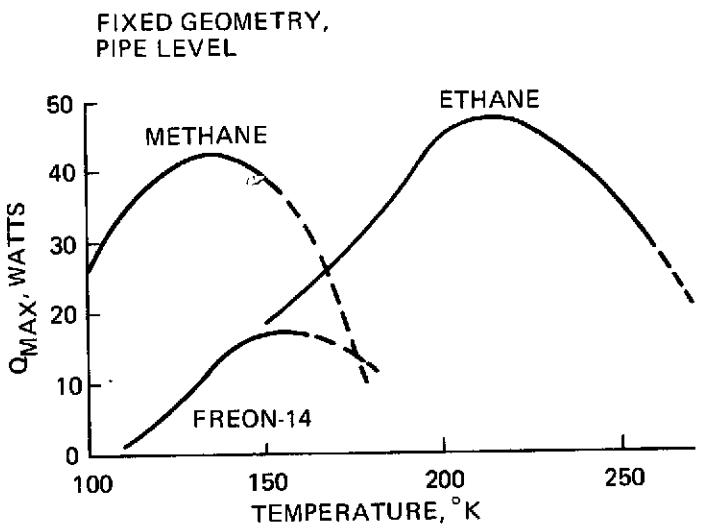

Figure 6-33 Transport Capacity vs Temperature

The reverse-mode heat transfer is less than .2 watt for all cases at the 30°K (54°F) temperature difference and is primarily due to pipe wall conductance. Energy for shutdown, based on evaporating liquid in the reservoir, is less than .2 watt-hr, but does not account for thermal energy transmitted during shutdown.

6.4 DIODE FABRICATION

The fabricated diode consisted of four sections: an evaporator, a transport section, a condenser and a reservoir as shown in Figure 6-34. The pipe was made with a charge tube having a 90° bend, permitting the charge valve to be left on for easy change of working fluid. Methane was selected as the initial working fluid. The diode envelope was made from Type 304 stainless steel, 1/8 hard tubing. This material was chosen to minimize thermal conduction in the reverse-mode.

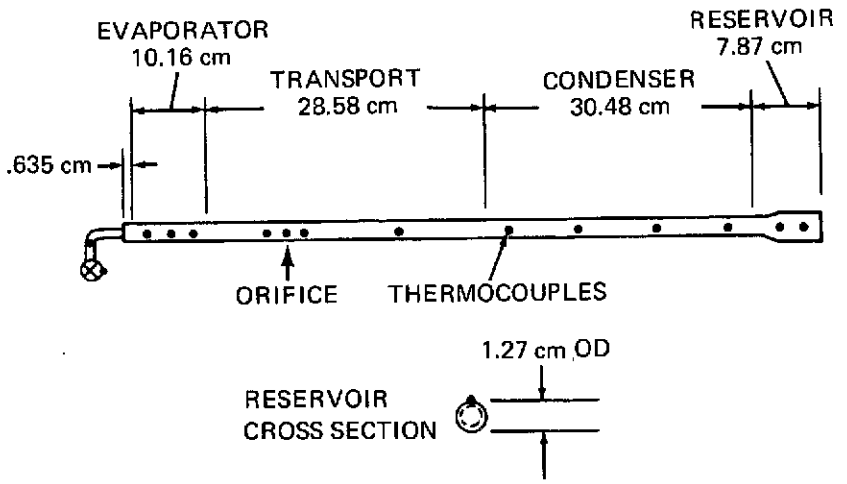

Figure 6-34 Pipe Schematic

The excess liquid reservoir construction is similar to that used previously in the ATFE diode (Reference 1). The reservoir consists of a stainless steel shell .071 cm (.028 in. thick) containing a tightly fitted aluminum cylinder, 1.130 cm (.445 in.) in diameter by 5.888 cm (2.318 in.) in length. Thirty holes .119 cm (.047 in.) diameter by 5.842 cm (2.3 in.) long were drilled in the cylinder to provide a volume of 1.966 cc (.12 cu. in.) (.86 grams of methane at 100°K). For ease of drilling, the cylinder was made in five sections, each carefully aligned and fitted to simulate single-block construction. The small holes were sized to retain excess liquid during normal-mode operation in a gravity environment. Aluminum provides a good conduction path to each hole for rapid evaporation of fluid during shutdown.

The artery is centrally positioned in the condenser and evaporator portions of the pipe by a three-legged mesh retainer assembly that also serves as a liquid communication link between the circumferential wall grooves and the artery. There are no retainers in the transport section. The artery extends the full length of the pipe but is not in liquid communication with the reservoir. Details of the diode construction are given in Figure 6-35 (Grumman Dwg No. 278AD001).

It may be noted that for this small inside diameter, and methane as the fluid, the vapor space in the condenser is self priming at temperatures below 139°K (-209°F). Excess liquid can thus fully block a portion of the condenser at colder temperatures during ground tests in a manner similar to what might be expected in space. Also, because of the small dimensions used, fluid fillets at the web junctions with pipe wall

QTY	PART NO.	NAME	MATERIAL	GOVT SPEC	STOCK SIZE
1	600-R-4-316	REDUCER	SWAGE-LOK - CONVERED FTG CO. SOLON, OHIO		
1	3NB54-316	VALVE	MFG BY WHITEY RESEARCH TOOL CO., RIVERVILLE, CAL		
6	-37	RETAINER	NICHROME	.002 x .12 x .12	
6	-35	SHIELD	NICHROME	.002 x .18 x 3.0	
1	-33	RETAINER	304 S. STL. SCREEN	RR-W-360	250 MESH x .0076 WD
1	-31	CHARGE TUBE	304 S. STL. MW ROD	QQ-S-763b	.250 DIA x 5.0 LGTH
2	-29	END DISK	304 S. STL. (SCREEN)	RR-W-360	250 MESH x .0076 WD
1	-27	ORIFICE	AL ALY 6061-T6 SH - QQ-A-250/8		.038 x .10 x .10
7	-25	SPACER WIRE	304 S. STL. WIRE	RR-W-360	.009 DIA x 2.81 LGTH
1	-23	SOCK	304 S. STL. (SCREEN)	RR-W-360	250 MESH x .0076 WD
1	-21	ARTERY WEB	304 S. STL. (SCREEN)	RR-W-360	250 MESH x .0076 WD
1	-19	END CAP	304 S. STL. SHT	MIL-S-5059	.063 x 3.0 x 1.0
1	-17	CORE SEGMENT	AL ALY 6061-T6 ROD	QQ-A-225/11	.500 D. x .73 LGTH
4	-15	CORE SEGMENT	AL ALY 6061-T6 ROD	QQ-A-225/11	.500 D. x .37 LGTH
1	-13	TUBE (SEAMLESS)	304 HD S. STL. TUBE	MIL-T-5695	.750 O.D. x .028 WALL x 4.0
1	-11	TUBE (SEAMLESS)	304 HD S. STL. TUBE	MIL-T-5695	.250 O.D. x .028 WALL x 29.0
4	-5	RETAINER ASSY			
1	-3	ARTERY ASSY			
1	278AD001-1	CRYO DIODE HEAT PIPE ASSY			

DETAIL "A"

-1 CRYO DIODE HEAT PIPE ASSY
(SCALE = FULL)

8.00 (REF)

LOCATION OF -27 ORIFICE

.25

200-R-4-316 REDUCER

3NB54-316 VALVE

.050 .055

.250 DIA

A-1

.188-.002 DIA

@-A-003

0.00-0.010 CORNER RAD

.015-.020 x 45° CHAMFER

2.93-3.00

.125 RAD

.098-.082 DIA (DRILL THRU)

.125 DIA @-A-003

MACHINING/BEFORE FORMING POSITION

.125-.150

.315 RAD

1.50

DETAIL -31 CHARGE TUBE
(SCALE = 4X)

NOTES

1- WELD -1 ASSY PER MIL-W-8611 (OR GAC-QCP 6.001) INSPECT. TO GSS 62-03

2- ALL SPOTWELDING PER MIL-W-6858-CLA

3- CHARGING PROCEDURE PER DPCS-1 FOR -1 ASSY

4- -15 & -17 CORE SHALL BE ALKALINE CLEAN PER GSS-7030

5- MAX PROOF PRESSURE 5000 PSIA
MAX BURST PRESSURE 8800 PSIA

-19 -17 1 REQ'D -15 4 REQ'D -13

INSTL NOTE - ALL 30 HOLES IN -15 AND -17 MUST BE ALIGNED

.445 DIA (-.195)

.030

.320 (REF)

.900 (REF)

.500 DIA .818

.015 R

.043 (REF)

2.318

2.678

NECK DOWN AS SHOWN

.250 DIA

@-.030 (CONST)

@-.165 RAD

@-.861 BSD

DETAIL A
(SCALE = 4X)

DETAIL "B"

27.75

.250 DIA REF

.028 WELD (REF)

.015-.020 x 45° CHAMFER (WELD PREP) (TYP)

70°

.144 ± 20 GROOVES PER INCH

.0013-.0015

.0095-.0075

DETAIL B
(NO SCALE)

DETAIL -11 TUBE
(SCALE = 4X)

C

4.00 (TYP -33 -35)

C

DETAIL -5 RETAINER ASSY
(SCALE = 4X)

D

-27

E

.37 (4)

8.00

EVAPOR. FOR END OF ARTERY

-29

27.25 (TYP -21 & -23)

D

E

SLOPE ORIENTATION

-29 (SPOT WELD IN POSITION SHOWN)

DETAIL -3 ARTERY ASSY
(SCALE = 4X)

.194 DIA

SPOTWELD -33 & -35 TOGETHER AS REQ'D

-35 SHIELD (6 REQ'D)

.101 DIA

.109 .101

.032 (-.35)

.046 (REF -33)

-33

SECTION C-C
(SCALE = 20X)

.101 DIA (-.23 O.D.)

.045-.050 DIA HOLLOW CORE

SPACER ROD -25

-21 ARTERY WEB

-23 SOCK

.035 DIA (-.21 OUTSIDE DIA)

SECTION D-D
(SCALE = 20X)

-37 RETAINER (6 REQ'D)

SPOTWELD TO ARTERY AS SHN

.193-.195 DIA

-27 ORIFICE

.030 TYP

.101 DIA

-37

.035

.098 (REF)

.010 (REF)

SECTION E-E
(SCALE 20X)

63 63 63 63

.018 TYP

DEPTH OF DRILLED HOLE

.318

.500

DETAIL -17 (1 REQ'D)
(SCALE = 10X)

DETAIL -15 (4 REQ'D)
(SCALE = 10X)

.445 ±.002 DIA

.042-.047 DIA - 30 HOLES DRILL THRU ON -15 ONLY SEE -17 DETAIL FOR DRILLED DEPTH

2.318 ± .004 DIA (10 EQUAL SPACES)

.0344 ±.004 DIA (16 EQUAL SPACES)

.0294 ±.004 DIA (4 EQUAL SPACES)

TYP SECTION FOR -15 & -17 (EXCEPT AS SHN)
(SCALE = 10X)

Fig. 6-35 Cryo Diode Heat Pipe Assembly

6-49/50

FOLDOUT FRAME 1

ORIGINAL PAGE IS OF POOR QUALITY

FOLDOUT FRAME 2

FOLDOUT FRAME 3

and artery represent a greater precentage of liquid volume than would be true for larger pipes. The final shipment charge weight was 3.95 grams of methane.

Section 7

MECHANICAL TEST

Prior to charging the diode with methane, the pipe was pressure tested with GN_2 to 3.4×10^7 Nm^{-2} (5000 psi), which is the maximum attainable with the pressurization rig. This pressure was maintained for 15 minutes and no anomolies were noted. Calculations indicate a burst pressure of 6.07×10^7 Nm^{-2} (8800 psi).

When charged with 3.95 grams of methane, the specific volume is 3.75 cc/gram (.06 ft^3/lbm). The corresponding pipe internal pressure at 300°K (80°F) is estimated to be 3.65×10^7 Nm^{-2} (5300 psi). Because of the large calculated margin and the small quantity of working fluid, this was considered acceptable. During shipment, the pipe might experience environmental temperatures as high as 344°K (160°F), however, and as a precaution, the pipe was shipped in a dry ice container.

Section 8

TEST SETUP AND INSTRUMENTATION

Low temperature thermal tests were conducted in both the normal and shutoff modes of operation. Normal-mode tests were performed at various temperatures and adverse tilts (evaporator end above condenser). Reverse-mode operation was performed with the diode in a horizontal attitude. Testing was performed in an insulated ambient enclosure cooled by vaporized LN_2. A special cryogenic sink/adjustable support fixture (Reference 5) was used to mount the diode in the insulated enclosure. This enclosure provided a controllable heat pipe environment which was kept above the operational diode temperature except for reverse-mode tests. Then the environment was maintained at or below evaporator temperature.

The diode pipe was instrumented with 15 copper-constantan thermocouples. The method of thermocouple attachment to the pipe was by welding each thermocouple bead to the outer envelope. This ensured excellent thermal contact. An additional four thermocouples within the insulated ambient enclosure measured pipe environment temperature. All testing used nichrome ribbon heaters, a condenser heater to simulate a reverse-mode flux, a reservoir heater with the same function, and an evaporator heater to simulate forward mode heat loads. A guard heater was installed on the charging valve to null the charge tube/charge valve heat leak during testing.

Appendix A is a Grumman thermal test plan and procedures followed in the testing of the cryogenic thermal diode.

Section 9

THERMAL PERFORMANCE TESTS

Performance testing of the cryogenic diode consisted of thermal tests to demonstrate forward-mode throughput and reverse-mode shutoff. Testing was accomplished with two different methane charges; 3.0 and 3.95 grams.

9.1 FORWARD-MODE RESULTS

Test data for transport capacity as a function of pipe tilt is shown in Figure 9-1 for a charge of 3.0 grams of methane. The data was obtained with the reservoir heated, so that all working fluid was in the operating portion of the pipe. The artery would not prime with the reservoir cold, indicating the charge was not sufficient to fill both wick and reservoir.

Filled symbols denote steady state operating points, and the O's denote points which resulted in evaporator dry-out. Transport capacity for this pipe is limited by the capillary rise capability of the screening. Experimental values seem to correspond to a capillary pore size of 38.1 microns. This is slightly better than had been expected, since values determined from lift testing the artery indicated a pore size of 43.2 microns.

Only limited data, shown in Figure 9-1, was taken with the 3.95-gram charge with the reservoir cold. The pipe carried 16.2 watts at 2.5 cm adverse tilt at 130^{o}K, indicated a primed tunnel condition. A local dry-out (increased wall temperature but not burn-out) was noted at 22 watts for the same temperature and tilt. Note that high heat load tests were run primarily to determine wick capacity. Evaporator and condenser lengths are too short to handle these high loads without an excessive temperature drop.

Temperature profiles for normal mode operation are shown in Figure 9-2 for the 3.0-gram charge with reservoir heated. The 4.1-watt case was with the artery tunnel unprimed, verified by evaporator dry-out for a small increase in power. The 6.5-watt case was with the tunnel primed, verified by subsequent increases in power up to 39 watts. The 4.1-watt case shows a considerable larger temperature drop in the condenser, believed due to the larger puddle with the tunnel drained. The tunnel at this temperature would contain approximately .3 grams of liquid if fill.

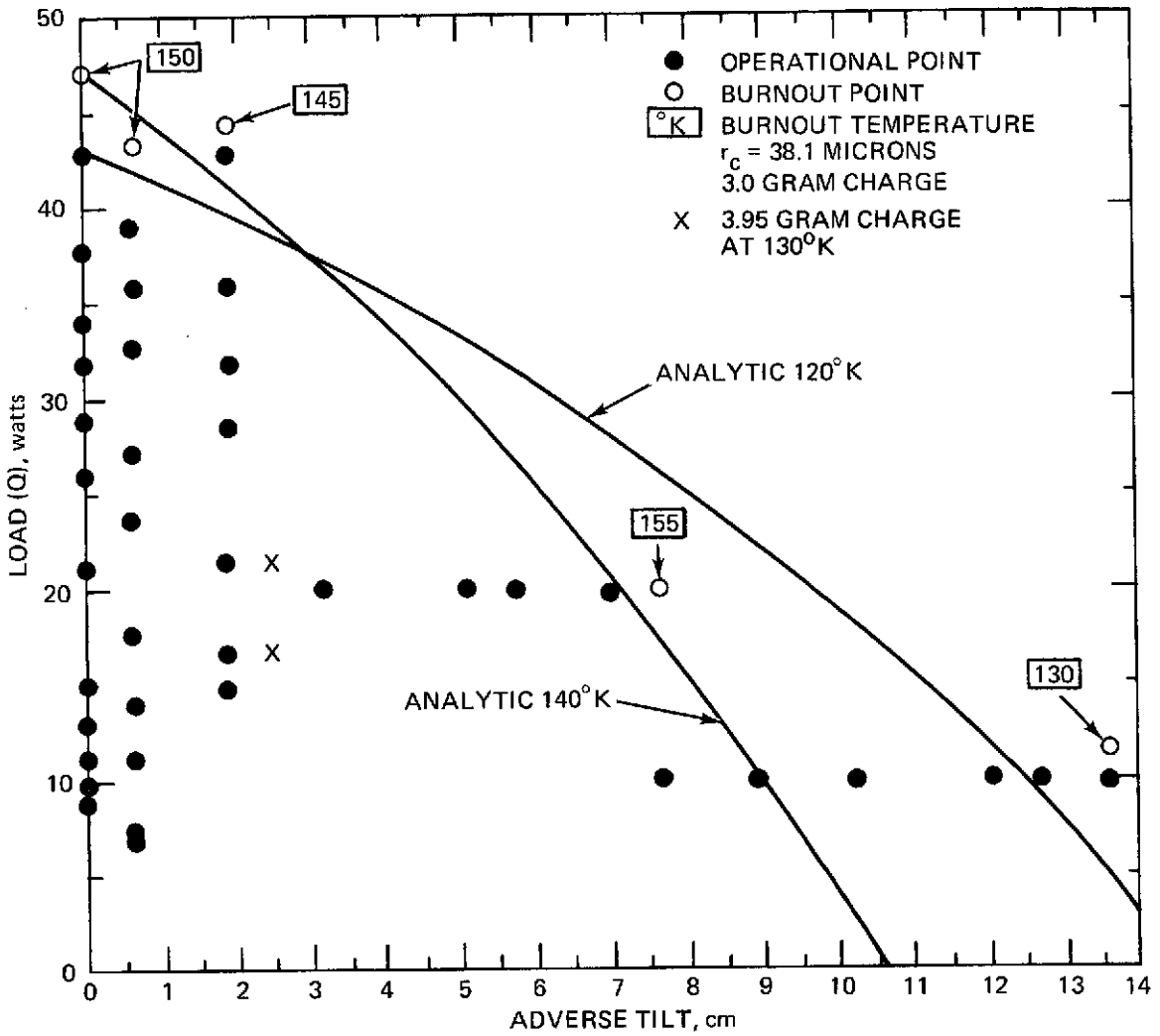

Figure 9-1 Forward-Mode Performance Map

Figure 9-3 shows normal-mode temperature profiles with the diode containing 3.95 grams of methane. The reservoir in this case is colder than the condenser and contains approximately .83 grams of liquid. Compared with Figure 9-2, there is slightly more free liquid in the condenser, and slightly larger temperature drops. Figure 9-3 is with the pipe level. There was some blockage of the condenser vapor space at adverse tilt at this charge, which might be expected since the vapor space can self prime if free liquid is available at temperatures below approximately 139°K (-209°F).

Evaporator film coefficients for these cases were approximately 1702 w/m^{2o}K (300 Btu/hr ft^{2o}R), based on inside surface area. Condenser film coefficients were

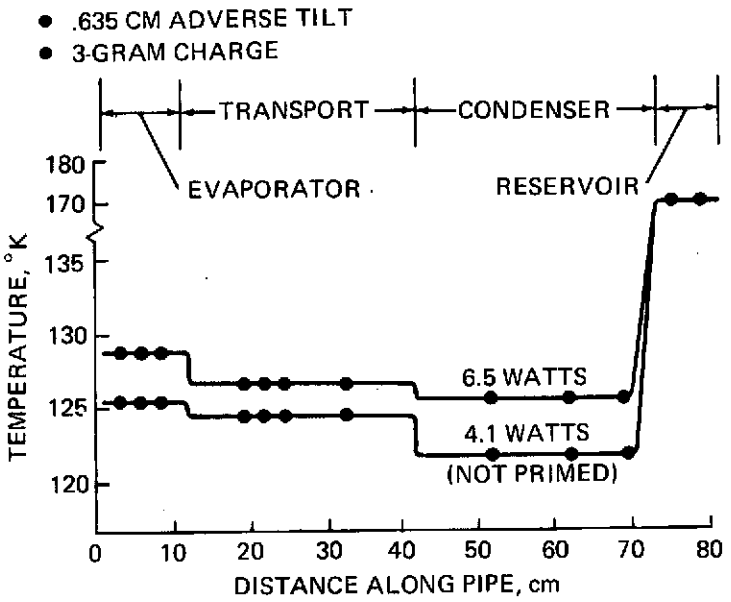

Figure 9-2 Forward-Mode Temperature Profile

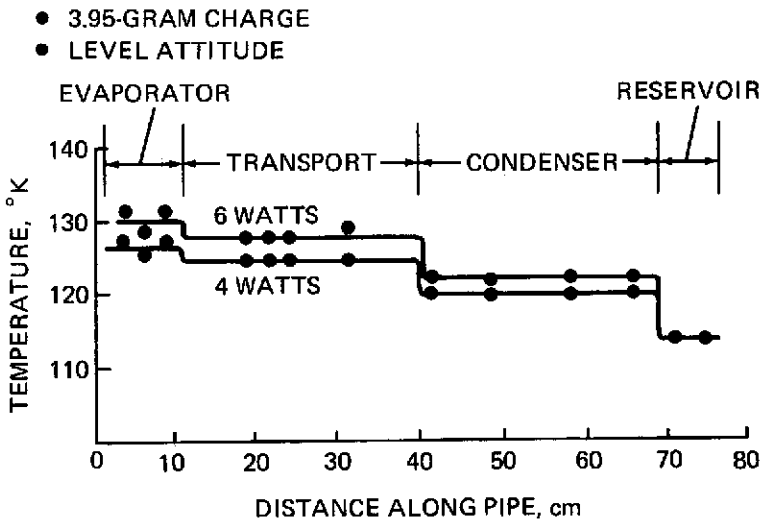

Figure 9-3 Forward-Mode Temperature Profile

not evaluated because of excess fluid effects. The bottom of the condenser is believed to be blocked by puddling, and the upper condenser surfaces may be partially blocked by large fillet radii near the webs. Free liquid seems to have a pronounced effect on condenser performance because of the small diameter and vapor passage height used.

9.2 REVERSE-MODE RESULTS

Testing for the reverse-mode characteristic was performed by shutting off evaporator power and applying power to reservoir and condenser heaters. Partial shutoff was achieved with the 3.0-gram charge. This is attributed to an insufficient amount of liquid to completely fill the vapor space from the evaporator up to the orifice plate. Figure 9-4 shows the results of the pipe in the shutoff mode of operation for the 3.0 and 3.95 gram charges. Shutoff of the pipe is evident from the sharp gradient with the 3.95 gram charge, characteristic of conduction heat transfer in the 10.16 cm (4-in.) blocked portion, measured from the evaporator to the orifice plate, of the transport section. No measurements of total reverse-mode energy were made due to the fact that the relatively large condenser block utilized for forward-mode operation provided too large a surface area for heat transfer with the environment. A more realistic shutoff mode test for this pipe is scheduled at ARC. In that test, both the reservoir and condenser portions are to be thermally coupled to a radiator(s) with heater(s) to simulate orbital flux heat loads.

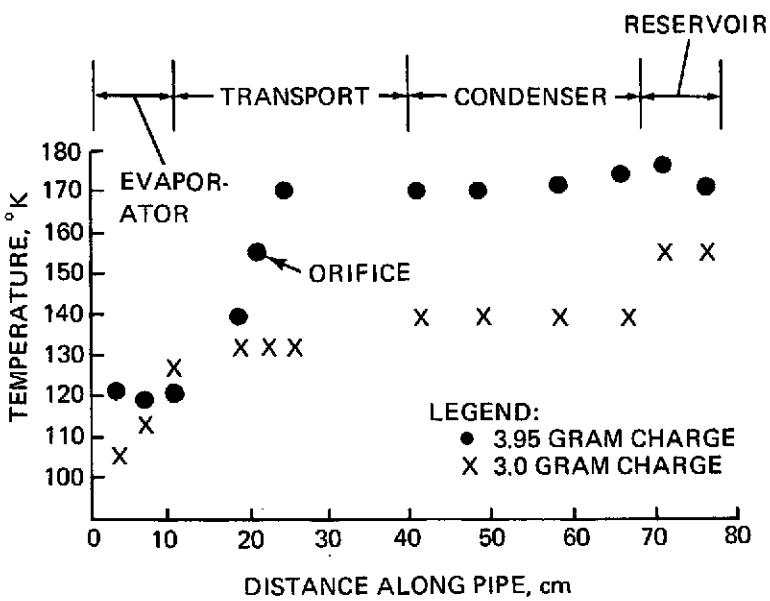

Figure 9-4 Reverse-Mode Temperature Profile, Level

Section 10

REFERENCES

1. Swerdling, B., and Kosson, R.," Design, Fabrication and Testing of a Thermal Diode," Grumman Aerospace Corporation, November 1972.

2. Swerdling, B., Kosson, R., Urkowitz, M., and Kirkpatrick, J., "Development of a Thermal Diode Heat Pipe for the Advanced Thermal Control Flight Experiement (ATFE)," AIAA Progress in Astronautics and Aeronautics, Vol. 31, "Thermal Control and Radiation," edited by Chang-Lin Tieu, The MIT Press, Cambridge, Massachusetts, and London, England, pp. 35-50.

3. Cooper, H.W. and Goldfrank, J.C., "B-W-R Constants and New Correlations," Hydrocarbon Processing, Vol. 46, No. 12, December, 1967, pages 141-146.

4. Kosson, R. Quadrini, J., and Kirkpatrick, J., "Development of a Blocking Orifice Thermal Diode Heat Pipe," AIAA Paper No. 74-754. To be published in Progress in Astronautics and Aeronautics Series.

5. Dominquez, P. and Kosson, R., "Development of a High Capacity Cryogenic Heat Pipe," AIAA Progress in Astronautics and Aeronautics, Vol. 35, "Thermophysics and Spacecraft Thermal Control," edited by R. G. Hering, The MIT Press, Cambridge, Massachusetts, and London, England, pp. 395-407.

Section 11

NOMENCLATURE

A	cross sectional area
A'_o	dimensionless coefficient
a'	dimensionless coefficient
B'_o	dimensionless coefficient
b'	dimensionless coefficient
C	loss coefficient
C'_o	dimensionless coefficient
c'	dimensionless coefficient
D	diameter
g_c	gravitational constant
g	gravitational acceleration
h_o	orifice opening
h	pipe tilt
ID	inner diameter
J	Joule constant (mechanical equivalent of heat)
K	temperature
k	conductivity
L	length
OD	outer diameter
P	pressure
Q	thermal transport rate
r	radius

$\bar{r}$	mean radius
S	allowable fiber stress
T	temperature
t	vapor annulus height or thickness
v	specific volume
α'	dimensionless coefficient
γ'	dimensionless coefficient
Δ	differential
Θ	time
λ	latent heat
μ	absolute viscosity
ρ	density
σ	surface tension
τ	modified reduced volume, dimensionless
ϕ	half angle
Ω	angular velocity

Subscripts

CAP	capillary structure
c	critical parameter
D,d	orifice discharge coefficient
GRAV	gravity
i	inside
L,ℓ, LIQ	liquid or laminar
o	orifice or outside
ROT	rotation
r	reduced parameter

T	turbulent
t	total
u	unblocked
V, v, VAP	vapor
w	wall

CONTRACT REQUIREMENTS	CONTRACT ITEM	MODEL	CONTRACT NO.
Par. C.3, SOW		Engineering	NAS 2-7492

Appendix

REPORT

NO. _____ DATE: 15 August 1974

THERMAL PERFORMANCE TEST PLAN AND
PROCEDURE FOR THE CRYOGENIC THERMAL DIODE
HEAT PIPE

CODE 26512

PREPARED BY: J. Quadrini

CHECKED BY:

DEPARTMENT:

SECTION:

TECHNICAL APPROVAL:

APPROVED BY: R. Haslett

APPROVED BY:

APPROVED BY:

REVISIONS

DATE	REV. BY	REVISIONS & ADDED PAGES	REMARKS

FORM G324A REV 1 8/67 15M

GRUMMAN AIRCRAFT ENGINEERING CORPORATION

1.0 SCOPE

1.1 General: This test plan and procedure define the test procedures and data requirements for the thermal performance testing of Cryogenic Thermal Diode Heat Pipe.

1.2 Applicability: This test plan and procedure is applicable to the Engineering Model Heat Pipe defined by GAC drawing 278AD001.

1.3 Diode Description: The Diode to be tested is made from stainless steel tubing and has outside diameters of 0.500 inch and 0.250 inch. The shape of the pipe is straight except for the fill tube which makes a 90° bend to the axis of the pipe. A valve is attached to the fill tube. The longest dimension is approximately 33 inches. The pipe is charged with Methane as the working fluid.

1.4 Objective: The objective of this test is to demonstrate diode throughput and feasibility of the shut-off technique. The Cryogenic Diode Heat Pipe shall be tested under two conditions as follows:

Condition A: Forward Modes: $\left\{\begin{array}{l}\text{Level, } Q_{max} \text{ vs. tilt,} \\ Q \text{ vs } \Delta T\end{array}\right\}$

Condition B: Reverse Mode: (Level)

2.0 APPLICABLE DOCUMENTS

2.1 Government Documents

None

2.2 Grumman Documents

Drawing

278AD001 Cryo Diode Heat Pipe Assy.

3.0 REQUIREMENTS

3.1 General: The Cryo Diode shall be tested in accordance with the requirements specified in Section 4.

3.2 Test Environment: The Cryo Diode shall be tested in two environments. Condition A shall be tested in either standard atmospheric conditions or in a vacuum chamber of at least 10^{-5} mm of mercury. Condition B shall be tested in a vacuum chamber of at least 10^{-5} mm of mercury.

3.3 Test Conditions: The Cryo Diode shall be subjected to the thermal performance conditions as specified in Table I.

3.4 Acceptance Criteria: Two conditions shall determine compliance to the test conditions as specified in 3.3. These conditions are:

(a) Temperature Difference (ΔT) : Compliance to the ΔT requirement of Condition A of Table I shall be based on average evaporator temperature to average transport temperature and average transport temperature to average condenser temperature.

(b) Reverse Heat Flow: Compliance to the Reverse Heat Flow requirement of Condition B of Table I shall be based on an average rate under steady state conditions. This rate shall be calculated from temperature measurements on the Cryo Diode.

3.5 Test Equipment Required: The following test equipment or equivalent shall be used for the performance of the tests specified herein. Test equipment marked * shall be calibrated in accordance with current established calibration procedures. The equipment shall bear an approved calibration certificate dated not more than six months prior to date of use. The equipment marked ** shall mean "or equivalent."

	Test Equipment Nomenclature	Manufacturer and Model No.
*	Thermocouple Readout	Bristol Strip Chart Recorder (-350°F to +300°F)
*	Ammeter - AC	Weston Instrument Div. **
*	Voltmeter - AC	Weston Instrument Div. **
	Heater Wire	Driver Harris Ribbon
	Test Fixture	
	Thermocouples (15)	Copper Constantan
	Vernier Height Gage	L.S. Starrett Co.
	Vacuum Chamber with LN_2 Cold Wall or equivalent insulated chamber	

3.6 Test Facilities: All testing shall be performed in the Grumman Bethpage facilities and/or Ames Research Center.

3.7 Data Recording: The results of the test shall be recorded in the appropriate documentary and check-off spaces provided by the Test Engineer. All recorded data shall be sufficiently legible such that copies can be submitted with the test report. The following is a listing of the data to be recorded during the thermal performance test of the Cryo Diode Heat Pipe.

(a) Date
(b) Time
(c) Power Input
(d) Temperatures
(e) Test Condition

Prior to recording data, the Cryo Diode temperatures shall reach steady state as achieved not sooner than 10 minutes after a power set point change. A second set of readings shall be taken within 5 minutes to establish the relative stability of the Cryo Diode. In the event steady state conditions cannot be achieved, recording of data shall be determined by the GAC Test Engineer or ARC Test Engineer.

3.8 Test Summary: Within five (5) days after completion of the performance test, a test summary shall be prepared which will contain test results as well as test conclusions.

3.9 Test Reports: Within thirty (30) days after completion of performance testing, a test report shall be prepared which will contain the following:

(a) Test Objectives
(b) Test Description
(c) Test Assessment Criteria
(d) Test Results
(e) Conclusions

3.10 Working Fluid Re-Test: The Cryo Diode is equipped with a valve for the purpose of testing other cryogenic fluids. The following information is necessary for the charging of the Cryo Diode designated by the drawing in Section 2.2.

(a) Pipe Dry Weight - Dry weight of pipe for a given configuration. Prior to determining this weight, the pipe shall be evacuated to a pressure less than 10^{-5} mm Hg.

(b) Weight of Charge - The total weight of the cryogenic fluid charge shall be based on the following volumes:

(1) Liquid: 8.9 cc
(2) Vapor: 6.2 cc
(3) Void: 15.1 cc

(c) Charging Cryo Diode - At the discretion of the Test Engineer, a charging procedure shall be determined.

4.0 METHOD OF TESTING

WARNING: The Cryo Diode Heat Pipe contains Methane as the working fluid. This fluid is under high pressure at room temperature (300°K). Exercise great care in handling.

4.1 Test Set-up for Condition A:

(a) Instrument pipe with suitable thermocouples and heaters as detailed by the Test Engineer. Install heater and thermocouple on Cryo Diode valve. Install heaters on reservoir and condenser cooling block.

(b) Check out all Cryo Diode instrumentation prior to next step.

(c) Mount Cryo Diode to test fixture. The test fixture can be part of an ambient insulated chamber or vacuum system. Either environment is acceptable. Ensure pipe is level and maintains this position during ambient/pipe environments.

(d) Insulate transport and evaporator sections, including valve, with proper thermal insulation as determined by the Test Engineer.

(e) Provide condenser and reservoir cooling by LN_2 spray and LN_2 condenser block if ambient insulated chamber is used. Otherwise condenser and reservoir cooling must be accomplished with a vacuum chamber LN_2 shroud supplemented with a LN_2 condenser block.

(f) Connect supporting test equipment up and perform preliminary functional check-out as detailed by the Test Engineer.

4.2 Test Procedure for Condition A:

(a) Adjust test fixture such that the entire system is level.

(b) Adjust ambient and/or condenser LN_2 flow rate/heater power to maintain desired forward mode temperature.

(c) Adjust reservoir temperature via reservoir heater such that it always remains several degrees Kelvin below vapor temperature.

(d) Adjust valve temperature via valve heater such that its temperature is several degrees Kelvin above vapor temperature.

(e) Apply 3 watts to evaporator or evaporator block and readjust condenser LN_2 flow rate/heater power to maintain desired forward mode temperature.

(f) Record temperature, current and voltage.

(g) Repeat steps (b) thru (e) 3 watt increments up to incipient burnout.

(h) After step (f) is complete, apply 3 watts to evaporator or evaporator block.

(i) Adjust test fixture to the desired tilt as specified by the Test Engineer such that the evaporator is higher than the condenser.

(j) Repeat steps (b) thru (h) to a maximum tilt as specified by the Test Engineer.

NOTE: If artery does not prime, return pipe to level & adjust condenser block temperature such that its temperature and rate of temperature increase is greater than the evaporator. Once this is established apply 5 to 7 watts to evaporator or evaporator block.

4.3 Test Set-up for Condition B:

(a) Insulate completely the Cryo Diode with superinsulation, after pipe is mounted in test fixture.

(b) Install in vacuum chamber equipped with LN_2 shroud.

(c) Adjust test fixture to ensure pipe is level.

NOTE: At the discretion of the Test Engineer, cooling may be accomplished by other means.

4.4 Test Procedure for Condition B:

(a) Evacuate chamber to a pressure lower than 10^{-5} mm Hg and begin LN_2 filling of chamber shroud.

(b) After chamber pressure stabilization, repeat steps (b) thru (e) of Test Procedure for Condition A.

(c) Repeat (b) above with 10 watts applied to evaporator or evaporator block. This ensures artery is primed and reservoir is filled with excess liquid.

(d) Apply power to condenser and reservoir heaters at the same time reducing evaporator or evaporator block power to zero.

(e) Record temperature, voltages and currents at least every 30 seconds until condenser temperature is 30° to 40°K higher than the initial forward mode temperature.

(f) Assuming solid conduction, the Test Engineer can determine the reverse mode heat leakage from the temperature gradient in the blocked portion of the pipe.

TABLE I

TEST REQUIREMENTS*

Condition	Mode	Q (watts)	Tilt (in.)	T vapor (°K)	ΔT
A	Forward	Q max	Level 1/4 1/2 3/4 . . . 3.0	100, 120, 140	TBD
A	Forward	Q	Level 1/4 1/2 3/4 . . . 3.0	100, 120, 140	TBD
B	Reverse	0	Level	30 to 40 higher than forward mode	

Shut off energy < 2 BTU's

* At the discretion of the Test Engineer, these requirements may be changed.